VOL. 6 NO. 3 SEPTEMBER 1963

Journal of

ELECTROANALYTICAL CHEMISTRY

International Journal Dealing with all Aspects of Electroanalytical Chemistry, Including Fundamental Electrochemistry

ELSEVIER

GENERAL INFORMATION

See also Suggestions and Instructions to Authors which will be sent free, on request to the Publishers.

Types of contributions

(a) Original research work not previously published in other periodicals.
(b) Reviews on recent developments in various fields.
(c) Short communications.
(d) Bibliographical notes and book reviews.

Languages

Papers will be published in English, French or German.

Submission of papers

Papers should be sent to one of the following Editors:

Professor J. O'M. Bockris, John Harrison Laboratory of Chemistry, University of Pennsylvania, Philadelphia 4, Pa., U.S.A.
Dr. R. Parsons, Dehartment of Chemistry, The University, Bristol 8, England.
Professor C. N. Reilley, Department of Chemistry, University of North Carolina, Chapel Hill, N.C., U.S.A.

Authors should preferably submit two copies in double-spaced typing on pages of uniform size. Legends for figures should be typed on a separate page. The figures should be in a form suitable for reproduction, drawn in Indian ink on drawing paper or tracing paper, with lettering etc. in thin pencil. The sheets of drawing or tracing paper should preferably be of the same dimensions as those on which the article is typed. Photographs should be submitted as clear black and white prints on glossy paper.
All references should be given at the end of the paper. They should be numbered and the numbers should appear in the text at the appropriate places.
A summary of 50 to 200 words should be included.

Reprints

Twenty-five reprints will be supplied free of charge. Additional reprints can be ordered at quoted prices. They must be ordered on order forms which are sent together with the proofs.

Publication

The *Journal of Electroanalytical Chemistry* appeared monthly and has six issues per volume and two volumes per year, each of approx. 500 pages.

Subscription price (post free): £ 10.15.0 or $ 30.00 or Dfl. 108.00 per year; £ 5.7.6 or $ 15.00 or Dfl. 54.00 per volume.

Additional cost for copies by air mail available on request.
For advertising rates apply to the publishers.

Subscriptions

Subscriptions should be sent to:

ELSEVIER PUBLISHING COMPANY, P.O. Box 211, Spuistraat 110-112, Amsterdam-C., The Netherlands.

CHROMATOGRAPHY *for* BIOCHEMISTS

a comprehensive survey of all chromatographic procedures and applications with special emphasis on the field of biochemistry

SEPARATION METHODS

VOLUME 4 IN THE SERIES COMPREHENSIVE BIOCHEMISTRY

edited by

MARCEL FLORKIN, Department of Biochemistry, University of Liège, Belgium

and

ELMER H. STOTZ, Department of Biochemistry, University of Rochester, N.Y., U.S.A.

xiii + 282 pages 91 illus. 43 tables 1507 references approx. 1300 index entries 70s.

Contents

Also available

TECHNIQUES IN PROTEIN CHEMISTRY

by **J. LEGGETT BAILEY**

x + 308 pages 42 tables 90 illustrations 537 refs. 1962 60s.

Contents. Paper chromatography of aminoacids and peptides. High-voltage paper electrophoresis. Ion-exchange chromatography of aminoacids and peptides. Disulphide bonds. Selective cleavage of peptide chains. N-terminal sequence determination. C-terminal sequence determination. Dialysis and gel filtration. Column chromatography of proteins. Zone electrophoresis of proteins. Miscellaneous analytical methods. Subject index.

ELSEVIER PUBLISHING COMPANY

AMSTERDAM LONDON NEW YORK

ZONE ELECTROPHORESIS IN BLOCKS AND COLUMNS

by H. BLOEMENDAL
Senior Research Fellow in Biochemistry at The Netherlands Cancer Institute, Amsterdam, The Netherlands

Zone electrophoresis in porous media or in density gradients has a number of advantages over moving boundary electrophoresis. Several stabilizing materials are used, e.g. paper, granular or hydrolyzed starch, agar, gelatin, glass wool or beads, foam rubber, polyvinyl chloride resin, asbestos and, recently, polyacrylamide gels. In this monograph the reports of a number of workers are presented regarding the various possibilities opened up by improved methods, with a discussion of their merits and limitations. The current literature is reviewed, and advice based on the author's own experience given, enabling the reader to make an informed choice of the analytical or preparative techniques suited to his purposes.

CONTENTS

5 × 7½"
viii + 219 pages
13 tables
75 illustrations
444 references
1963
40s.

ELSEVIER PUBLISHING COMPANY
AMSTERDAM LONDON NEW YORK

207 E

SUMMARIES OF PAPERS PUBLISHED IN JOURNAL OF ELECTRONALYTICAL CHEMISTRY

Vol. 6, No. 3, September 1963

REPORT OF THE CITCE COMMISSION FOR NOMENCLATURE AND ELECTROCHEMICAL DEFINITIONS, AND OF THE IUPAC SUBCOMMISSION FOR SYMBOLS AND ELECTROCHEMICAL TERMINOLOGY

PIERRE VAN RIJSSELBERGHE, *J. Electroanal. Chem.*, 6 (1963) 173–182.

ELECTROCHEMICAL BEHAVIOUR OF NITROSOBENZENE IN DIMETHYLFORMAMIDE

Nitrosobenzene is reduced in a solution of 0.2 *N* $NaNO_3$ in dimethylformamide in two polarographic waves. In the first reduction wave the free radical anions of nitrosobenzene form primarily. The free radical anions are unstable and react with formation of azoxybenzene as a final product. This was ascertained by means of controlled potential electrolysis at the potential of the first reduction wave of azoxybenzene. Nitrobenzene is formed during simultaneous electrochemical reduction of oxygen and nitrosobenzene in a solution of 0.2 *N* $NaNO_3$ in dimethylformamide. This was ascertained by means of electrolysis and also by oscillopolarography.

W. KEMULA AND R. SIODA, *J. Electroanal. Chem.*, 6 (1963) 183–186.

TRANSIENTS *IN* CONVECTIVE SYSTEMS

I. THEORY OF GALVANOSTATIC, AND GALVANOSTATIC WITH CURRENT REVERSAL TRANSIENTS, AT A ROTATING DISC ELECTRODE

The theory of a galvanostatic transient at a rotating disc electrode is reviewed, and an accurate solution obtained by a numerical method. Methods of analysis into kinetic and diffusion parameters are proposed. Current-reversal transients are treated, and a criterion presented for diagnosis of the applicability of the model.

J. M.HALE, *J. Electroanal. Chem.*, 6 (1963) 187–197.

POLAROGRAPHY OF Ni^{2+} IN DIFFERENT SUPPORTING ELECTROLYTES IN AQUEOUS AND NON-AQUEOUS MIXTURES

The reduction of Ni^{2+} in 0.1 *M* sodium formate, sodium sulphate and sodium iodide supporting electrolytes gives only one reduction wave. As the concentration of the supporting electrolytes is increased from 0.5–1–1.5 *M*, two reduction waves are obtained. In all cases the total limiting current was found to be diffusion-controlled which provides a method for the polarographic determination of Ni^{2+}. The half-wave potential of the first wave in each case corresponds to the reduction of the $Ni(H_2O)_6^{2+}$ complex. In the case of the second wave, the shift in half-wave potential indicates the co-ordination of the anion of the supporting electrolyte with Ni^{2+}.

In ethanol, propanol and ethylene glycol aqueous mixtures the two waves show a tendency to unite to form a single wave. This is more apparent in the case of propanol.

K. ZUTSHI, *J. Electroanal. Chem.*, 6 (1963) 198–204.

A METHOD FOR THE DETERMINATION OF ELECTROLYTIC HYDROGENTRITIUM SEPARATION FACTORS

A new method for the determination of electrolytic H/T separation factors is described. Copper or mercury was used as the test electrode. electrode. Vacuum systems, used in previous methods, were eliminated in the present technique. Instead, helium was used to carry the electrolytically evolved gases (H_2 and HT) into an oxidation train and also to carry the resulting water over into a collection system, whereafter the activity of the tritium was measured. The method has an accuracy of $\pm$ 6%.

J. O'M. BOCKRIS, S. SRINIVASAN AND M. A. V. DEVANATHAN,
J. Electroanal. Chem., 6 (1963) 205–210.

NULL-POINT POTENTIOMETRIC DETERMINATION OF ZINC

A null-point potentiometric method employing ferrocyanide as titrant has been described for the determination of zinc. The end point in the titration is indicated by balancing the E.M.F. of two half-cells, one containing ferrocyanide–ferricyanide solution and the unknown zinc solution, and the other the same quantity of ferrocyanide–ferricyanide solution and ferrocyanide is complexed by zinc in unknown and standard sufficient standard zinc solution to obtain the balance. Interferences of mineral acids and other metal ions have been studied.

N. K. MATHUR AND C. K. NARANG,
J. Electroanal. Chem., 6 (1963) 211–213.

POLAROGRAPHIC AND pH-METRIC STUDIES ON THE INTERACTION OF LEAD WITH TRANSFUSION GELATIN

Polarographic and pH-metric studies of mixtures containing lead nitrate and transfusion gelatin were undertaken to ascertain how plumbous ions were bound to the protein. Experiments carried out with varying concentrations of the reactants at a fixed ionic strength and under varying pH conditions have shown the existence of a metal–protein complex in the pH range 3.7–5.57. Experiments carried out at a higher pH range (5.9–6.8) gave little or no evidence for the binding of lead to the imidazole groups. An alternative procedure, identical in principle with BJERRUM's method, was employed to calculate V_M from the difference in hydrogen ion concentration data in the presence and absence of metal. Evidence is presented for a one-to-one binding of plumbous ion to the carboxylate ion of tranfusion gelatin, for which the intrinsic association constant was calculated as 1.87 and the free energy change of the combination as $-$ 2.593 kcal.

W. U. MALIK AND M. MUZAFFARUDDIN,
J. Electroanal. Chem., 6 (1963) 214–220.

CHRONOPOTENTIOMETRY WITH CURRENT REVERSAL EFFECT OF THE UNEQUAL FORWARD AND REVERSE CURRENT DENSITIES

The theory of current reversal chronopotentiometry has been extended to take into account unequal forward and reverse current densities. Equations have been derived for the potential–time dependence on the current density ratio for reversible and irreversible re-oxidations. The dependence of the ratio of the reverse to forward transition time current density ratio was established. The time at which the potential is equal to the half-wave potential for the re-oxidation step was shown to depend on the current density ratio and verified experimentally.
A study was made of the irreversible nickel–nickelous system in 1 *M* sodium perchlorate, using the equations derived. A value of $k_{b,h}{}^{\circ}$ equal to $2.74 \cdot 10^{-4}$ cm sec^{-1} at 25°. was calculated for the re-oxidation step and the value of -0.246 V *vs.* N.H.E. established as the formal reduction potential of the $Ni^{2+}-Ni$ system.

D. J. MACERO AND L. B. ANDERSON,
J. Electroanal. Chem., 6 (1963) 221–226.

VOLTAMMETRY OF IRON IN MOLTEN LITHIUM FLUORIDE–POTASSIUM FLUORIDE–SODIUM FLUORIDE

The voltammetry of iron(II) in molten LiF–NaF–KF was investigated over the temperature range 470–545°. The current–voltage curves were recorded using a controlled-potential polarograph and a stationary platinum micro-electrode coupled with a platinum quasi-reference electrode. A third platinum electrode, which was isolated, served as the counter electrode. The reduction of iron(II) to the metal and the oxidation of iron(II) to iron(III) appeared to proceed reversibly under the existing experimental conditions. The limiting current (wave height) of the cathodic wave was proportional to the concentration of iron in the melt. An activation energy of about 12 kcal/mole was calculated for the current limiting process which corresponded to the reduction of iron(II) to the metal.

D. L. MANNING, *J. Electroanal. Chem.*, 6 (1963) 227–233.

THE POLAROGRAPHIC BEHAVIOR OF NICKEL(II) IN ACETONITRILE IN THE PRESENCE OF CHLORIDE ION

In the presence of small amounts of chloride ion, nickel(II) undergoes a two-step reduction in acetonitrile. Analysis of the dependency of the half-wave potential of the first step on the logarithm of the CDMBCl concentration, indicates that this polarographic step involves the reversible reduction of the four nickel-chloride complexes, $NiCl_4^{2-}$, $NiCl_3^-$, $NiCl_2$ and $NiCl^+$, and that these complexes have nearly identical formation constants in acetonitrile *ca.* 0.02 *M* in H_2O. The potential and characteristic of the second step suggest that it involves the reduction of hydrated nickel II) ion. With high concentrations of chloride ion, only one step, corresponding to the first step in the two-step polarograms obtained at low concentrations of chloride, is obtained. The chemistry of the nickel–chloride system in water is undoubtedly governed by a similar equilibrium situation to that in acetonitrile.

I. V. NELSON AND R. T. IWAMOTO,
J. Electroanal. Chem., 6 (1963) 234–241.

VERIFICATION OF THE COULOMETRIC METHOD FOR THE ANALYSIS OF ABSORBED HYDROGEN

A coulometric method of analysis for hydrogen absorbed in palladium was checked against a gas flow method which used a programmed temperature rise for the sample and a thermal conductivity detector. It was found that the amount of hydrogen determined coulometrically was linearly proportional to the amount of hydrogen driven out of the metal thermally.

T. C. FRANKLIN AND N. F. FRANKLIN,
J. Electroanal. Chem., 6 (1963) 242–244.

THE CATALYTIC REDUCTION OF NITRITE IONS DURING POLAROGRAPHIC REDUCTION OF VANADIUM(V)

Enhances limiting currents for the polarographic reduction of vanadium(V) in HN_3–NH_4Cl electrolyte are observed in the presence of nitrite ions. The limiting current is independent of the head of mercury and is proportional to the square root of the nitrite ion concentration. The enhanced current is attributed to the catalytic reduction of nitrite ion, involving the following reactions:

$$V(V) + 3\,e \rightarrow V(II)$$

$$V(II) + NO_2^- \rightarrow V(IV) \text{ (reduction of products of } NO_2^-$$

$$V(IV) + e\,2 \rightarrow (VII)$$

F. BAUMANN, *J. Electroanal. Chem.*, 6 (1963) 245–249.

REPORT FOR DISCUSSION AND COMMENT

RAPPORT DE LA COMMISSION CITCE* "NOMENCLATURE ET DÉFINITIONS ÉLECTROCHIMIQUES" ET DE LA SOUS-COMMISSION IUPAC** "SYMBOLES ET TERMINOLOGIE ÉLECTROCHIMIQUES

PIERRE VAN RYSSELBERGHE
RAPPORTEUR

Departments of Chemistry & Chemical Engineering, Stanford University (Stanford, California, U.S.A.)

(avec la collaboration de RAYMOND DEFAY (Université de Bruxelles), NORBERT IBL (Ecole Polytechnique Fédérale, Zurich), ERICH LANGE (Universität Erlangen)***, EUGÈNE LEWARTOWICZ (Centre National de la Recherche Scientifique, Bellevue-Paris), GIULIO MILAZZO (Istituto Superiore di Sanità, Roma) et GABRIEL VALENSI (Université de Poitiers)).

(Reçu le 12 janvier, 1963)

La Commission CITCE de "Nomenclature et Définitions Electrochimiques", fonctionnant simultanément comme Sous-Commission IUPAC de "Symboles et Terminologie Electrochimiques", présente ci-dessous le Chapitre 6 du rapport de "Nomenclature et Définitions Electrochimiques," dont les Chapitres 1 à 5 ont été publiés, dans leur plus récente forme, aux Electrochimica Acta (vol. 5, pp, 28–53, (1961)) et au Journal of Electroanalytical Chemistry (vol. 2, pp. 265–290 (1961)).

Ce Chapitre 6, intitulé "Cinétique et Polarisation Electrochimiques", est basé sur des discussions ayant eu lieu à Bruxelles en avril 1961, à Montréal en août 1961 et à Rome en septembre 1962. Sous la forme présentée ici il remplace les versions anglaise et française du Chapitre 5 du rapport publié aux Comptes Rendus de la réunion CITCE de 1957 à Paris (Butterworths, Londres, 1959, pp. 176–219).

Ce Chapitre, ainsi que le reste du rapport, sera graduellement amélioré et complété. Une nouvelle version anglaise du rapport entier est prévue pour l'avenir immédiat. Des traductions en d'autres langues seraient souhaitables et sont invitées par la Commission.

* CITCE = Comité International de Thermodynamique et de Cinétique Electrochimiques.
** IUPAC = Union Internationale de Chimie Pure et Appliquée – International Union of Pure and Applied Chemistry.
*** Le Professeur Lange se déclare d'accord avec les points à la discussion desquels il a participé. Sur d'autres points, au moment de la mise sous presse du présent rapport, il nous a fait part d'observations dont il sera tenu compte ultérieurement.

6. CINÉTIQUE ET POLARISATION ÉLECTROCHIMIQUES

6.1 – Au contact des deux phases d'une électrode (ce mot étant pris dans le sens général de la définition 3.1), il existe une région, dite *région interphase*, ayant des propriétés (chimiques, électriques, hydrodynamiques) différentes de celles existant dans les régions profondes des deux phases.

Nous ne considérerons, dans ce qui suit, que des électrodes dont la phase I est métallique (voir 3.2 et 3.18) et dont la symétrie est idéalement plane.

On peut concevoir la décomposition de la région interphase en couches successives à caractères différents, bien qu'il n'y ait pas nécessairement de discontinuités marquées à leurs frontières mutuelles.

La région interphase comporte, de la phase I vers la phase II, une *couche de transfert a–b* (voir diagramme ci-dessous), suivie d'une *couche diffuse b–c*, laquelle est elle-même suivie, lors du passage de courant, d'une *couche de diffusion c–d*. A l'équilibre électrochimique la couche diffuse est suivie de la portion uniforme de la phase II.

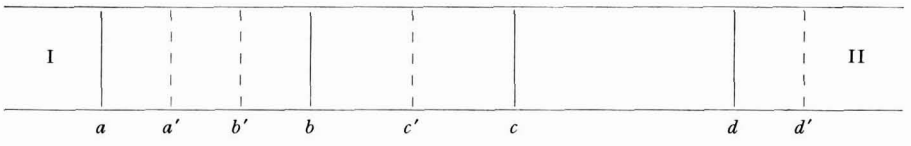

La phase métallique I, notamment quand elle est liquide, peut aussi présenter une couche diffuse (négligeable, vu la conductibilité élevée du métal) et, lors du passage de courant, une couche de diffusion entre la couche de transfert et la portion uniforme de la phase I.

Afin d'assurer autant de clarté que possible, considérons par exemple la réaction

$$X^{x+}(II) + x e^{-}(I) \rightarrow X(I)$$

écrite dans le sens cathodique et pour laquelle la charge réactionnelle zF est négative et égale à $-xF$.

La réaction ci-dessus pourrait également s'écrire (voir 4.5).

$$X^{x+}(II) \rightarrow X^{x+}(I).$$

6.2 – La *couche de transfert a–b* est la couche dont les propriétés sont celles d'une couche d'adsorption et dans laquelle les électrons participent aux réactions d'électrode. Les propriétés de la couche de transfert peuvent présenter des discontinuités.

A l'équilibre les potentiels électrochimiques des divers constituants du système ont les mêmes valeurs en tous points des phases ou couches où ils se trouvent présents. L'indice *équ.* représentant les valeurs d'équilibre, on a:
en a', par exemple:

$$(\tilde{\mu}_{e^-}^{a'})_{équ.} = (\tilde{\mu}_{e^-}^{I})_{équ.}$$

ou:

$$(\mu_{e^-}^{a'} - F\varphi^{a'})_{équ.} = (\mu_{e^-}^{I} - F\varphi^{I})_{équ.}$$

en b', par exemple:

$$(\tilde{\mu}_{X^{x+}}^{b'})_{équ.} = (\tilde{\mu}_{X^{x+}}^{II})_{équ.},$$

ou:

$$(\mu_{x^+}^{b'} + xF\varphi^{b'})_{équ.} = (\mu_{x^+}^{II} + xF\varphi^{II})_{équ.}$$

6.3 – La *couche diffuse b–c* est la portion d'électrolyte ou de solution dans laquelle, tant à courant nul qu'à courant non-nul, il existe en tout point une densité de charge non-nulle et des gradients non-nuls de potentiel électrique et de potentiels chimiques. A l'équilibre on a:
en c', par exemple:

$$(\tilde{\mu}_{x^+}^{c'})_{équ.} = (\tilde{\mu}_{x^+}^{II})_{équ.},$$

avec:

$$(\text{grad}\ \varphi^{c'})_{équ.} = -(\text{grad}\ \mu_{x^+}^{c'})_{équ.}/xF$$

A l'équilibre la différence de potentiel électrique $(\varphi^b - \varphi^c)$ *équ.* est la *tension électrocinétique* ζ, appelée couramment *potentiel électrocinétique.*

Les paragraphes 6.2 et 6.3 ci-dessus complètent les considérations présentées en 3.7.

6.4 – La *couche de diffusion c–d* est la portion d'électrolyte ou de solution dans laquelle, en présence de courant, la composition est différente de celle de la partie profonde de la phase II, les gradients de potentiels électrique et chimique étant sensiblement plus faibles que dans la couche diffuse et la densité de charge électrique étant en tout point pratiquement négligeable ou nulle.

La surface *d* serait située à l'infini en l'absence de toute convection. En pratique, la convection est inévitable et l'emplacement de la surface *d* dépend à la fois de l'intensité du courant, de l'agitation de la solution et des forces naturelles de convection (telles que la pesanteur).

A l'équilibre la surface *d* se confond avec la surface *c*. Toutefois, pour tout courant non-négligeable, l'épaisseur de la couche de diffusion est considérablement plus grande que celle de la couche diffuse.

La surface *c* devrait théoriquement se trouver à distance infinie de *a*, mais se place pratiquement à la distance au-delà de laquelle, vers la droite, la densité de charge électrique peut être considérée comme négligeable.

6.5 – La *double couche électrochimique* est formée, même en présence de courant, de la couche de transfert et de la couche diffuse, à l'exclusion de la couche de diffusion. C'est donc seulement la portion de la région interphase où les charges électriques locales ne sont pas nulles, la densité de charge variant avec la distance à *a*.

6.6 – La *tension électrique d'une électrode traversée par un courant* doit être considérée comme le potentiel électrique du métal I diminué de celui de la solution à l'extrémité *d* de la couche de diffusion.

Ainsi qu'il a été expliqué en 4.14, la tension électrique relative d'une électrode est égale à la tension électrique d'une *cellule tensiométrique* auxiliaire, non-parcourue par le courant, dans laquelle l'électrode étudiée correspond aux phases de gauche, 1/2, et l'électrode de référence aux phases de droite, 3/4, de cette cellule tensiométrique.

Cette grandeur n'est elle-même expérimentalement accessible que d'une manière approchée à cause de l'impossibilité de placer en *d* l'extrémité du capillaire de Haber-Luggin nécessaire à la mesure. Cette extrémité est en effet placée en *d'* dans la région uniforme II et il est difficile de connaître exactement la chute ohmique entre *d'* et *d*.

6.7 – La *couche de diffusion de Nernst* est une couche stylisée qui répond à l'image suivante:

Le nombre de moles d'ion X^{z+} provenant de la phase II qui entrent par unité de temps dans l'unité de surface de la couche de transfert est $-i/xF$, où i désigne la densité de courant (voir 6.12). En l'absence pratique d'effet de champ électrique, en particulier quand un électrolyte indifférent (dit *électrolyte-support*) est présent en grand excès, on considère le flux de diffusion pure équivalent au flux réel précédent et qui aurait lieu dans une couche fictive d'épaisseur δ où la concentration varierait linéairement depuis $C^{II}_{X^{z+}}$ jusqu'à la concentration $C^{e}_{X^{z+}}$ qui existe au contact de la couche diffuse. Cette épaisseur δ est donc définie par l'équation

$$-i/xF = D_{X^{z+}} \cdot (C^{II}_{X^{z+}} - C^{e}_{X^{z+}})/\delta$$

(voir loi de Fick, 2.9(c)), où le coefficient de diffusion $D_{X^{z+}}$ est pris égal à sa valeur au sein de la solution.

Dans le cas fréquent d'une espèce réductible X^{z+}, dont la concentration stationnaire au contact de la couche diffuse peut être considérée comme nulle, on a:

$$\delta_l = D_{X^{z+}} \cdot C^{II}_{X^{z+}}/(-i_l/xF)$$

où l'indice l se rapporte au *courant limite* (voir 6.24).

6.8 – Lorsqu'une réaction d'électrode donnée transfère une charge positive au métal de l'électrode, le courant correspondant est désigné comme étant *cathodique* et la réaction elle-même est dite *cathodique* ou *de réduction*. Lorsque cette réaction transfère une charge négative au métal, le courant correspondant est désigné comme étant *anodique* et la réaction elle-même est dite *anodique* ou *d'oxydation*.

Dans les systèmes métal-solution les courants anodiques sont positifs et les courants cathodiques sont négatifs. L'inverse sera le cas dans les systèmes solution-métal.

6.9 – A une électrode simple (voir 3.17(a)), le courant correspondant à la réaction d'électrode ou *courant réactionnel* est la somme algébrique d'une composante anodique et d'une composante cathodique traversant simultanément la couche de transfert dans des sens opposés.

6.10 – A l'équilibre électrochimique les composantes anodique et cathodique du courant réactionnel dans la couche de transfert sont égales en valeur absolue. Cette valeur absolue commune des deux composantes est appelée *courant d'échange de transfert* ou, en abrégé, *courant d'échange*.

6.11 – A une polyélectrode (voir 3.17(b)), le courant total est la somme des *courants réactionnels* qui correspondent aux diverses réactions d'électrode. Chaque courant

réactionnel est la somme algébrique d'une composante anodique et d'une composante cathodique traversant simultanément la couche de transfert dans des sens opposés.

6.12 – Dans le présent rapport on appellera *densité de courant réactionnel* d'une réaction d'électrode ayant lieu à une électrode simple ou *densité de courant réactionnel partiel* d'une réaction d'électrode ayant lieu à une polyélectrode le courant ou le courant partiel de la réaction divisé par *l'aire apparente* de la surface de l'électrode à laquelle la réaction a lieu.

6.13 – La *vitesse d'une réaction d'électrode par unité de surface* ou *densité de vitesse réactionnelle électrochimique* est égale à la densité de courant ou de courant partiel de cette réaction divisée par la charge réactionnelle.

6.14 – Aux composantes anodique et cathodique du courant réactionnel dans la couche de transfert (voir 6.9) correspondent semblablement (voir 6.13) des *densités de vitesses réactionnelles anodique et cathodique* de transfert.

6.15 – Lorsque les densités définies en 6.14 sont divisées par les concentrations des espèces réagissantes aux seins des phases I ou II, on obtient les *constantes de vitesses réactionnelles anodique et cathodique* de transfert. (Ces concentrations sont, éventuellement, élevées aux puissances requises par l'ordre de la réaction.)

Pour l'analyse du mécanisme réactionnel les densités définies en 6.14 sont, dans certains cas, divisées par les concentrations en c ou en b ou ailleurs (voir diagramme de la définition 6.1) et les constantes de vitesses sont modifiées de manière correspondante.

Les unités des diverses grandeurs en jeu ici sont reliées par les formules dimensionnelles suivantes (voir 3.8 pour la définition de l'avancement d'une réaction):

$$\begin{aligned}(\text{densité de courant}) &= (\text{charge réactionelle}) \times (\text{avancement}) \times (\text{longueur})^{-2} \times (\text{temps})^{-1} \\ &= (\text{charge}) \times (\text{longueur})^{-2} \times (\text{temps})^{-1}, \\ (\text{densité de vitesse réactionnelle}) &= (\text{avancement}) \times (\text{longueur})^{-2} \times (\text{temps})^{-1} \\ &= (\text{constante de vitesse}) \times (\text{concentration})^{n}.\end{aligned}$$

A température et pression données ces constantes de vitesses réactionnelles électrochimiques dépendent des tensions électriques entre I et II ou, éventuellement, entre les limites de la portion considérée de la région interphase. Elles comprennent les coefficients d'activité des réactifs et du complexe activé et ne sont donc pas nécessairement indépendantes de la composition.

6.16 – On appelle qualitativement *polarisation* l'ensemble des effets du passage de courant qui rendent la tension électrique d'une électrode (ou celle d'une cellule galvanique) différente de sa valeur sous courant total nul.

Quantitativement la *polarisation d'une cellule* désigne sa tension électrique lors du passage de courant diminuée de sa valeur sous courant total nul.

Pour une électrode métal-solution on peut considérer comme "polarisation expérimentale" la mesure approchée de la tension électrique de cette électrode (non-dépouillée de la chute ohmique dans la région uniforme) diminuée de sa valeur sous

courant total nul. Elle est dite *anodique* quand sa valeur est positive et *cathodique* quand sa valeur est négative.

La polarisation électrochimique dont il est question ici ne doit évidemment pas être confondue avec la polarisation diélectrique.

6.17 – Lorsque, à densité de courant donnée, une électrode est le siège d'une réaction déterminée et unique, sa *surtension*, à un instant donné, est égale à la tension électrique relative de l'électrode à cet instant, diminuée de la tension électrique relative réversible correspondant à cette réaction. Cette tension électrique réversible ou d'équilibre est celle que possède l'électrode à l'équilibre électrochimique et pour le même état chimique aux seins des phases que celui correspondant à l'instant pour lequel la surtension est évaluée.

Dans le cas de l'électrode simple considérée ci-dessus la "polarisation expérimentale" ne diffère de la surtension que par le terme ohmique mentionné en 6.6.

Pour une électrode métal-solution la *surtension* et la *tension électrochimique* sont identiques en grandeur et en signe.

6.18 – Si plusieurs réactions d'électrode ayant des tensions électriques réversibles distinctes ont lieu simultanément à la même électrode, la tension électrique de cette électrode est appelée *tension électrique mixte*.

Dans de nombreux cas les réactions ayant lieu à une électrode ne sont pas connues. On appellera alors la tension mixte sous courant, diminuée de la tension mixte sous courant total nul, *excès de tension*.

La polarisation expérimentale ne diffère de l'excès de tension que par le terme ohmique mentionné en 6.6.

6.19 – Lorsqu'une électrode est le siège de plusieurs réactions d'électrode simultanées, on peut évaluer une *surtension* par rapport à la tension électrique réversible de chacune de ces diverses réactions.

6.20 – (a) – En régime stationnaire on appelle *résistance de surtension de l'unité de surface* le quotient de la surtension par la densité de courant ou de courant partiel correspondant à la réaction envisagée. On appelle *résistance d'excès de tension de l'unité de surface* le quotient de l'excès de tension par la densité de courant.
(b) – La *résistance différentielle de l'unité de surface*, pour une réaction d'électrode, est la dérivée de la surtension stationnaire par rapport à la densité de courant correspondante.

6.21 – La *surtension* η d'une électrode métal-solution I/II étant identique à sa *tension électrochimique* (voir 6.17), on a, la charge négative $-xF$ allant de I vers II pour la réaction écrite en 6.1:

$$\eta = \tilde{A}/zF = -\tilde{A}/xF$$

L'affinité électrochimique $\tilde{A}$ de la réaction d'électrode est donnée par:

$$\tilde{A} = \tilde{\mu}^{II}_{X^{z+}} + x\tilde{\mu}^{I}_{e^-} - \mu^{I}_{X}$$

expression que nous pouvons décomposer en les trois termes suivants:

$$\tilde{A}^{dc} = \tilde{\mu}^{II}_{x^{x+}} - \tilde{\mu}^{c}_{x^{x+}}$$

$$\tilde{A}^{cb} = \tilde{\mu}^{c}_{x^{x+}} - \tilde{\mu}^{b}_{x^{x+}}$$

$$\tilde{A}^{ba} = \mu^{b}_{x^{x+}} + x\tilde{\mu}^{I}_{e^-} - \mu^{I}_{x}$$

Nous avons alors les trois contributions suivantes à la surtension totale:

$$\eta^{cd} = \tilde{A}^{dc}/F = -\tilde{A}^{dc}/xF = (\mu^{II}_{x^{x+}} - \mu^{c}_{x^{x+}})/(-xF) + \varphi^{c} - \varphi^{d}$$

$$\eta^{bc} = \tilde{A}^{cb}/zF = -\tilde{A}^{cb}/xF = (\mu^{c}_{x^{x+}} - \mu^{b}_{x^{x+}})/(-xF) + \varphi^{b} - \varphi^{c}$$

$$\eta^{ab} = \tilde{A}^{ba}/zF = -\tilde{A}^{ba}/xF = (\mu^{b}_{x^{x+}} + x\mu^{I}_{e^-} - \mu^{I}_{x})/(-xF) + \varphi^{a} - \varphi^{b}.$$

La première, η^{cd}, est la *surtension de diffusion électrochimique*. Elle comprend un terme de diffusion:

$$\eta_D = (\mu^{II}_{x^{x+}} - \mu^{c}_{x^{x+}})/(-xF) = (RT/xF) \cdot \ln(a^{c}_{x^{x+}}/a^{II}_{x^{x+}}),$$

ou, en présence d'un électrolyte-support de concentration suffisante:

$$\eta_D = (RT/xF) \cdot \ln(C^{c}_{x^{x+}}/C^{II}_{x^{x+}})$$

et un terme électrique $\varphi^{c} - \varphi^{d}$.

La deuxième, η^{bc}, correspondant à la couche diffuse, est mal connue, mais probablement négligeable en présence d'un électrolyte-support de concentration suffisante.

La troisième, η^{ab}, correspondant à la couche de transfert, est la *surtension de transfert*. Dans le cas étudié ici elle est encore appelée *surtension d'activation*.

6.22 – Lorsque la surtension de diffusion électrochimique est négligeable, la surtension d'une réaction d'électrode, au-delà d'un seuil de l'ordre de quelques millivolts, est souvent une fonction linéaire du logarithme de la valeur absolue de la densité de courant. Une telle relation est appelée *loi de Tafel*. On écrit alors, pour le cas anodique et le cas cathodique respectivement:

$$\eta_a = a_a + b_a \cdot \ln i \qquad \text{et} \qquad |\eta_c| = a_c + b_c \cdot \ln |i|.$$

On admet généralement que ces relations s'appliquent à la composante anodique i_a et à la composante cathodique i_c de la densité de courant résultante $i = i_a - |i_c|$, même au voisinage de l'équilibre. On a alors, à la tension électrique $U_{\text{rév.}} + \eta$ commune aux deux composantes:

$$\eta = a_a + b_a \cdot \ln i_a \qquad \text{et} \qquad -\eta = a_c + b_c \cdot \ln |i_c|.$$

Lorsque η est positif et suffisamment grand, $|i_c|$ devient négligeable devant i_a et la

valeur de i tend vers i_a. Lorsque η est négatif et suffisamment grand en valeur absolue, i_a devient négligeable devant $|i_c|$ et la valeur de i tend vers i_c. On a:

$$i = i_a - |i_c| = \exp\left(\frac{\eta - a_a}{b_a}\right) - \exp\left(\frac{-\eta - a_c}{b_c}\right).$$

Puisque $i = 0$ lorsque $\eta = 0$, on doit avoir:

$$a_a/b_a = a_c/b_c = -\ln i_0$$

où i_0 désigne la valeur absolue du *courant d'échange* (voir 6.10).
Posons:

$$b_a = RT/\beta_a F \quad \text{et} \quad b_c = RT/\beta_c F$$

La densité de courant s'écrit alors:

$$i = i_0 [\exp(\beta_a F\eta/RT) - \exp(-\beta_c F\eta/RT)$$

Notons que les coefficients β_a et β_c multiplient l'affinité électrochimique divisée par le nombre de charges élémentaires transportées ($\bar{A}/z = zF\eta/z = F\eta$).

6.23 – Si l'on envisage la réaction dont la couche de transfert est le siège comme une succession d'étapes élémentaires, le *nombre stoechiométrique* de chacune de ces étapes est le nombre de fois qu'elle joue quand la réaction globale joue une fois. Lorsque l'une de ces étapes est seule régulatrice, il peut être utile de mettre les coefficients β_a et β_c sous les formes:

$$\beta_a = (|z|/\nu) \cdot \alpha_a \quad \text{et} \quad \beta_c = (|z|/\nu) \cdot \alpha_c$$

dans lesquelles ν désigne le nombre stoechiométrique de cette étape régulatrice. Les coefficients α_a et α_c sont alors appelés *coefficients de transfert.*

A titre d'example et sans discuter la valeur des hypothèses, envisageons seulement les deux mécanismes (respectivement dits *de Volmer* et *de Tafel*) interprétant la décharge de l'ion hydrogène H^+.

La réaction d'électrode étant écrite:

$$2\ H^+ + 2\ e^- \rightarrow H_2,$$

ce qui correspond à $z = 2$, les étapes élémentaires que l'on suppose localisées dans la couche de transfert seraient:

$$H^+ + e^- \rightarrow H \text{ (adsorbé)}$$

$$2\ H \text{ (adsorbés)} \rightarrow H_2$$

La première étape joue deux fois et la seconde une fois quand la réaction globale joue une fois. Leurs nombres stoechiométriques sont donc respectivement 2 et 1.

Le mécanisme dit de Volmer suppose la première régulatrice. On aurait donc $\nu = 2$. L'expérience donnant d'autre part, avec certains métaux, $\beta_c = 0.5$ environ, il en résulte que le coefficient de transfert α_c est aussi égal à 0.5 environ.

Le mécanisme dit de Tafel suppose la seconde étape régulatrice. On aurait donc $\nu = 1$. L'expérience donnant d'autre part, avec d'autres métaux, $\beta_c = 2$ environ, il en résulte que le coefficient de transfert α_c est maintenant égal à 1 environ.

6.24 – Si, dans la courbe qui représente la densité de courant en fonction de la tension électrique appliquée, cette densité atteint une valeur qui ne peut être dépassée

sans changer la réaction d'électrode, cette valeur est appelée la densité de *courant limite* de cette réaction. Elle correspond à la vitesse maximale du transport de matière lié à cette réaction, dans des conditions expérimentales données (régime hydrodynamique, concentration au sein de la solution, etc).

Dans le cas où une espèce dissoute est consommée dans la réaction d'électrode (cas du dépôt d'un métal, par exemple, en présence d'un électrolyte-support), le courant limite est atteint lorsque la concentration de cette espèce devient négligeable en c (voir 6.1 et 6.6).

6.25 – Une *électrode simple* est dite *réversible* lorsque toute surtension, si petite soit-elle, s'accompagne d'un courant stationnaire *non-nul*.

Si, au contraire, une petite surtension ne provoque aucun courant stationnaire, l'électrode est dite *indifférente*.

En pratique, la distinction entre une électrode réversible et une électrode indifférente est graduelle et se situe différemment suivant les valeurs minimales décelables des surtensions et des densités de courant.

Du point de vue cinétique, l'évaluation des courants d'échange à l'équilibre permet d'estimer le degré de réversibilité d'une électrode: plus les courants d'échange sont grands, plus l'électrode s'approche de la réversibilité.

Du point de vue thermodynamique, une électrode simple réversible est une électrode dont l'équilibre électrochimique est un *équilibre véritable*, tandis qu'une électrode simple indifférente est une électrode susceptible de demeurer dans un état de faux équilibre sans passage de courant.

Il y a lieu de remarquer que, dès que la densité de courant totale est différente de zéro, l'électrode réversible devient le siège de *phénomènes irréversibles*, comme c'est le cas pour tout système qui évolue hors de son état d'équilibre.

6.26 – Pour une *polyélectrode* la réversibilité doit être considérée relativement à chacune des réactions possibles à cette électrode.

Une polyélectrode est réversible relativement à une réaction d'électrode lorsque, en portant la tension électrique à une valeur très peu différente de la tension électrique d'équilibre de cette réaction, on provoque l'avancement de cette réaction avec une vitesse *non-nulle*.

Une polyélectrode peut être *réversible* relativement à une réaction et *indifférente* relativement à une autre réaction.

Par exemple, une électrode de platine poli plongée dans une solution contenant des ions H^+, Fe^{2+}, Fe^{3+}, etc. peut être réversible relativement à la réaction

$$Fe^{2+} \rightarrow Fe^{3+} + e^-$$

et indifférente relativement à la réaction

$$2\,H^+ + 2\,e^- \rightarrow H_2.$$

Finalement, dans un intervalle limité de tension électrique appliquée, une polyélectrode peut être indifférente relativement à toutes les réactions éventuellement possibles à cette électrode.

6.27 – La tension électrique relative d'une électrode simple pour laquelle la densité d'un courant de polarisation anodique est égale à la sensibilité de sa propre mesure (par exemple 10^{-8} amp./cm^2) peut être appelée *tension électrique d'oxydation* pour la sensibilité spécifiée.

La tension électrique d'une électrode simple pour laquelle la densité d'un courant de polarisation cathodique est égale à la sensibilité de sa propre mesure peut être appelée *tension électrique de réduction* pour la sensibilité spécifiée.

Dans le cas d'une électrode simple indifférente (voir 6.25), la tension électrique d'oxydation ainsi définie est plus élevée et la tension électrique de réduction ainsi définie est plus basse que la tension électrique réversible théorique de cette électrode simple.

Dans le cas limite d'une électrode simple réversible (voir 6.25), les tensions électriques d'oxydation et de réduction correspondant à un courant décelable minimum coïncident. Leur valeur commune est alors la *tension électrique d'oxydoréduction* ou *tension électrique rédox*, laquelle est donc alors une tension électrique réversible ou d'équilibre.

Ces définitions s'appliquent également à chacune des réactions d'une polyélectrode.

ELECTROCHEMICAL BEHAVIOUR OF NITROSOBENZENE IN DIMETHYLFORMAMIDE

W. KEMULA AND R. SIODA

Institute of Physical Chemistry, Polish Academy of Sciences, Warsaw (Poland)

(Received May 23th, 1963)

Nitrosobenzene is reduced in two polarographic waves in 0.2 N $NaNO_3$ in dimethylformamide[1,2]. The first reduction wave is slightly irreversible, as follows from the slope (0.075) of the line on the E_d *vs.* log $i/(i_d - i)$ diagram. A certain degree of irreversibility can also be inferred from the cyclic chrono-voltamperometric curves on the hanging mercury electrode, for nitrosobenzene[2]. On the other hand by using oscillopolarography with a frequency of 5 c/sec we obtained at the potentials of the first reduction wave of nitrosobenzene, a reduction–oxidation system corresponding to the reduction of nitrosobenzene and the oxidation of the reduction product (Fig. 2A). During electrolyses of solutions of nitrosobenzene on the mercury pool cathode at potentials corresponding to the potentials of the diffusion current of the first reduction wave of nitrosobenzene in 0.2 N $NaNO_3$ in dimethylformamide, the first polarographic

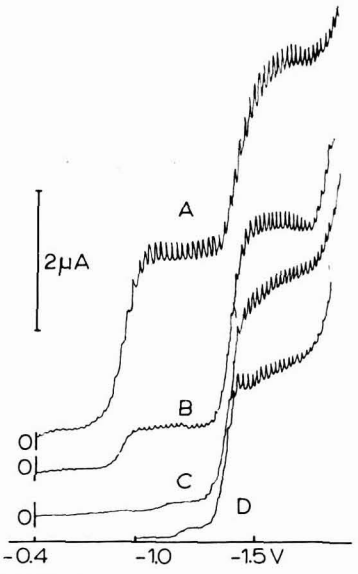

Fig. 1. Polarograms in 0.2 N $NaNO_3$ in dimethylformamide: (A), $1 \cdot 10^{-3}$ M nitrosobenzene before electrolysis; (B), after partial electrolysis; (C), at end of the electrolysis; (D), $3.5 \cdot 10^{-4}$ M azoxybenzene. Potentials *vs.* S.C.E.

reduction wave decayed completely after passing a charge of less than 1 electron per molecule of nitrosobenzene through the solution. No distinct anodic polarographic current of oxidation of stable free radical anions was obtained, contrary to the behaviour of nitrobenzene[2]. After a prolonged electrolysis there remained a second

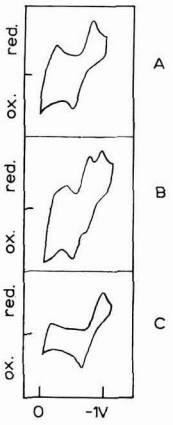

Fig. 2. Oscillograms: (A), $2.0 \cdot 10^{-4}$ *M* soln. of nitrosobenzene in 0.2 *N* $NaNO_3$ in dimethylformamide; (B), as (A), but containing a little of oxygen from the air; (C), $3.0 \cdot 10^{-4}$ *M* soln. of nitrobenzene in 0.2 *N* $NaNO_3$ in dimethylformamide. Oscillopolarograms were made using the hanging mercury drop electrode[4]. Frequency 5 c/sec. Potentials measured against aqueous S.C.E.

polarographic wave at a potential $E_{1/2} = -1.34$ V *vs.* S.C.E., similar to the reduction wave of azoxybenzene in dimethylformamide (Fig. 1). The absorption spectrum of the solution at the end of the electrolysis did not show maxima of nitrosobenzene at 283 mμ and 307 mμ, but a new absorption maximum appeared at 323 mμ, identical with the absorption maximum of azoxybenzene. If trace amounts of oxygen penetrated in to the electrolytical cell during electrolysis, an additional small reduction wave at $E_{1/2} = -1.01$ V *vs.* S.C.E., similar to the first reduction wave of nitrobenzene, was recorded on the polarogram of the solution after the electrolysis. The light absorption of the solution was increased at wavelengths between 260 and 300 mμ, where the absorption maximum of nitrobenzene occurs (260 mμ). This has previously been described by us[2]. The small reduction wave at $E_{1/2} = -1.01$ V did not form, when we used very pure hydrogen, specially purified from traces of oxygen by means of a special catalytic apparatus[3], for de-aerating and mixing the electrolysed solution.

The formation of nitrobenzene could also be observed during the oscillopolarographic investigation of a solution of nitrosobenzene containing a small quantity of oxygen from the air. There appeared then a secondary, reversible redox system of nitrobenzene as well as the original system of nitrosobenzene (Fig. 2B). Oxygen is

reduced irreversibly and does not give a distinct reduction peak under these conditions. The formation of nitrobenzene from nitrosobenzene takes place on the surface of the electrode during the electrochemical process and not directly from nitrosobenzene and oxygen in the bulk of solution.

Taking into account the two-stage reduction of nitrosobenzene in 0.2 *N* $NaNO_3$ in dimethylformamide, and also the reversibility of oscillopolarographic reduction and oxidation of nitrosobenzene, (where the original reduction product can be re-oxidised before it undergoes secondary reactions), we assumed that, at the potential of the first reduction wave of nitrosobenzene, the free radical anion C_6H_5—NO^- was formed[1]. From the slight irreversibility of the first wave and also from the results of prolonged electrolysis, it follows that such a free radical anion is unstable[2]. It is known, that nitrosobenzene easily reacts with free radicals. We assume that the free radical anion of nitrosobenzene can react with a molecule of nitrosobenzene or another such free radical anion, and that azoxybenzene is the final product of a not yet fully known radical reaction.

The formation of nitrobenzene during the electrochemical reduction of a solution of nitrosobenzene in the presence of oxygen can also be interpreted as a radical reaction in which the attacking reagent would be the nitroso-benzene free radical anion or possibly molecular oxygen anion.

Oxygen is reduced in 0.2 *N* $NaNO_3$ in dimethylformamide in two irreversible polarographic waves at $E_{1/2} = -0.63$ V and $E_{1/2} = -1.62$ V *vs.* S.C.E. Because of the more positive potential of the first reduction wave of oxygen than the first reduction wave of nitrosobenzene ($E_{1/2} = -0.81$ V), the formation of nitrobenzene can be preceded by transference of the electron from the nitrosobenzene free radical anion to O_2 with formation of a molecular oxygen anion, which then reacts with nitrosobenzene to give nitrobenzene. The transference of the electron and the reaction can be simultaneous. It may also be that the unstable molecular oxygen anion, formed probably as the primary electrode reduction product in the first reduction wave of oxygen in dimethylformamide, can react with nitrosobenzene or its free radical anion with formation of nitrobenzene.

Summarizing, we assume that in the first reduction wave of nitrosobenzene in 0.2 *N* $NaNO_3$ in dimethylformamide, the free radical anion C_6H_5—NO^- is formed primarily. This free radical anion is unstable and reacts with a molecule of nitrosobenzene or maybe with another such free radical anion and the result of the radical reaction is azoxybenzene. This instability of the nitrosobenzene free radical anion causes the slight irreversibility of the first reduction wave of nitrosobenzene. The second reduction wave of nitrosobenzene in 0.2 *N* $NaNO_3$ in dimethylformamide has a complex character. The free radical anion of nitrosobenzene may add a second electron with formation of C_6H_5—NO^{2-}, which may abstract protons from the dimethylformamide. At the same time because of a sufficiently negative potential, azoxybenzene formed on the drop by the reactions of mono-negative free radical anions (C_6H_5—NO^-), may also be reduced.

SUMMARY

Nitrosobenzene is reduced in a solution of 0.2 *N* $NaNO_3$ in dimethylformamide in two polarographic waves. In the first reduction wave the free radical anions of nitrosobenzene form primarily. The free radical anions are unstable and react with formation

of azoxybenzene as a final product. This was ascertained by means of controlled potential electrolysis at the potential of the first reduction wave of azoxybenzene. Nitrobenzene is formed during simultaneous electrochemical reduction of oxygen and nitrosobenzene in a solution of 0.2 *N* $NaNO_3$ in dimethylformamide. This was ascertained by means of electrolysis and also by oscillopolarography.

REFERENCES

1 W. KEMULA AND R. SIODA, *Bull. Acad. Polon. Sci., Ser. Sci. Chim.*, 10 (1962) 107.
2 W. KEMULA AND R. SIODA, *Bull. Acad. Polon. Sci., Ser. Sci. Chim.*, 10 (1962) 507.
3 W. KEMULA AND R. SIODA, *Chem. Anal. (Warsaw)*, 8 (1963) 629.
4 W. KEMULA AND Z. KUBLIK, *Anal. Chim. Acta*, 18 (1958) 104.

TRANSIENTS IN CONVECTIVE SYSTEMS

I. THEORY OF GALVANOSTATIC, AND GALVANOSTATIC WITH CURRENT REVERSAL TRANSIENTS, AT A ROTATING DISC ELECTRODE

J. M. HALE

Royal Aircraft Establishment, Farnborough, Hants (England)

(Received May 24th, 1963)

INTRODUCTION

Although the measurement of a transition time, the time required to reduce to zero the surface concentration of a reacting species during galvanostatic polarisation of an electrode, is a familiar experimental technique in unstirred solutions, its application in stirred systems has been neglected due to the lack of a theoretical interpretation. In principle however, transient phenomena induced in the presence of a well defined convective regime, should be more meaningful than analogous experiments under quiescent conditions because natural convention interferes with the supply of reactant to the electrode surface. Furthermore, transition times are longer in the stirred system, other parameters being equal, and are therefore measured more accurately.

Theoretical analysis of the boundary value problem for a rotating disc electrode appropriate to this technique, was first undertaken by LEVICH[1], but his solution may be shown to apply only to the first milliseconds of electrolysis. In a recent re-examination of the problem, SIVER[2] derived an approximate solution, and claimed agreement with experiment. His method was an analytic one, and his formulation in fact identical with that treated much earlier by ROSEBURGH AND LASH-MILLER[3a], and by MCKAY[3b], in an entirely different application. The purpose of this paper, is to derive a numerical solution of the complete problem, to examine the meaing and effectiveness of SIVER's approximation, and to propose means of analysis of the experimental datum into kinetic parameters.

The case of galvanostatic transients with current reversal is also discussed, and a table is appended which enables the elucidation of diffusion parameters from experimental results.

THE BOUNDARY VALUE PROBLEM

The concentration of reacting species C, satisfies the one-dimensional convective diffusion equation:

$$\frac{\partial C}{\partial t} = D\frac{\partial^2 C}{\partial x^2} - V\frac{\partial C}{\partial x}$$

in which D is the diffusion coefficient, V is the velocity vector—a function of position, but not of time in the case of a hydrodynamic steady state — and t and x are the in-

dependent time and distance variables respectively. Initially there is a uniform distribution of concentration throughout the solution,

$$C = C^b \quad \text{at} \quad t = 0$$

and one assumes electrolysis to continue only for short times, such that the bulk concentration is unaffected

$$C = C^b \quad \text{at} \quad x \to \infty$$

The galvanostatic condition at the electrode, taken as the origin of the one-dimensional system, can be interpreted as a constant gradient of reacting species, (in the presence of an excess of an indifferent electrolyte), because the fluid is stationary with respect to the electrode at this point.
Therefore

$$\frac{\partial c}{\partial x} = \frac{I}{nFAD} \quad \text{at} \quad x = 0$$

where I/A is the constant current density, F the Faraday, and n the number of electrons involved in unit reaction. There is a convenient substitution

$$\psi = \int_0^x \exp\left\{\int \frac{V}{D}\,dx\right\} dx$$

which transforms the problem into the finite domain $0 \leqslant \psi \leqslant \delta$, where

$$\delta = \int_0^\infty \exp\left\{\int \frac{V}{D}\,dx\right\} dx$$

may be demonstrated to have the properties of the *thickness of the diffusion layer*, of classical NERNST[4] diffusion theory. δ was first introduced by LEVICH[5] in connection with steady state applications of the rotating disc electrode. He used COCHRAN'S[6] asymptotic solution, for the velocity vector of fluid stirred by the disc, at low values of x

$$\frac{V}{D} = -\frac{3x^2}{(\delta')^3} + \cdots$$

where

$$\delta' = 1.82\left(\frac{D}{\nu}\right)^{1/3}\sqrt{\frac{\nu}{\omega}}$$

ω is the rotation speed of the disc, in radians/sec, and ν is the kinematic viscosity.
Hence

$$\delta = \delta' \int_0^\infty e^{-t^3}\,dt = 0.893\,\delta'$$

and

$$\psi = \delta' \int_0^x e^{-t^3}\,dt = \frac{\delta'}{3}\int_0^x e^{-u}\,u^{-2/3}\,du$$

The integral

$$\Gamma_x(1 + p) = \int_0^x e^{-u} u^p \, du$$

is the incomplete Gamma function of argument p, and has been tabulated as a function of x by PEARSON[7], in the form

$$I(r, p) = \frac{\int_0^r e^{-u} u^p \, du}{\int_0^\infty e^{-u} u^p \, du} = \frac{\int_0^x \sqrt{1+p} \, e^{-u} u^p \, du}{\Gamma(1 + p)}$$

The denominator is the complete Gamma function of argument p.

Evidently $I(x, -2/3) = z = \psi/\delta$, which gives a convenient relationship between ψ and x. In terms of the new variable ψ, the diffusion equation and its associated boundary conditions take the form

$$\frac{\partial C}{\partial t} = D \frac{\partial^2 C}{\partial \psi^2} \left(\frac{d\psi}{dx}\right)^2 \tag{1}$$

$$C = C^b \quad \text{at} \quad t = 0, \quad C = C^b \quad \text{at} \quad \psi = \delta$$

and

$$\frac{\partial C}{\partial \psi} = \frac{I}{nFAD} \quad \text{at} \quad \psi = 0$$

The coefficient $(d\psi/dx)^2$ is a slowly varying function of x, and renders the differential equation insoluble by an analytic route. It is plotted against the parameter $z = \psi/\delta$

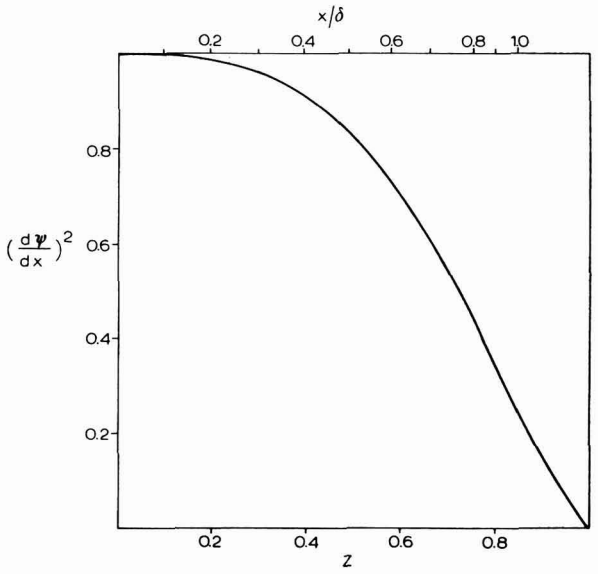

Fig. 1

in Fig. 1. z was determined as a function of x, by interpolation within PEARSON's table to $p = -2/3$, using EVERETT's[8] method; then $(\mathrm{d}\psi/\mathrm{d}x)^2$, calculated at the same values of x, was interpolated at convenient values of z, by application of NEWTON's[9] divided difference formula. The relationship between z and x/δ is indicated on the abscissa of Fig. 1, from which it may be seen that $x = \delta$ at $z \simeq 0.85$.

SIVER's approximation to the present problem, is equivalent to the neglect of the variation in this coefficient throughout the range of x; *i.e.*, he makes $(\mathrm{d}\psi/\mathrm{d}x)^2 = 1$. Then, the solution is required of a simple diffusion problem in a finite domain, and may be found by Laplace transformation or otherwise. The surface concentration according to this approximation is:

$$C(o) = C^b - \frac{I\delta}{nFAD} F\left(\frac{\pi^2 \mathrm{D}t}{4\delta^2}\right) \tag{2}$$

where

$$F(v) = 1 - \frac{8}{\pi^2} \sum_{n=1}^{\infty} \frac{1}{(2n-1)^2} \exp\left[-(2n-1)^2 v\right]$$

$F(v)$ was tabulated by MCKAY[3b] for the range $0 \leqslant v \leqslant 3.59$.

The physical implication of this approximation, in neglecting the attenuation of the rate of concentration change at the outside of the diffusion layer, is to underestimate the supply of reactant by convection. It must predict shorter values of the transition time than those observed in practice. From eqn. (2) and MCKAY's table, it follows that

$$0 \leqslant \tau \leqslant 3.5 \frac{4\delta^2}{\pi^2 D}$$

for the transition times must fall within the range of variation of $F(v)$. Experimental values outside this range have indeed been observed[10].

Since there is no means of removing the approximation $(\mathrm{d}\psi/\mathrm{d}x)^2 = 1$ whilst retaining the analytic method of solution, resort has to be made to a purely numerical method. Fortunately in the present case, only advantage results, for the form of presentation of the solution can be arranged identically with the analysis considered.

Of the available methods, the CRANK–NICHOLSON[11] difference representation was chosen for stability and accuracy. Some preliminary rearrangement of the problem into dimensionless variables is effected as follows:

$$y = \frac{nFADC^b}{\delta I} \cdot \frac{(C - C^b)}{C^b}; \quad z = \frac{\psi}{\delta}; \quad \theta = \frac{Dt}{\delta^2}$$

Then

$$\frac{\partial y}{\partial \theta} = \left(\frac{\mathrm{d}\psi}{\mathrm{d}x}\right)^2 \frac{\partial^2 y}{\partial z^2} \qquad 0 \leqslant z \leqslant 1$$

$$\frac{\partial y}{\partial z} = 1 \quad \text{at} \quad z = 0, \quad y = 0 \quad \text{at} \quad z = 1, \quad y = 0 \quad \text{at} \quad \theta = 0.$$

The difference equivalent of the diffusion equation is:

$$\frac{2(\Delta z)^2}{a_l^2(\Delta\theta)} (y_l - y_k) = y_{l+1} - 2y_l + y_{l-1} + y_{k+1} - 2y_k + y_{k-1}.$$

Here a_l^2 represents the value of $(\mathrm{d}\psi/\mathrm{d}x)^2$ at the point l and is independent of time. l refers to a point in the range of z in the *current* time line, and k, to the same point in the *previous* time line. This equation may be expressed:

$$y_{l-1} - \pi_l y_l + y_{l+1} = b_l$$

where

$$\pi_l = 2 + \frac{2(\Delta z)^2}{a_l^2(\Delta\theta)}$$

$$b_l = -y_{k+1} + \left(2 - \frac{2(\Delta z)^2}{a_l^2(\Delta\theta)}\right) y_k - y_{k-1}$$

The two additional equations required for solution are provided by the boundary conditions, namely,

$$y_2 - y_o = 2(\Delta z) \quad \text{and} \quad y_n = 0$$

for any time line. The first of these equations replaces the derivative of y at the electrode surface, $l = 1$, by a central difference approximation; the second refers to the boundary $z = 1$, $l = n$. In the first line of calculation the initial condition gives $y_k = 0$, $1 \leqslant k \leqslant n$.

These equations may be written in the shortened form,

$$Ay = B$$

where A is a band matrix of width three. These equations were solved with the aid of a Mercury computer, by resolution of the A matrix into a product of upper and lower triangle matrices. The range of z was divided into ten strips, $\Delta z = 0.1$, whilst the semi-infinite range of θ was divided such that $(\Delta z)^2/(\Delta\theta) = 1$.

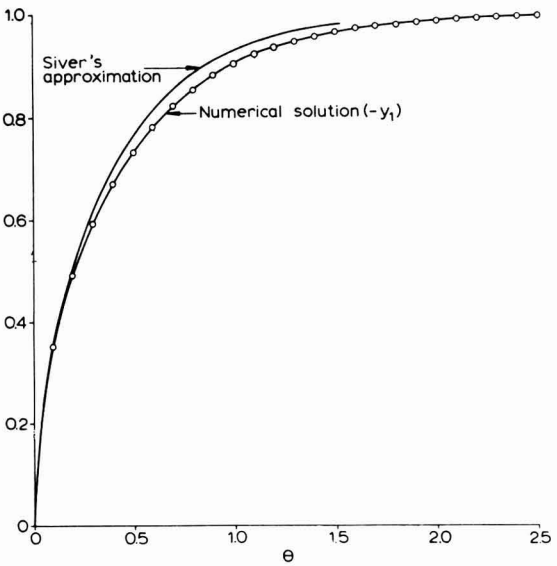

Fig. 2

y_1, the value of the function y at the electrode surface, was printed out at a function of θ, and may be compared directly with McKAY's function $F(v)$ since they represent the same expression (see Fig. 2*, and Table 1)

$$y_1 = \frac{nFAD}{I\delta}(C(o) - C^b)$$

TABLE 1

θ	$-y_1$	$-y_1/\theta^2$	θ_2/θ_1
0.1	0.352	35.164	0.327
0.2	0.492	12.301	0.311
0.3	0.593	6.586	0.292
0.4	0.671	4.192	0.276
0.5	0.733	2.932	0.257
0.6	0.783	2.175	0.239
0.7	0.824	1.681	0.222
0.8	0.857	1.339	0.206
0.9	0.884	1.091	0.192
1.0	0.905	0.905	0.179
1.1	0.923	0.763	0.168
1.2	0.937	0.651	0.157
1.3	0.949	0.562	0.148
1.4	0.959	0.489	0.139
1.5	0.966	0.429	0.131
1.6	0.973	0.380	0.124
1.7	0.978	0.338	0.118
1.8	0.982	0.303	0.112
1.9	0.985	0.273	0.107
2.0	0.988	0.247	0.102
2.1	0.990	0.225	0.097
2.2	0.992	0.205	0.093
2.3	0.994	0.188	0.089
2.4	0.995	0.173	0.086
2.5	0.996	0.159	0.082

Evidently SIVER's approximation is quite close to the true solution, being accurate as $\theta \to 0$, and only about 4% too high over most of the range of θ. The error is cubed during subsequent calculation of the diffusion coefficient, but the approximation is certainly realistic. The new solution indicates that the steady state surface concentration is attained when $\theta \sim 2.5$, *i.e.*,

$$t \sim 2.5\,\delta^2/D\text{, for } I < i_d = \frac{nFADC^b}{\delta}.$$

i_d is the steady state limiting current observed at the electrode under ambient conditions of concentration and rotation speed. A typical value of t, here, is 0.66 sec for $\omega \sim 100$ radians/sec and $D \sim 10^{-5}$ cm^2/sec.

TRANSITION TIMES

For interpretation of experimental results, the function $(-y_1/\theta^2)$ is in fact more useful, for

* In Fig. 2, $(-y_1)$ is the plotted quantity.

$$(-y_1/\theta^2) = \frac{\delta^4}{D^2t^2}\,\frac{nFAD(C^b - C(o))}{I\delta} = \left(\frac{1.626\,\nu^{1/6}}{\omega^{1/2}}\right)^3 \frac{nFA(C^b - C(o))}{It^2} \qquad (3)$$

which is independent of D, and may be calculated from immediately accessible experimental quantities, at the transition time where $C(o) = 0$, $t = \tau$. $(-y_1/\theta^2)$ is tabulated as a function of θ in Table 1. The procedure for analysis of experimental data, is to calculate the appropriate magnitude of $(-y_1/\theta^2)$ from the right hand side of eqn. (3) at the transition time. Hence the diffusion coefficient may be derived from the appropriate value of θ which is best interpolated from a plot of log $(-y_1/\theta^2)$ *vs.* θ (Fig. 3)

$$\theta = \frac{D\tau}{\delta^2} = \frac{D^{1/3}\tau}{(1.626\nu^{1/6}\omega^{-1/2})^2}$$

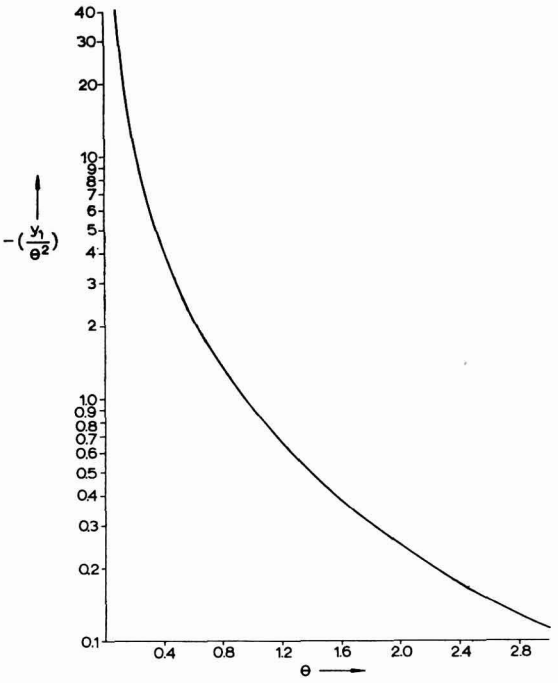

Fig. 3

POTENTIAL–TIME CURVES

In order to interpret the shape of potential–time curves, generated by galvanostatic polarisation of the rotating disc electrode, it is necessary to consider the surface concentration of all potential-determining substances. Here we restrict attention to the simple n-electron transfer reaction

$$O + n\,e \rightarrow R$$

in which both O and R are soluble in the solution.

The boundary value problem for species O is that treated above, and the distribu-

tion of R satisfies the same set of equations, except that C_R replaces C_o and the surface concentration gradient of R is opposite to that of O, *i.e.*,

$$\frac{\partial C_R}{\partial x} = -\frac{I}{nFAD_R} \quad \text{at} \quad x = 0 .$$

These equations are not coupled in any way, so that the solution derived above is immediately applicable, and we can write:

$$y_1(o) = \frac{nFAD_oC_o^b}{I\delta_o}\,\frac{C_o(o) - C_o^b}{C_o^b} = -u_1$$

$$y_2(o) = \frac{nFAD_RC_R^b}{I\delta_R}\,\frac{C_R^b - C_R(o)}{C_R^b} = -u_2$$

During cathodic polarisation, the u's are positive quantities; y_1 and y_2 are not independent of each other, they may be interpolated from Fig. 2 at their respective values of θ, $\theta_1 = D_ot/\delta_o^2$ and $\theta_2 = D_Rt/\delta_R^2$. Writing the steady state limiting currents of the cathodic and anodic processes as i_1 and i_2

$$i.e.,\ i_1 = \frac{nFAD_oC_o^b}{\delta_o} \quad \text{and} \quad i_2 = \frac{nFAD_RC_R^b}{\delta_R}$$

then the surface concentrations may be evaluated from:

$$C_o(o) = \left(1 - \frac{I}{i_1}u_1\right)C_o^b$$

$$C_R(o) = \left(1 + \frac{I}{i_2}u_2\right)C_R^b$$

EQUILIBRIUM CASE

If the electrode reaction is reversible, then the electrode potential obeys the Nernst equation, so that

$$E - E_e = \frac{RT}{nF}\ln\frac{C_o(o)}{C_R(o)} = \frac{RT}{nF}\ln\left[\frac{i_1 - Iu_1}{i_2 + Iu_2}\,\frac{D_2}{D_1}\right]$$

and a plot of the right hand side versus potential should yield a straight line. E_e is the rest potential of the electrode.

IRREVERSIBLE CASE

When equilibrium does not exist at the electrode, and its potential is to some extent determined by the rate of the electrode reaction, analysis of the shape of the potential–time curve allows determination of the kinetic parameters of the electron transfer.

The surface concentrations are to be introduced into the kinetic equation:

$$\frac{I}{nFA} = k_f C_o(o) - k_b C_R(o)$$

k_f and k_b are the potential dependent rate constants of the electrode reaction. Thus

$$\frac{I}{nFA} = k_f C_o^b\left(1 - \frac{I}{i_1}u_1\right) - k_b C_R^b\left(1 + \frac{I}{i_2}u_2\right)$$

That is

$$\frac{1}{nFAk_fC_o^b} = \frac{1}{I} - \frac{u_1}{i_1} - e^{nf\eta}\left(\frac{1}{I} + \frac{u_2}{i_2}\right) \tag{4}$$

$f = F/RT$ and $\eta = E - E_e$, is the total over-potential of the electrode, experimentally accessible. Equation (4) provides a relationship between four parameters, I, η, ω and t. Hence there are six feasible means of analysis, in which any two of these *variables* are held constant. For example, the potential–time curve itself may be analysed directly, by taking logarithms of each side of eqn. (4), and plotting the right hand side against potential (compare reference[12]).

$$\alpha nf\eta - \log(nFAk_{of}C_o^b) = \log\left\{\frac{I}{I} - \frac{u_1}{i_1} - e^{nf\eta}\left(\frac{I}{I} + \frac{u_2}{i_2}\right)\right\}$$

because[13]

$$k_f = k_{of}\exp(-\alpha nf\eta)$$

k_{of} is the magnitude of the forward rate constant at the equilibrium potential. The transfer coefficient is determined by the slope of the resulting straight line, and the parameter k_{of} is accessible from the intercept at $E = E_e$. Whilst this method might be tedious in the complexity of analysis, yet it might be most convenient from the experimental point of view, because the solid electrode may be poisoned by long exposure to a solution.

DIFFUSION-CONTROLLED CURRENT-REVERSAL TRANSIENTS

It is difficult to detect the transition of an electrode to a higher potential, if there is an electro-reducible species also present in solution, whose reduction potential is only

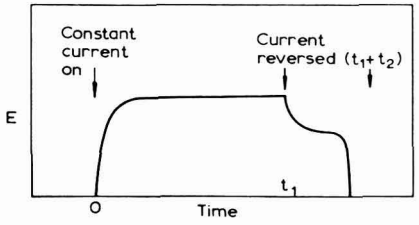

Fig. 4

slightly more negative than that of the species under study. This situation can arise, for example, in the study of many electro-active organic substances in acid solution. In such cases it is convenient to oxidise the product of electro-reduction, by reversal of the current (See Fig. 4).

For interpretation of this kind of experiment, it is necessary to express the time

required for complete oxidation of a species R from the surface layers of solution adjacent to the anode, as a function of diffusion parameters, and the time of electroreduction.

$O + n\,e \rightarrow R$ Charge for t_1 seconds

$R \rightarrow O + n\,e$ Discharge to the transition time, t_2.

For simplicity, we consider the case in which R is initially absent from the solution, and for which the discharge current has the same magnitude though the opposite sign, as the charging current.

The boundary value problem for charge differs from that stated earlier, only in that $C_R{}^b = 0$, and that

$$\frac{\partial C_R}{\partial x} = -\frac{I}{nFAD_R}$$

Hence we may write, as before:

$$\frac{\partial y}{\partial \theta} = a^2 \frac{\partial^2 y}{\partial z_1{}^2}$$

$$y = 0\,,\ z_1 = 1\,,\ \theta_1 \geqslant 0$$

$$y = 0\,,\ \theta_1 = 0\,,\ 0 \leqslant z_1 \leqslant 1$$

$$\frac{\partial y}{\partial z_1} = -1 \text{ at } z_1 = 0\,,\ \theta_1 \geqslant 0$$

where

$$y = \frac{nFAD_R C_R}{I\delta_R}$$

During discharge, the surface gradient has the opposite sign,

$$\frac{\partial y}{\partial z_2} = 1 \text{ at } z_2 = 0\,,\ \theta_2 \geqslant 0$$

The initial condition is

$$y(\theta_2 = 0) = y(\theta_1)$$

expressing the continuity of y at the instant of switching cathodic to anodic. Other boundary conditions, and the diffusion equation, for discharge, have the same form as written for the charge.

These equations were expressed in difference form according to the CRANK–NICHOLSON procedure, and values of θ_2 corresponding to $y = 0$ at $z_2 = 0$ during discharge, computed for various values of θ_1. The result is expressed in the form of a table of $\theta_2/\theta_1 = t_2/t_1$, *vs.* θ_1, and is included as the third column in Table I. Hence θ_1 may be determined from an experimental ratio of t_2/t_1, by interpolation within a curve constructed from this table.

It follows from the boundary value problem for a galvanostat, solved earlier, that for $\theta_1 \sim 2.5$ and $i < i_1 = nFAD_o C_o{}^b/\delta_o$, the function y becomes independent of time, whence θ_2 reaches a constant value. This, for the conditions prescribed herein, is 0.207, *i.e.*,

$$t_2 = \frac{0.207}{D_R}\,\delta_R{}^2$$

Hence the diffusion coefficient of the reduced species is immediately accessible from the oxidation transient, when polarisation is started from a steady state concentration distribution. Under these conditions, t_2 is proportional to ω^{-1}, which is a sensitive criterion to be obeyed by this diffusion-controlled model. It will not hold, for example, in the presence of adsorption or of dissociation of the product, complications which will be further considered in a subsequent paper.

CONCLUSIONS

The analysis of galvanostatic transients at a rotating disc electrode into fundamental rate parameters, is feasible, with the tabulated functions of this paper. Apart from the academic interest in the solution of this problem, real advantages derive from experimental application, due to the complete specification of supply of the reactants.

SUMMARY

The theory of a galvanostatic transient at a rotating disc electrode is reviewed, and an accurate solution obtained by a numerical method. Methods of analysis into kinetic and diffusion parameters are proposed. Current-reversal transients are treated, and a criterion presented for diagnosis of the applicability of the model.

REFERENCES

1 V. G. LEVICH, *Acta Physicochim.*, 19 (1944) 133.
2 YU. G. SIVER, *Zh. Fiz. Khim.*, 34 (1960) 577.
3a T. R. ROSEBURGH AND W. LASH-MILLER, *J. Phys. Chem.*, 14 (1910) 816.
3b A. T. MCKAY, *Proc. Phys. Soc. (London)*, 42 (1930) 547.
R. P. BUCK AND H. E. KELLER, *Anal. Chem.*, 35 (1963) 400.
4 W. NERNST, *Z. Physikal. Chem.*, 47 (1904) 52.
5 V. G. LEVICH, *Acta Physicochim.*, 17 (1942) 257.
6 W. G. COCHRAN, *Proc. Cambridge Phil. Soc.*, 30 (1934) 365.
7 K. PEARSON, *Tables of the Incomplete Gamma Function*, 3rd edn., Biometrika, 1946.
8 H. JEFFREYS AND B. S. JEFFREYS, *Methods of Mathematical Physics*, 3rd edn., Cambridge University Press, 1953, p. 269.
9 H. JEFFREYS AND B. S. JEFFREYS, *ibid.*, p. 262.
10 J. M. HALE, *Thesis*, Bristol, 1961.
11 J. CRANK AND P. NICHOLSON, *Proc. Cambridge Phil. Soc.*, 43 (1947) 50.
12 J. E. B. RANDLES, *Can. J. Chem.*, 37 (1959) 238.
13 P. DELAHAY, *New Instrumental Methods in Electrochemistry*, 1st edn., Interscience Publishers Inc., New York, 1954, Chapter 1.

POLAROGRAPHY OF Ni^{2+} IN DIFFERENT SUPPORTING ELECTROLYTES IN AQUEOUS AND NON-AQUEOUS MIXTURES

KAMALA ZUTSHI

Department of Chemistry, University of Rajasthan, Jaipur (India)

(Received May 21st, 1963)

In non-complexing supporting electrolytes Ni^{2+} gives a single reduction wave the wave height of which is independent of the concentration of the supporting electrolyte. SANBORN AND ORLEMANN[1] have studied the reduction of Ni^{2+} in sodium chloride and potassium chloride and have reported that the reduction depends upon the concentration of the supporting electrolyte and is due to the formation of Ni^{+} ion. VLCEK[2] suggested that the reduction of nickel in sodium chloride was accompanied by a kinetic current. TAKAHASHI AND SHIRAI[3] have studied the reduction of Ni^{2+} in potassium nitrate, potassium bromide, potassium sulphate and potassium nitrite. They have reported that two waves are formed in all these supporting electrolytes, except potassium nitrate.

A detailed study of the reduction of Ni^{2+} in mixtures containing non-aqueous solvents has not yet been described in the literature.

This paper describes the reduction of Ni^{2+} in sodium formate, sodium iodide and sodium sulphate as supporting electrolytes, in water, water/ethanol, water/propanol and water/ethylene glycol solutions.

EXPERIMENTAL

Apparatus

Heyrovsky system L.P. 55 Polarograph was used manually in all the polarograms. The dropping mercury electrode had the following characteristics: $m = 2.12$ mg/sec, $t = 3.6$ sec (at an applied voltage of -1.5 V *vs.* S.C.E.).

Reagents

Reagent grade chemicals and conductivity water were used for the preparation of all the solutions. The sodium formate, sodium sulphate and sodium iodide were in crystalline form. Doubly distilled ethanol, propanol, and ethylene glycol were used in the solvent mixtures. A stock solution of Ni^{2+} was prepared and the nickel content accurately determined.

All the reported diffusion currents have been corrected for the residual currents. In the water/alcohol mixtures the iR drop correction was made by measuring the resistance of the cell with the help of a L.P. 024 conduscope. The potentials reported refer to the saturated calomel electrode. All the experiments were carried out at a temperature of 25° by means of a Haake type N 61174 thermostat. The temperature

coefficient of the diffusion current in aqueous solution was determined by raising the temperature from 25° to 45° and then to 65°. Purified hydrogen was used for the removal of dissolved oxygen. In the case of volatile solvents the gas was pre-saturated by passing it through a solution having the same composition as that of the experimental mixture.

RESULTS

Sodium formate as supporting electrolyte

A well-defined reduction wave of nickel ion was obtained in 0.1 *M* sodium formate (Fig. 1, curve 1). On increasing the concentration of the supporting electrolyte from 0.5–1–1.5 *M* two reduction waves were obtained. The half-wave potential of the first wave varied from −1.09 to −1.15 V and for the second wave from −1.35 to −1.6 V (Fig. 1, curves 1, 2, 3, 4). As the concentration of Ni^{2+} was increased, the total wave

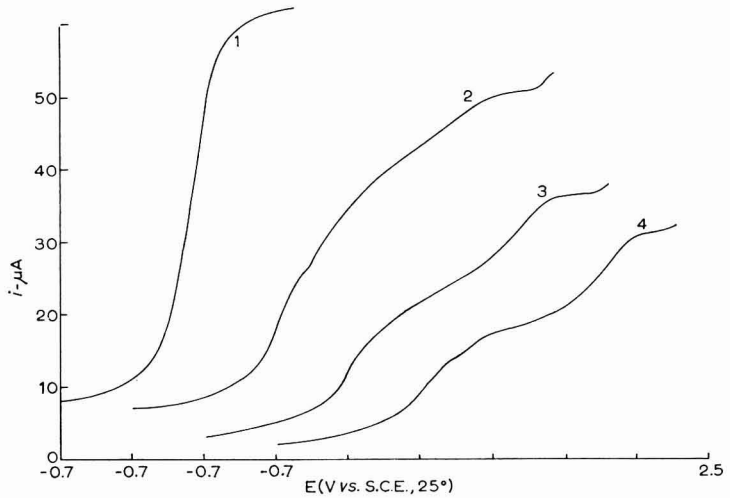

Fig. 1. Polarograms of nickel in sodium formate and 0.001% Triton x-100: (1), 1 m*M* Ni^{2+} in 0.1 *M* H.COONa; (2), 1 m*M* Ni^{2+} in 0.5 *M* N.COONa; (3), 1 m*M* Ni^{2+} in 1.0 *M* H.COONa; (4), 1 m*M* Ni^{2+} in 1.5 *M* H.COONa. Each curve begins at −0.7 V and each interval along the axis corresponds to 0.2 V.

height increased correspondingly showing thereby that the total limiting current is diffusion-controlled (Fig. 2, curve 3). The individual currents, however, were not found to be diffusion-controlled. The log-plot of $i/(i_d - i)$ *vs.* E was found to be linear, with a slope of 0.086 showing that the reduction is irreversible. The temperature coefficient of the diffusion current was found to be 3%. In the presence of dissolved oxygen a wave appeared which was removed on de-aerating the solution. The maximum which appeared in the absence of a maxima suppressor was suppressed by adding 0.001% Triton X-100 (Fig. 2, curves 1, 2). The plot of i/h against the total wave height passes through the origin indicating that the limiting current is diffusion-controlled. The straight lines obtained by plotting i/h against the individual wave heights do not pass through the origin, indicating the presence of a kinetic current.The addition of 0.005% gelatine solution did not affect the shape or the number of the reduction waves.

The reduction of Ni^{2+} was also studied in 20%, 40% and 60% aqueous ethanol and aqueous propanol and 20% aqueous ethylene glycol using 1.5 *M* sodium formate as supporting electrolyte. No appreciable effect was noticed either in the shape or height of the curve by the addition of ethanol or ethylene glycol to the aqueous solution of

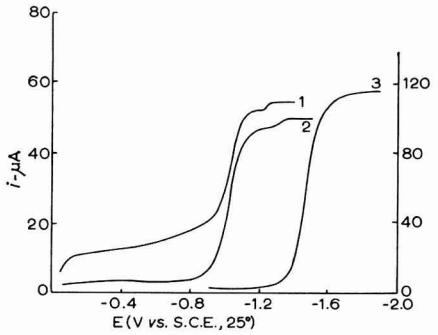

Fig. 2. Polarograms of nickel in 0.1 *M* sodium formate: (1), 1 m*M* Ni^{2+} with oxygen; (2), 1 m*M* Ni^{2+} without oxygen; (3), 2 m*M* Ni^{2+} without oxygen +0.001% Triton x-100. Curve (3) begins at −0.5 V and for this curve each interval along the axis corresponds to 0.4 V and each interval along the vertical axis corresponds to 40 sub-divisions.

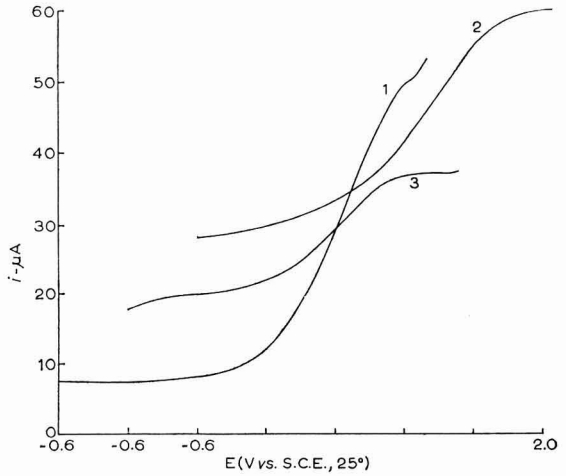

Fig. 3. Polarograms of nickel in 1.5 *M* sodium formate and 0.001% Triton x-100: (1), 1 m*M* Ni^{2+} and 20% propanol; (2), 1 m*M* Ni^{2+} and 40% propanol; (3), 1 m*M* Ni^{2+} and 40% propanol; (3), 1 m*M* Ni^{2+} and 60% propanol. Each curve begins at −0.6 V and each interval along the axis corresponds to 0.2 V.

sodium formate. The two curves, however, tended to approach each other and the shape becomes ill-defined. There was a marked difference on the addition of propanol (Fig. 3, curves 1, 2, 3). The two waves combined to form one and the total diffusion current decreased with increasing concentration of propanol. The half-wave

potentials of the 20, 40 and 60% aqueous mixtures were found to be −1.38, −1.24 and −1.17 V respectively, *vs.* S.C.E.

The product of the square root of the viscosity (n) and diffusion current constant (K) for each solution was calculated. The product $Kn^{\frac{1}{2}}$ remains constant for all concentrations of ethylene glycol and ethanol but decreases for the propanol solution.

Sodium sulphate as supporting electrolyte

In 0.1 M sodium sulphate Ni^{2+} gave a single reduction wave having a half-wave potential of −1.1035 V *vs.* S.C.E. (Fig. 4, curve 1). As the concentration of sodium sulphate was increased from 0.5–1–1.5 M, two reduction waves were obtained in each case. The half-wave potential of the first wave varied from −1.09 to −1.04 V and that of the second wave from −1.52 to −1.685 V (Fig. 4, curve 2, 3, 4). The log-

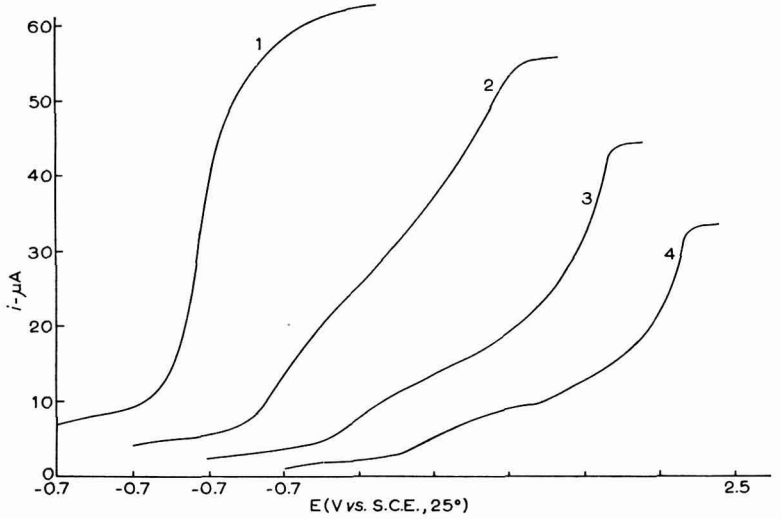

Fig. 4. Polarograms of nickel in sodium sulphate and 0.001% Triton x-100: (1), 1 mM Ni^{2+} in 0.1 M Na_2SO_4; (2), 1 mM Ni^{2+} in 0.5 M Na_2SO_4; (3), 1 mM Ni^{2+} in 1.0 M Na_2SO_4; (4), 1 mM Ni^{2+} in 1.5 M Na_2SO_4. Each curve begins at −0.7 V and each interval along the axis corresponds to 0.2 V.

plot of $i/(i_d - i)$ *vs.* E was found to be linear but the reduction of Ni^{2+} is irreversible. The value of the slope was found to be 0.053. The total wave height decreased with increasing concentration of the supporting electrolyte. The total limiting current was found to be diffusion-controlled (Fig. 5, curve 3). but the individual current is not diffusion-controlled. In the presence of oxygen a wave appeared which disappeared on de-aeration. A maximum appeared in the absence of a maxima suppressor; it was removed by adding 0.001% Triton x-100 (Fig. 5, curves 1, 2). In the presence of 0.005% gelatine the shape of the curve remained unchanged. A graph of wave height against $\sqrt{h}$ was plotted for the each wave. The resulting line does not pass through the origin, indicating the presence of a kinetic current but the line expressing the relationship between the total wave height and $\sqrt{h}$ does pass through the origin showing that the limiting current is controlled by the diffusion rate. The value of the tempera-

ture coefficient was found to be 2.85% showing that the reduction of Ni^{2+} is irreversible. In 20, 40 and 60% aqueous ethylene glycol and ethanol there was a decrease in the total wave height and the two waves tended to approach each other. Polarograms could not be obtained in aqueous propanol because of the immiscibility of propanol in sodium sulphate solution. The product $Kn^{\frac{1}{3}}$ remains constant at all concentrations of ethanol and ethylene glycol.

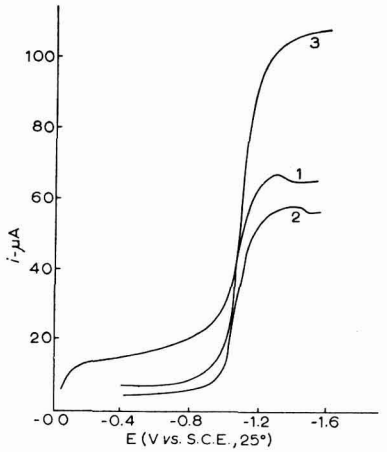

Fig. 5. Polarograms of nickel in 0.1 *M* sodium sulphate: (1), 1 m*M* Ni^{2+} with oxygen; (2), 1 m*M* Ni^{2+} without oxygen; (3), 2 m*M* Ni^{2+} without oxygen + 0.001% Triton x-100.

Sodium iodide as supporting electrolyte

A single reduction wave with a half-wave potential of −1.04 V was obtained with Ni^{2+} with 1 *M* sodium iodide as supporting electrolyte (Fig. 6, curve 1). As the concentration of the supporting electrolyte was increased from 0.5–1–1.5 *M* a two-wave polarogram was obtained in each case. The $E_{\frac{1}{2}}$ of the first wave did not appreciably change with the changing concentration of the supporting electrolyte. The half-wave potential of the second wave varied from −1.40 to −1.5 V (Fig. 6, curves 2, 3, 4). As the concentration of the Ni^{2+} was increased the wave height increased proportionately showing that the current is diffusion-controlled (Fig. 6, curve 5). The log-plot of $i/(i_d - i)$ *vs.* E, is linear with a slope of 0.045 at 25°, indicating the irreversible reduction of Ni^{2+}. The temperature coefficient of the diffusion current was found to be about 3%. In presence of dissolved oxygen Ni^{2+} gave an oxygen wave which was eliminated by de-aeration. A maximum appeared in the absence of a maximum suppressor; it was removed by adding Triton x-100.

The reduction of Ni^{2+} in 20, 40 and 60% aqueous ethanol, propanol and aqueous ethylene glycol in 1 *M* sodium iodide gave only one wave (Fig. 7, curves 1, 2, 3). The individual height of the single wave was slightly less than the total height of the two waves at the same concentration in aqueous solutions of 1 *M* sodium iodide. The product $Kn^{\frac{1}{3}}$ remains constant in aqueous ethanol and aqueous ethylene glycol but decreases in aqueous propanol.

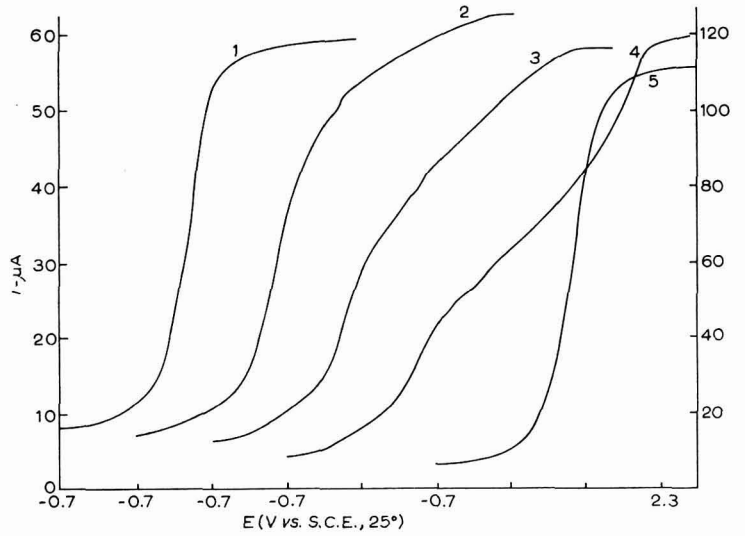

Fig. 6. Polarograms of nickel in sodium iodide and 0.001% Triton x-100: (1), 1 mM Ni^{2+} in 0.1 mM NaI; (2), 1 mM Ni^{2+} in 0.5 M NaI; (3), 1 mM Ni^{2+} in 1.0 M NaI; (4), 1 mM Ni^{2+} in 1.5 M NaI; (5), 2 mM Ni^{2+} in 0.1 M NaI. Each curve begins at −0.7 V and each interval along the axis corresponds to 0.2 V.

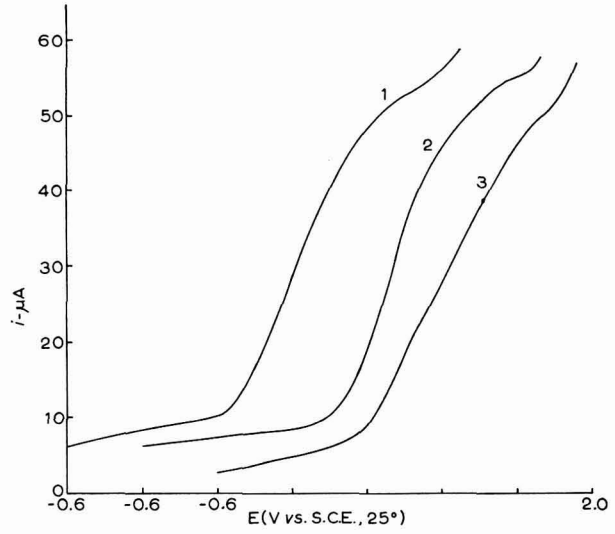

Fig. 7. Polarograms of nickel in 1.0 M sodium iodide and 0.001% Triton x-100: (1), 1 mM Ni^{2+} containing 20% ethanol; (2), 1 mM Ni^{2+} containing 20% propanol; (3), 1 mM Ni^{2+} containing 20% ethylene glycol. Each curve begins at −0.6 V and each interval along the axis corresponds to 0.2 V.

DISCUSSION

In 0.1 M solutions of all three supporting electrolytes *viz.*, sodium formate, sodium sulphate, and sodium iodide, nickel gives only one reduction wave. The half-wave

potential of this wave corresponds to the reduction of $Ni(H_2O)_6^{2+}$. As the concentration of the supporting electrolyte is gradually increased above 0.1 *M* the formation of two reduction waves starts. When the concentration reaches 1.5 *M* two distinct waves are obtained. The half-wave potential of the first wave in all cases corresponds to the reduction of $Ni(H_2O)_6^{2+}$ but the half-wave potential of the second wave in every case shifts to a more negative potential with increasing concentration of the supporting electrolyte. This suggests that at higher concentrations (0.5–1.0–1.5 *M*) a co-ordinated compound, in addition to $Ni(H_2O)_6^{2+}$, is formed with the anion of the supporting electrolyte. The presence of the kinetic wave indicates that the compounds are in a state of equilibrium. Although the total limiting current is diffusion-controlled, the reduction of $Ni(H_2O)_6^{2+}$ is irreversible in all the supporting electrolytes. This is evident from the fact that the half-wave potential is more negative than what would be expected for the reversible potential of the Ni^{2+}–Ni couple. This is also confirmed by the abnormally low value of the slope of the nickel wave and the high value of the temperature coefficient. When the two waves are resolved the second wave is also found to be irreversible.

The increase in the second wave height and the corresponding decrease in the first wave height, with increasing concentration of the supporting electrolyte, may be attributed to the fact that the concentration of $Ni(H_2O)_6^{2+}$ decreases as the concentration of the anion increases and the former may be more easily reduced than the anion complex. This supports the views expressed by SANBORN[1]. The constant value of $Kn^{\frac{1}{2}}$ in aqueous ethanol and aqueous ethylene glycol in all the supporting electrolytes shows that the decrease in the total wave height is due to the increased viscosity of the solution.

The addition of propanol, however, gives only one reduction wave in sodium formate and the product $Kn^{\frac{1}{2}}$ is not constant either in sodium iodide or sodium formate. This is due to the fact that the viscosity of the solution is not the only factor affecting the diffusion current but that probably ion-pair formation takes place. The single wave results because propanol prevents the co-ordination of the anion of the supporting electrolyte with nickel ion.

SUMMARY

The reduction of Ni^{2+} in 0.1 *M* sodium formate, sodium sulphate and sodium iodide supporting electrolytes gives only one reduction wave. As the concentration of the supporting electrolytes is increased from 0.5–1–1.5 *M*, two reduction waves are obtained. In all cases the total limiting current was found to be diffusion-controlled which provides a method for the polarographic determination of Ni^{2+}. The half-wave potential of the first wave in each case corresponds to the reduction of the $Ni(H_2O)_6^{2+}$ complex. In the case of the second wave, the shift in half-wave potential indicates the co-ordination of the anion of the supporting electrolyte with Ni^{2+}.

In ethanol, propanol and ethylene glycol aqueous mixtures the two waves show a tendency to unite to form a single wave. This is more apparent in the case of propanol.

REFERENCES

1 R. H. SANBORN AND E. F. ORLEMANN, *J. Am. Chem. Soc.*, 78 (1956) 4852.
2 A. A. VLCEK, *Z. Elektrochem.*, 61 (1957) 1014.
3 T. TAKAHASHI AND H. SHIRAI, *J. Electroanal. Chem.*, 3 (1962) 313–320.

A METHOD FOR THE DETERMINATION OF ELECTROLYTIC HYDROGEN-TRITIUM SEPARATION FACTORS

J. O'M. BOCKRIS, S. SRINIVASAN AND M. A. V. DEVANATHAN

The Electrochemistry Laboratory, University of Pennsylvania, Philadelphia 4, Penna. (U.S.A.)

(Received June 25th, 1963)

A knowledge of H/T separation factors is of fundamental importance in the determination of mechanism of hydrogen evolution. It is also of value in heavy water enrichment experiments. Previous methods for the determination of H/D[1] or H/T[2] separation factors utilized vacuum systems. In the present communication, a new method[3] is described for the determination of H/T separation factors.

EXPERIMENTAL

Apparatus

Cell. The test cell, made of pyrex glass, is shown diagramatically in Fig. 1. The main features are: (1) A furnace compartment (h) to heat the test electrode to 700–800°C in hydrogen and introduce the electrode into the cathode compartment out of contact with air; (2) a vacuum tight fit of the test electrode holder (k) at the conical joint by means of a teflon sleeving; (3) a side arm from the central cathode compartment to which a vacuum tight teflon stop cock and a socket joint (e) are attached; (4) the cylindrical platinum gauze (b) to ensure an even distribution of current lines.

Oxidation train and collection system. — The oxidation train and collection system are represented diagramatically in Figs. 2 and 3. The oxidation train is connected to the cell at the socket joint on the side arm of the test cell. The central tube, on the cap of the collection system, ended about $^1/_2$ cm from the base of the sampling vial. All joints in the oxidation train were greased (Apiezon T – high temperature grease to ensure a vacuum tight seal).

Run procedure

Electrolysis and oxidation of evolved gas. — All three compartments in the cell were filled with tritiated electrolyte – 0.5 N H_2SO_4 (activity $\simeq$ 6 μc/ml). After heating the test electrode (Cu, area 10 cm^2) in the furnace compartment (h in Fig. 1) at 700°C in a purified hydrogen atmosphere and then cooling it, the electrode was lowered into position so that there was a tight fit on the conical joint, provided with a teflon sleeve. It was necessary to insert the electrode into the solution with a small current ($< 10^{-4}$ A) for the cathodic protection of the electrode. The oxidation train was assembled in

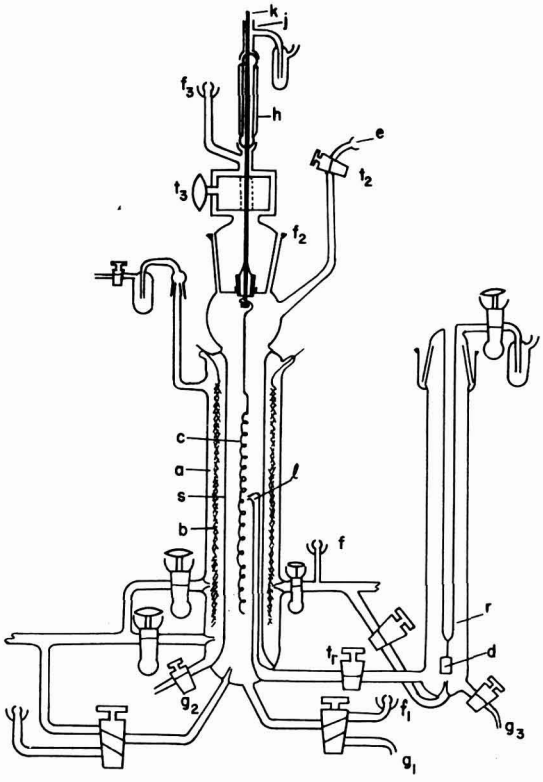

Fig. 1. Test cell

a anode compartment
b cylindrical platinum gauze anode
c cathode compartment
d platinized platinum reference electrode
e socket joint for connection of oxidation train
f inlet for purified hydrogen or helium
g_1 outlet tap from cathode compartment
g_2 outlet tap from anode compartment
g_3 outlet tap from reference electrode compartment
f_1 water sealed ball joint for pre-electrolysis cell
f_2 conical joint
f_3 inlet for purified hydrogen into furnace compartment
h furnace compartment for heating electrode
k electrode holder
j ground glass sleeve
l Luggin capillary
r reference electrode compartment
s fritted tube separating anode and cathode compartments
t_1 Teflon stopcock separating reference electrode and cathode compartments
t_2 Teflon stopcock on side arm of cathode compartment
t_3 large stopcock separating furnace and cathode compartments

its position. Helium was passed through the anode and cathode compartments. The reference electrode compartment was maintained in a hydrogen atmosphere. The electrolytic current was increased to 10^{-1} A and continued for a period of 15 minutes. The electrolytic gas from the cathode compartment was carried over with the helium into the oxidation train. Water vapor, which was also carried over from the cell, was absorbed in the sulphuric acid trap and any small traces were frozen out in the liquid air trap. The electrolytic gas was next oxidized to water in the cupric oxide furnace

(cupric oxide, used in wire form, was maintained at 720°C). This water was carried over with the helium into the collection system immersed in liquid air where it was trapped. The lead from the cupric oxide furnace to the collection system was electrically heated to prevent any condensation of water in this tube. The water generally

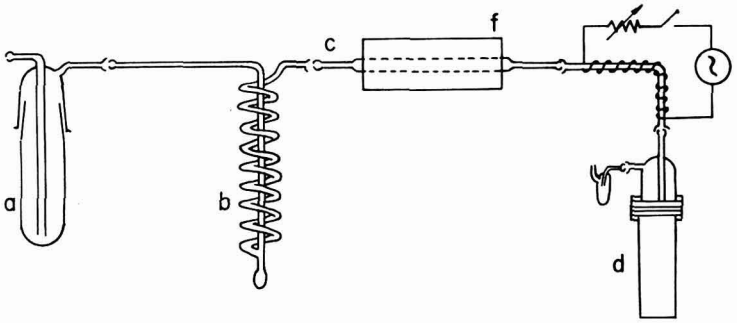

Fig. 2. Train for oxidation of electrolytic gas

a concentrated sulphuric acid trap
b spiral liquid air trap
c Vycor glass tube containing CuO
d collection system
f electric furnace

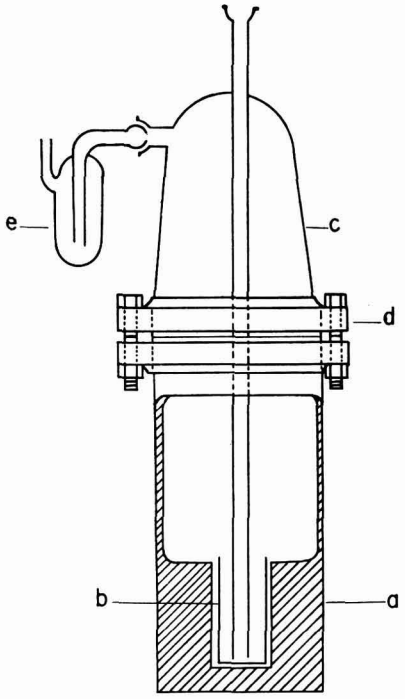

Fig. 3. Collection system for gas sample

a brass vessel
b sampling vial
c cap
d pipe flange arrangement connecting cap and brass vessel
e sulphuric acid bubbler

froze out in the central tube of the cap of the collection system. The passage of helium was continued for a further period of 15 minutes (after reducing the electrolytic current to 10^{-4} A) to flush the cell free of any evolved gas into the oxidation train and and the steam into the collection system.

The collection system was then disconnected from the train and the inner and outer sides of the central tube of the cap washed with scintillation mixture (composition: toluene – 1000 ml, dioxane – 1000 ml, ethyl alcohol – 600 ml, naphthalene – 600 g, PPO (2,5 diphenyl oxazole) – 2.6 g, POPOP (1,4-bis-2-phenyl oxazolyl-benzene) – 0.13 g) into the sampling vial which was then directly counted. The quantity of hydrogen (light and heavy) liberated and converted to water was calculated using Faradays' laws.

The amount of hydrogen evolved during the period of flushing the cell and train (when the current was maintained at 10^{-4} A) is only a negligible fraction (0.1%) of the hydrogen evolved during electrolysis at 10^{-1} A.

Preparation of samples for counting. — Besides the electrolytic gas samples, the following samples were also prepared:

Electrolytic solution samples

0.5 ml of the electrolytic solution was diluted accurately a hundred times with equilibrium water and 0.1 ml portions of this diluted solution were transferred with a Hamilton microliter syringe into each of three sampling vials containing 10 ml of scintillation mixture.

Blank samples

To obtain the activity (measured activity diminished by background) of the electrolytic solution and gas samples, blanks were also prepared, one blank containing only 10 ml of scintillation mixture and the other 10 ml of scintillation mixture and 0.1 ml of equilibrium water.

Counting techniques

All the above samples were counted in the automatic liquid scintillation counter (Packard Tricarb Model 314X) which was set to record the count for a predetermined time (10 min) or the time for a predetermined total number of counts (10^5). These predetermined values were used in order to limit the error due to counting statistics to within 1%. Counting measurements were repeated three times and then after the addition of 0.1 ml of a tritiated toluene standard to each sample, the counting was repeated as previously.

RESULTS

Expression for separation factor

The H/T separation factor is defined by

$$S_T = \left(\frac{C_H}{C_T}\right)_g \Big/ \left(\frac{C_H}{C_T}\right)_s \qquad (1)$$

where $(C_H/C_T)_g$ and $(C_H/C_T)_s$ are the ratios of atomic concentrations of H to T in the

electrolytic gas and solution respectively. It may easily be shown that when the H to T atomic ratio is high (in our case $10^8 : 1$), equation (1) reduces to

$$S_T = \frac{(a_T)_s}{(a_T)_g} \tag{2}$$

where $(a_T)_g$ and $(a_T)_s$ are the activities of the electrolytic gas and solution samples respectively for the same total quantities of water in each[2,3].

Separation factor on copper

The average value of the separation factor on Cu as determined by this method is 18.1 ± 2.4. There was some scatter in S_T values in a few experiments. A number of experiments were carried out to check the method[3]. A few of the main ones are described in the following section (see also Ref. 3).

EXPERIMENTS CARRIED OUT TO TEST METHOD

Pregl tube experiment

After the separation factor determinations in an experiment, a Pregl tube was connected in place of the collection system. The percentage conversion and recovery in all of Pregl tube experiments was over 97% and in most cases nearly 100%. Thus, there were no leaks in the system up to the end of the oxidation train.

*Experiment with calibrated H–T gas mixture**

Instead of the electrolytic gas, a known quantity of a calibrated H–T gas mixture was passed from the cell into the oxidation train, with helium again as carrier gas. An average percentage conversion and recovery of 93–94% was obtained in all experiments. The small error reported is probably accounted for by counting errors. The efficiency of the collection system is checked by this experiment.

Separation factor on mercury

Separation factors were determined on mercury, using this technique (a similar cell was used with mercury at the base of the central cathode compartment). The experiments were carried out both under crude and high purity conditions of solution preparation. The S_T values were quite reproducible in all the experiments, the average value being 5.8 ± 0.3.

CONCLUSION

The experiments, carried out to test the method, show that S_T values can be determined to within an accuracy of 6–7%. Due to the greater reproducibility in the separation factors on mercury, it may be concluded that the scatter in S values in some experiment on copper, was due to the irreproducible behavior of the Cu electrode. The present technique was applied to a number of other metals in acid and alkaline solution with the aim of determining the mechanism of hydrogen evolution on these metals. These results and mechanistic conclusions are discussed in a separate paper[4].

* The authors wish to thank D. B. MATTHEWS for carrying out this experiment.

ACKNOWLEDGEMENTS

This work was sponsored by the Aeronautical Systems Command, Air Force Systems Command, United States Air Force AF 33(657)-8823.

The facilities of the liquid scintillation counter afforded by Dr. R. J. RUTMAN, Mrs. S. C. JONES and Mrs. N. GOLDSTEIN are gratefully acknowledged. The authors also wish to thank Mrs. V. DRAZIC and Mr. D. B. MATTHEWS for their assistance in some of the experimental work.

SUMMARY

A new method for the determination of electrolytic H/T separation factors is described. Copper or mercury was used as the test electrode. Vacuum systems, used in previous methods, were eliminated in the present technique. Instead, helium was used to carry the electrolytically evolved gases (H_2 and HT) into an oxidation train and also to carry the resulting water over into a collection system, whereafter the activity of the tritium was measured. The method has an accuracy of $\pm$ 6%.

REFERENCES

1 G. P. LEWIS AND P. RÜETSCHI, *J. Phys. Chem.*, 66 (1962) 1487. (Earlier references found in this paper.)
2 M. L. EIDENHOFF, *J. Am. Chem. Soc.*, 69 (1947) 2507.
3 S. SRINIVASAN, *Ph.D. Thesis*, University of Pennsylvania (1963).
4 J. O'M. BOCKRIS AND S. SRINIVASAN, to be published.

NULL-POINT POTENTIOMETRIC DETERMINATION OF ZINC

N. K. MATHUR AND C. K. NARANG

Department of Chemistry, University of Jodhpur, Jodhpur (India)

(Received May 27th, 1963)

The volumetric determination of zinc using ferrocyanide was suggested by GALLETTI[1] and until the development of the complexometric methods[2] of titration using various amino-polycarboxylic acids, this was the only reliable titrimetric method for the determination of zinc. The controversy over the composition of the zinc ferrocyanide precipitate was settled by the studies of DE KONINCK AND PROST[3]. It has been stated that initially the potassium zinc ferrocyanide precipitate is gelatinous[4] and capable of reacting with uranyl ions, which is a major limitation in the use of uranyl nitrate as an external indicator. CONE AND CADY[5] introduced the use of certain redox indicators such as diphenylamine and diphenylbenzidine for ferrocyanide titrations, incorporating indicator amounts of ferricyanide in the titrant. KOLTHOFF AND PEARSON[6] suggested the addition of ammonium sulphate to improve the coagulation of the precipitate and also suggested that the titration be carried out at 60–80°. The success of the titration depends upon uniformity of conditions during the titrations of the unknown and the standard zinc solution.

Potentiometric methods[7] have also been used in titrations involving ferrocyanide. Recently a new potentiometric method for the determination of fluoride and chloride was reported and has been referred to as a null-point potentiometric method[8,9]. The advantages of the new method over the conventional method have been described and this technique has therefore been tried out for the determination of zinc by ferrocyanide titration. Highly satisfactory results have been obtained.

EXPERIMENTAL

Apparatus

The titration cell consisted of two, 250-ml beakers used as half-cells connected through an agar–potassium chloride bridge. Each half-cell was provided with a platinum wire electrode and suitable stirring arrangements. The complete titration cell was placed in a large water bath at 60–80°. A simple Pye student potentiometer was used for e.m.f. measurements.

Reagents and solutions

Exactly 0.1 *M* solutions of potassium ferrocyanide and potassium ferricyanide were prepared in distilled water from A.R. reagents. For the determination of zinc in unknown solutions, it is not necessary to prepare these solutions of exact strength, but for studying the effect of acid concentration on the formal potential of the ferrocyan-

ide–ferricianide couple and for other exploratory work it was considered necessary to prepare solutions of exact strength. Equal volumes of the solutions were mixed to give solutions, containing ferrocyanide and ferricyanide in ratio 1 : 1. A standard 0.05 *M* zinc solution was prepared from A.R. zinc sulphate.

Effect of acid concentration on the formal potential of the ferrocyanide–ferricyanide couple

The standard redox potential[10] of the ferrocyanide-ferricyanide couple has been reported to be + 0.36 V but there is a considerable variation in this potential depending on acid concentration. It has also been reported that in solutions containing different mineral acids at the same concentration, the formal potential is the same, indicating that it is dependent on the hydrogen ion concentration rather than the nature of anion. Since the success of the proposed method would depend on the constancy of the formal potential it was considered necessary to study the effect of acetic acid and the formal potential of the couple was found to be constant over the acetic acid concentration range 0.5–1.5 *M* In the presence of acetic acid the addition of anions (Cl^-, SO_4^{2-}, NO_3^-, ClO_4^-) in the form of neutral salts had no effect on the formal potential of the couple.

Procedure

50.0-ml portions of ferrocyanide–ferricyanide solution were measured into each half-cell and about 0.5 g of solid ammonium sulphate added to each. The half-cells were connected and checked for zero e.m.f. A suitable aliquot of the unknown solution was added to one half-cell and the same volume of distilled water to the other. The difference in the potential of the two half-cells was measured. Standard zinc solution was then added in small volumes from a burette to the second half-cell. At the same time equal volumes of water were added to the first half-cell and the solutions were stirred thoroughly. The end point corresponds to the zero E.M.F. of the cell *i.e.*, when all the ferrocyanide in both half-cells has reacted with zinc to form the double salt. It is possible to plot a graph between the volume of the titrant added and the E.M.F.

Any free mineral acid in the unknown solution must be neutralised and the solution should be 0.6–1.5 *M* with respect to acetic acid. The results of typical determinations are given in Table 1.

TABLE 1

Acetic acid concn. (M)	*Amount of zinc (mg)*		*% Error*
	taken	*found*	
0.5	16.25	16.12	0.79
0.5	21.70	21.61	0.44
1.2	21.70	21.66	0.19
1.5	32.51	32.42	0.31
1.5	66.23	66.34	0.17
1.5	82.48	82.23	0.31

Interfering substances

The interfering action of strong mineral acids has been mentioned earlier. Cations such as iron(II) and iron(III) copper (II), cadmium(II) and mercury(II) interfere because of the formation of insoluble ferrocyanides. No interference was observed when

alkaline earths, alkali metals, aluminium and ammonium ions were present with zinc in 1 : 1 ratio. Common anions do not interfere.

Other experimental conditions

The concentration and ratio of ferrocyanide–ferricyanide in the mixed solutions can be varied depending on the concentration of the unknown zinc solution. 50 ml of ferrocyanide–ferricyanide solution 0.05 *M* with respect to each salt can be used satisfactorily for 20.0 ml of an unknown zinc solution the strength of which is about 0.05 *M*. There is a maximum difference of potential between the two half-cells on the addition of zinc solution, when the ratio of ferrocyanide : ferricyanide is 1 : 1 which justified the use of the solution having equimolar concentrations.

The method can be applied to the analysis of certain alloys such as brass after separation of copper; zinc is determined in the filtrate after the mineral acids have been neutralised and the required amount of acetic acid added.

SUMMARY

A null-point potentiometric method employing ferrocyanide as titrant has been described for the determination of zinc. The end point in the titration is indicated by balancing the E.M.F. of two half-cells, one containing ferrocyanide–ferricyanide solution and the unknown zinc solution, and the other the same quantity of ferrocyanide–ferricyanide solution and sufficient standard zinc solution to obtain the balance. Interferences of mineral acids and other metal ions have been studied.

REFERENCES

1 M. GALLETT, *Bull. Soc. Chim.*, 2 (1864) 83 and 9 (1868) 369.
2 F. J. WELCHER, *The Analytical uses of EDTA*, Van Nostrand Co., Inc., New York, 1958.
3 L. L. DE KONINCK AND E. PROST, *Z. Angew. Chem.*, 9 (1896) 460, 564.
4 I. M. KOLTHOFF AND V. A. STENGER, *Volumetric Analysis*, Vol. II, Interscience Publishers, Inc., New York, 1947.
5 W. H. CONE AND L. C. CADY, *J. Am. Chem. Soc.*, 49 (1927) 356.
6 I. M. KOLTHOFF AND E. A. PEARSON, *Ind. Eng. Chem., Anal. Edn.*, 4 (1932) 147.
7 I. M. KOLTHOFF AND N. H. FURMAN, *Potentiometric Titrations*, John Wiley and Sons, Inc., New York, 1931.
8 H. V. MALMSTADT AND J. D. WINEFORDNER, *Anal. Chim. Acta*, 20 (1959) 283.
9 T. A. O'DONNELL AND D. F. STEWART, *Anal. Chem.*, 33 (1961) 337.
10 E. H. SWIFT, *A System of Chemical Analysis for Common Elements*, *Prentice Hall*, New York, 1939, pp. 540–3.

POLAROGRAPHIC AND pH-METRIC STUDIES ON THE INTERACTION OF LEAD WITH TRANSFUSION GELATIN

WAHID U. MALIK AND M. MUZAFFARUDDIN

Chemical Laboratories, Aligarh Muslim University, Aligarh (India)

(Received June 6th, 1963)

Very little is known regarding the binding of heavy metal ions to gelatin. The process can be better investigated by using a simple and well characterised gelatin like transfusion gelatin[1] and the first work of this kind was undertaken in this laboratory, when many interesting results on the binding of hydrogen ion[2] and heavy metal ions[3,4] to this particular protein were obtained. The behaviour of the Cu(II) complex at the dropping mercury electrode was particularly interesting[3] and it was, therefore, thought worthwhile to extend the studies to other metal ions. This paper deals with the polarography of lead ion in the presence of transfusion gelatin. Results on pH-metry have also been included to supplement the polarographic results.

A few valuable references on lead-protein binding are available in the literature. These are: (i) the work of TANFORD[5] on the binding of Pb(II) to bovine serum albumin (ii) polarographic estimation of lead in the presence of gelatin[6]; (iii) the investigation of GURD AND MURRAY[7] on the combination of lead ion with human serum albumin by the equilibrium dialysis technique and (iv) an indirect approach to the study of the lead complexes of egg albumin, haemoglobin and gelatin by SUZUTANI[8,9] who estimated free lead polarographically in the solution obtained after the complete adsorption of the complexes on animal charcoal.

EXPERIMENTAL

Transfusion gelatin (concn. 6%, mol.wt. = 75,000) supplied by the Director, N.C.L., Poona, was used throughout these investigations. Solution of lead nitrate and potassium nitrate were prepared by dissolving the appropriate A.R. salt in doubly distilled water. Walpole acetate and ammonium acetate buffers were prepared in the laboratory and their pH determined by the Beckman pH Meter, Model G.

Polarographic measurements were carried out by means of the Fisher Electropode in conjunction with the Multiflux Galvanometer (Type MG F2) in the external circuit. An H-shaped polarographic cell was found to be suitable for de-areation of the protein solution and for subsequent measurements at the D.M.E. The capillary used had a flow rate of 2.2 mg/sec with a drop time of 3.6–3.8 sec. The temperature of the solution was maintained at $30 \pm 0.1°$ by keeping the cell immersed in a thermostatic water bath (Townson and Mercer, Croydon).

The following sets were subjected to polarographic analysis:

(i) 1 ml of lead nitrate solution (0.01 *M*), 8 ml of acetate buffers pH 3.72, 4.45, 4.8,

5.2 and 5.57 and 2 ml of protein solutions were mixed and the total volume made up to 20 ml by adding potassium nitrate so that the ionic strength was adjusted to 0.15 in each case. Similar sets were analysed, using ammonium acetate–ammonia buffers of pH 5.5, 5.95, 6.35, and 6.8. The diffusion current of lead ions at different pH values in the absence of protein remained constant up to pH 5.5 and then decreased with increase in pH. This was attributed to the existence of aqua-complexes[5] at higher pH ranges. This fact was taken into consideration when computing the value of $i_d/(i_d)_0$. The results are shown in Table 1 (A and B) and Fig. 1.

TABLE 1A

CONCENTRATION OF PROTEIN, $0.8 \cdot 10^{-4}\ M$; CONCENTRATION OF Pb(II), $0.5 \cdot 10^{-3}\ M$; WALPOLE ACETATE BUFFER

pH	$i_d/(i_d)_0$	$C_b \cdot 10^{-3}\ M$	$\bar{V}_M$
3.72	0.918	0.136	1.7
4.45	0.910	0.150	1.9
4.80	0.902	0.163	2.0
5.20	0.869	0.218	2.7
5.57	0.853	0.245	3.1

TABLE 1B

CONCENTRATION OF PROTEIN, $0.8 \cdot 10^{-4}\ M$; CONCENTRATION OF Pb(II), $0.4 \cdot 10^{-3}\ M$; AMMONIUM ACETATE–AMMONIA BUFFER

pH	$i_d/(i_d)_0$	$C_b \cdot 10^{-3}\ M$	$\bar{V}_M$
5.50	0.810	0.253	3.2
5.95	0.790	0.280	3.5
6.35	0.780	0.293	3.6
6.80	0.780	0.293	3.6

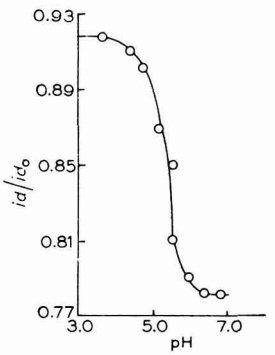

Fig. 1. Effect of pH on the diffusion current depression; $\mu = 0.15$.

(ii) Varying amounts of protein were mixed with a fixed amount of lead nitrate (1 ml) and acetate buffer (8 ml of pH 5.57) was added and the total volume made up to 20 ml with the ionic strength being kept at 0.15 in each case. Solutions of high protein content ($1.8–2.0 \cdot 10^{-4}\ M$) precipitated within an hour. In these cases analysis was carried out immediately after mixing. The results are shown in Table 2 and Fig. 2.

TABLE 2

CONCENTRATION OF Pb(II), $0.5 \cdot 10^{-3}$ *M*

Concn. of protein $\cdot 10^{-4}$ *M*	$i_d/(i_d)_0$	$C_b \cdot 10^{-3}$ *M*	$\overline{V}_M$
0.4	0.914	0.143	3.5
0.6	0.885	0.191	3.2
0.8	0.853	0.245	3.1
1.2	0.814	0.310	2.6
1.4	0.743	0.428	3.0
1.6	0.728	0.453	2.8
1.8	0.709	0.485	2.7
2.0	0.704	0.493	2.5

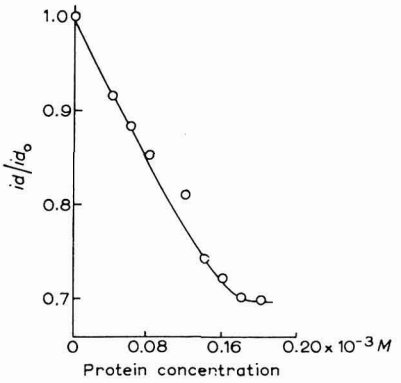

Fig. 2. Effect of protein concn. on the diffusion current decrease.

TABLE 3

CONCENTRATION OF PROTEIN, $0.8 \cdot 10^{-4}$ *M*

Concn. of Pb(II) $\cdot 10^{-3}$ *M*	$i_d/(i_d)_0$	$C_b \cdot 10^{-3}$ *M*	$\overline{V}_M$
1.0	0.893	0.356	4.4
0.75	0.866	0.335	4.1
0.50	0.853	0.245	3.1
0.35	0.840	0.186	2.3
0.20	0.725	0.183	2.2
0.10	0.700	0.100	1.2

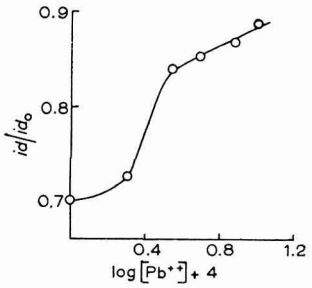

Fig. 3. Effect of metal ion concn. on diffusion current decrease.

(iii) Varying amounts of lead nitrate solution were mixed with a fixed amount of gelatin, and acetate buffer (8 ml of pH 5.57) was added keeping the total volume 20 ml and ionic strength at 0.15. The results are summarised in Table 3 and Fig. 3.

In all, 70 polarograms were taken. The typical ones are illustrated in Fig. 4. The reversibility was tested by the equation given by TOMES[10].

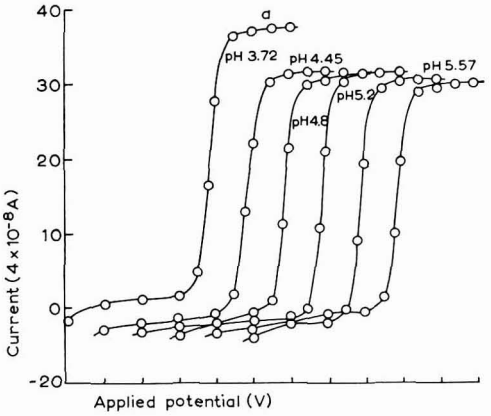

Fig. 4. Polarograms. Protein concn. $0.8 \cdot 10^{-4}$ M; Pb^{2+} concn. $0.5 \cdot 10^{-3}$ M; $\mu = 0.15$ Curve (a), protein absent. Each curve starts at 0 V, 1 cm $\simeq -0.1$ V.

The following method was adopted for pH-metry:

2 ml of transfusion gelatin (3%, pH 5.8), 2 ml of lead nitrate solution (pH 5.8) and varying amounts of hydrochloric acid were mixed in different test tubes keeping the total volume at 10 ml and the ionic strength at 0.15. The pH of each solution was recorded immediately after mixing and then again after 24 hours. The value were found to be the same in both cases. The measurements were repeated without lead ion but maintaining the same conditions. The results are given in Table 4.

RESULTS AND DISCUSSION

Taking the molecular weight of transfusion gelatin as 75,000, the number of metal ions bound per protein molecule, $\bar{V}_M$, was computed from the values obtained by the following relationship:

$$C_b = C - C_F$$

and TANFORD's equation

$$i_d/(i_d)_0 = \frac{C_F + kC_b}{C}$$

where C_F, C_b and C are the free, bound and total metal concentration; $id/(id)_0$ is the depression in diffusion current (given in column 2 of Tables 1, 2 and 3); k is the limiting value of $i_d(i_d)_0$ obtained from curves 2 and 3.

The values given in Table 4, column 2, are converted into free hydrogen ions assuming that the activity of hydrogen ion (a_{H^+}) depends only upon the non-protein constituent of the solution even in presence of protein. The pH is given as

$$pH = -\log a_{H^+}$$

The activity coefficients at ionic strength 0.15 (in extreme acid ranges) are taken from TANFORD[11]. The difference between added and free hydrogen ions gives the number of hydrogen ions bound to the protein (Table 4, column 4), From this the number of hydrogen ions dissociated per protein molecule is evaluated both in the presence and absence of metal ions (Table 4, column 5).

TABLE 4A

CONCENTRATION OF PROTEIN, $0.8 \cdot 10^{-4}$ M

H^+ added ($moles/l \cdot 10^{-3}$)	pH	Free H^+ ($moles/l \cdot 10^{-3}$)	Bound H^+ (moles/mole protein)	Moles of H^+ dissociated per mole protein
0	5.56	—	—	—
0.8781	4.9	0.01258	11.0	59
1.7562	4.6	0.02511	22.0	48
3.5124	4.0	0.1000	43.0	27
5.2686	3.5	0.3162	62.0	8
6.1467	3.15	0.7029	68.0	2
7.9029	2.7	2.223	71.0	0
12.2936	2.23	6.683	70.0	0

TABLE 4B

CONCENTRATION OF PROTEIN, $0.8 \cdot 10^{-4}$ M; CONCENTRATION OF Pb(II), $0.4 \cdot 10^{-3}$ M

H^+ added ($moles/l \cdot 10^{3}$)	pH	Free H^+ ($moles/l \cdot 10^{3}$)	Bound H^+ (moles/mole protein)	Moles of H^+ dissociated per mole protein
0	5.58	—	—	—
0.70248	4.7	0.01995	9.0	61
1.7562	4.3	0.05011	21.0	49
3.5124	3.7	0.1995	41.0	29
5.2686	3.3	0.5011	59.5	10
6.1467	3.08	0.8709	66.0	4
7.9029	2.65	2.494	67.0	3
12.2936	2.22	6.837	68.0	2

The appreciable reduction in diffusion current of metal ions in the presence of a large amount of protein has been ascribed to: (i) the probable complex formation[5,12,13,14] between metal and protein; (ii) adsorption[15] and (iii) viscosity[12] effects. Since the present investigations were carried out at pH 5.5 and above, and every care was taken to keep the protein in the native state, the influence of non-specific factors like adsorption and viscosity can very well be ruled out, and the relative depression in diffusion current can be safely taken as a measure of metal–protein combination. The fact that the value of $\bar{\nu}_M$, the number of metal ions bound per protein molecule, remained the same at all protein concentrations, and a limiting value for $i_d/(i_d)_0$ was realised either by changing the metal: protein ratio or pH, also leads to the same conclusion.

From Table 1 it is seen that C_b is highly dependent upon pH. The changes are most marked in the vicinity of pH 5.0, showing therefore that the uptake of metal ions by

the protein increases more rapidly in the pH range 5.2–5.57. Here all the 84 carboxyl groups of transfusion gelatin are deprotonated[2], and are thus available for the binding of metal ions. It may, therefore, be concluded that the carboxyl groups offer the principal sites for the binding of plumbous ions.

This view is further supported by the results on hydrogen ion equilibria in the presence and absence of metal ions (Table 4 A and B). Assuming that metal ions compete with hydrogen ions for the common site (carboxylate ion) on the protein molecule, the following conclusions may be drawn:

1. The amount of hydrogen ions given out by the protein is greater in the presence of lead than with protein alone (Table 4 A and B, column 3). This would be the case if the replacement of hydrogen ions by lead, from the carboxyl groups of the protein, is visualised, especially as the observations were made at the lower pH range.

2. There is a difference of two hydrogen ions per protein molecule for mixtures with and without metal ions (Table 4 A and B, column 5). Normally such data would point towards a possible combination of one lead ion with two carboxyl groups resulting an intramolecular cross-linking. But we assume, with GURD AND MURRAY[7], "a one-to-one binding", which appears to be more plausible in the case of the lead–protein complex[16]. This difference in hydrogen ion concentration directly determines the number of Pb(II) ions bound per protein molecule[17], thus $\bar{\nu}_M$ appears to be 2 at a total metal concentration $0.4 \cdot 10^{-3}$ M.

The intrinsic association constant for the lead–gelatin complex was calculated by applying SCATCHARD's equation.

$$K = \frac{\bar{\nu}_M}{(n - \bar{\nu}_H - \bar{\nu}_M)C}$$

where $\bar{\nu}_M$ and $\bar{\nu}_H$ are the active sites covered by the metal ions and hydrogen ions respectively, n is the total number of such sites, C is the total metal concentration and K is the intrinsic association constant, the values of n and $\bar{\nu}_H$ are taken from the literature[2]. Using this equation, log K was found to be 1.87 by inserting the value for $\bar{\nu}_M$ obtained by polarography, and 1.91 by inserting the value for $\bar{\nu}_M$ determined indirectly from pH-metry. The constancy of log K is proof of the assumption that only one Pb(II) ion is bound with one carboxyl group and that the pH-metric method is valid.

The free energy change of the combination at 30° was

$$\Delta F = -2.593 \text{ kcal.}$$

ACKNOWLEDGEMENT

Thanks are due to Prof. A. R. KIDWAI for providing facilities and to Prof. K. VENKATARAMAN, Director, National Chemical Laboratory, Poona, India for the supply of transfusion gelatin.

SUMMARY

Polarographic and pH-metric studies of mixtures containing lead nitrate and transfusion gelatin were undertaken to ascertain how plumbous ions were bound to the protein. Experiments carried out with varying concentrations of the reactants at a fixed ionic strength and under vaying pH conditions have shown the existence of a

metal–protein complex in the pH range 3.7–5.57. Experiments carried out at a higher pH range (5.9–6.8) gave little or no evidence for the binding of lead to the imidazole groups. An alternative procedure, identical in principle with BJERRUM's method, was employed to calculate $\bar{V}_M$ from the difference in hydrogen ion data in the presence and absence of metal. Evidence is presented for a one-to-one binding of plumbous ion to the carboxylate ion of transfusion gelatin, for which the intrinsic association constant was calculated as 1.87 and the free energy change of the combination as — 2.593 kcal.

RERERENCES

1 S. L. KALRA, G. SINGH AND M. RAM, *Indian J. Med. Res.*, 46 (1958) 171.
2 W. U. MALIK AND SALAHUDDIN, *J. Electroanal. Chem.*, 5 (1963) 68.
3 W. U. MALIK AND SALAHUDDIN, *J. Electroanal. Chem.*, 5 (1963) 147.
4 W. U. MALIK AND SALAHUDDIN, *Nature*, (in press).
5 C. TANFORD, *J. Am. Chem. Soc.*, 74 (1952) 211.
6 T. TACHIBANA, K. TAMAMUSHI AND R. TAMAMUSHI, *J. Biochem., (Tokyo)*, 44 (1957) 33; *C.A.* 51, 7748.
7 F. R. N. GURD AND G. R. MURRAY, *J. Am. Chem. Soc.*, 76 (1954) 187.
8 T. SUZUTANI, *Japan, J. Physiol.*, 1 (1951) 213, *C.A.* 45, 6895h.
9 T. SUZUTANI, Sbornik Mezinarod. Polarograf. Sgezdu Praze, Ist Congr. Pt., 1 (1951) 425; *C.A.* 46, 9931i.
10 J. TOMES, *Collection Czech. Chem. Communs.*, 9 (1937) 12.
11 C. TANFORD, *J. Am. Chem. Soc.*, 72 (1950) 441.
12 I. M. KOLTHOFF AND J. J. LINGANE, *Polarography*, Interscience Publishers Inc., New York, 1952, p. 397.
13 C. TANFORD, *J. Am. Chem. Soc.*, 73 (1951) 2066.
14 C. TANFORD, *ibid.*, 74 (1952) 6036.
15 K. WIESNER, *Collection Czech. Chem. Commun.*, 12 (1947) 594.
16 F. R. N. GURD AND P. E. WILCOX, *Advances in Protein Chemistry*, Vol. XI, Academic Press Inc. Publishers, New York, 1956, p. 311.
17 C. TANFORD, *Physical Chemistry of Macromolecules* John Wiley and Sons, Inc., New York, 1961, p. 576.

CHRONOPOTENTIOMETRY WITH CURRENT REVERSAL EFFECT OF UNEQUAL FORWARD AND REVERSE CURRENT DENSITIES

DANIEL J. MACERO AND LARRY B. ANDERSON

Department of Chemistry, Syracuse University, Syracuse 10, N.Y. (U.S.A.)

(Received June 10th, 1963)

In chronopotentiometry with current reversal, an electrode process in a given direction can be suddenly made to take place in the opposite direction by simple reversal of the current. This technique has been shown[2,7] to be extremely useful in evaluating thermodynamic and electrode kinetic quantities for both reduction and oxidation processes.

The general theory for a cathodic process followed by an anodic process on current reversal has been presented by BERZINS AND DELAHAY[1]. These authors, however, derived the relationships for potential variation and transition time for the reverse process, only for the specific case where the current densities are equal in both the forward and reverse direction. It seemed desirable to vary the current density of the reverse electrode process with respect to the forward current density and to ascertain the effect on the derived thermodynamic and kinetic quantities.

EXPERIMENTAL

Reagents

All chemicals were of analytical reagent grade.

Apparatus

The constant current was supplied by a variable 450 V regulated power supply feeding through a series of dropping resistors of from 400 KΩ–4.9 MΩ. By means of a suitable switching arrangement the ratio of the reverse to the forward current could be adjusted from 0.05 to 1.00 using the same load resistors for the forward and reverse process. The currents were determined by measuring the voltage drop across a General Radio Type 500-H precision resistance in series with the electrolysis cell.

The electrolysis cell was adapted from a design by DELAHAY AND MATTAX[4]. The mercury pool potential was measured against a saturated NaCl silver–silver chloride reference electrode ($E_{ref.} = 0.192$ V *vs.* N.H.E.). A platinum gauze electrode served as the auxiliary electrode and was separated from the mercury pool compartment by a medium porosity fritted glass disk. Solutions were de-aerated by bubbling purified nitrogen saturated with water vapor at 25° through the solution for 5–10 min before a run and over the solution during the course of the run. All measurements were made at 25.0 ± 0.1°.

The output from the electrolysis cell was fed into a Beckman, Model H pH-meter which was modified to serve as a cathode follower. This in turn was connected to a Minneapolis Honeywell Type Y153X Recorder with 2.5 mV fullscale sensitivity, $\frac{1}{2}$ sec full scan and a chart speed of 8 in. /min. The pH-meter output was shunted with a variable resistance to enable the voltage axis of the strip chart recorder to be expanded for precision potential measurements. The voltage axis of the recorder and the constant current were calibrated prior to each run.

The rectification of the experimental potential–time curves was accomplished with the aid of an I.B.M. 650 computer. A computer program was designed to calculate the appropriate ln $f(t)$ data, fit these data to a least-squares best straight line and then calculate from the slope and intercept the desired thermodynamic and kinetic quantities.

Transition times were measured after the method suggested by DELAHAY AND MAMANTOV[3].

DISCUSSION AND RESULTS

For the sake of simplicity a forward electrode process will be treated as a reduction and the reverse process as a re-oxidation. The treatment, of course, applies equally well to an oxidation process followed by re-reduction.

Reversible re-oxidation processes

For a reversible electrode reaction the forward process is simply reversed when the current is reversed, *i.e.*, $O + n\,e \rightleftharpoons R$. The concentration of substance R at the electrode surface during the re-oxidation process is given by BERZINS AND DELAHAY[1]:

$$C_R(O,t') = 2\theta\left[\frac{D_R(\tau + t')}{\pi}\right]^{1/2} - 2(\theta + \lambda')\left[\frac{D_R t'}{\pi}\right]^{1/2} \tag{1}$$

with

$$\theta = \frac{i_o}{nFD_R} \quad \text{and} \quad \lambda' = \frac{i_o'}{n'FD_R}$$

i_o and i_o' are the forward and reverse current densities respectively, τ is the transition time for the forward process and t' the time elapsed since reversal of the current.

The concentration of substance O at the electrode surface during re-oxidation is

$$C_o(O,t') = C^\circ - C_R(O,t') \tag{2}$$

assuming the diffusion coefficients of oxidized and reduced forms to be equal.

From these equations the potential–time relation for the reversible re-oxidation step using unequal current densities for the forward and reverse process is obtained:

$$E = E_{1/2} + \frac{RT}{nF} \ln\left\{\frac{\tau^{1/2} - [(\tau + t')^{1/2} - (1 + a)(t')^{1/2}]}{(\tau + t')^{1/2} - (1 + a)(t')^{1/2}}\right\} \tag{3}$$

where $a = i_o'/i_o$.

The potential is therefore dependent on the ratio of the reverse to forward current densities. At equal forward and reverse current densities, $a = 1$ and eqn. (3) reduces to DELAHAY's relationship (8–35)[2]:

$$E = E_{1/2} + \frac{RT}{nF} \ln \left\{ \frac{\tau^{1/2} - [(\tau + t')^{1/2} - 2t'^{1/2}]}{(\tau + t')^{1/2} - 2t'^{1/2}} \right\} \quad (4)$$

A plot of the potential, E, against the log term in eqn. (3) should be a straight line with slope equal to RT/nF and an intercept equal to $E_{1/2}$. Equation (3) was verified experimentally for the case of 1 mM Cd^{2+} in 0.1 M KCl solution.

Half-wave potential for reversible re-oxidation

When the fraction in the logarithmic term in eqn. (3) is equal to unity, the time t' corresponds to the time where $E = E_{1/2}$ for the forward process. For equal forward and reverse current densities ANSON *et al.*[6] have shown that this occurs when $t'/\tau' = 0.215$. For any current density ratio, however, the time at which E becomes equal to $E_{1/2}$ or $(t')_{E=E_{1/2}}$ is given by the expression:

$$(t')_{E=E_{1/2}}/\tau' = \frac{1}{4a(a+2)} \left[\sqrt{4a^2 + 8a + 1} - (1 + a) \right]^2 \quad (5)$$

A plot of the ratio $(t')_{E=E_{1/2}}/\tau'$ *vs.* the right hand portion of eqn. (5) for various values of a from 0–1 can be made to facilitate the evaluation of $(t')_{E=E_{1/2}}$. This is shown in Fig. 1. It can be seen that as the current density ratio becomes smaller the distortion of the potential–time curve becomes greater. It can also be shown that the curve asymptotically approaches the value 0.25 as a becomes infinite.

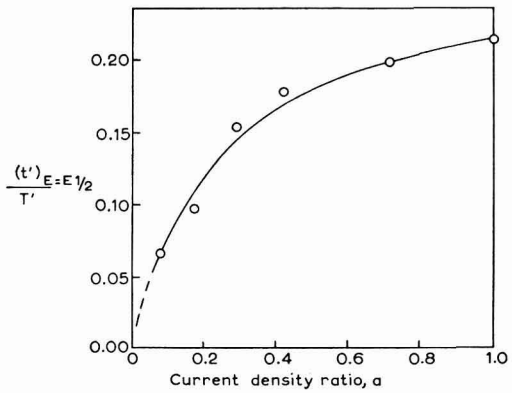

Fig. 1. Plot of $(t')_{E=E_{1/2}}/\tau'$ as a function of the current density ratio, a.

A test of eqn. (5) was made with chronopotentiograms of 1 mM Cd^{2+} in 0.1 M KCl solution. These values are represented in Fig. 1 by open circles.

Transition time ratio

The transition time, τ', for the re-oxidation process can be shown to be related to the transition time, τ, for the reduction process and the current density ratio by eqn. (6).

$$\tau'/\tau = \frac{1}{a(a+2)} \quad (6)$$

Note that when $a = 1$, $\tau'/\tau = 0.333$.

In Table 1 are given the predicted and observed values of the ratio, τ'/τ for the system containing 1 mM Cd^{2+} in 0.1 M KCl solution. Each experimentally observed ratio listed, is the average of four measurements.

TABLE 1

PREDICTED AND OBSERVED VALUES OF τ'/τ FOR VARIOUS CURRENT DENSITY RATIOS

a	τ'/τ (calc.)	τ'/τ (obs.)
1.000	0.333	0.335 ± 0.012
0.726	0.505	0.500 ± 0.017
0.431	0.954	0.964 ± 0.045
0.213	2.117	2.122 ± 0.035

The use of a smaller current density in the reverse direction expands the experimental potential–time trace but it is evident from Table 1 above that no increase in precision is obtained since all the values have an uncertainty of approximately 4%.

Irreversible re-oxidation processes

For a totally irreversible re-oxidation process the rate of the electrode reaction is given by:

$$\frac{i_o'}{n'F} = k_{b,h}{}^{\circ} C_R(O,t') \exp\left[\frac{(1-\alpha')n_a' FE}{RT}\right] \tag{7}$$

where i_o' is the current density for the re-oxidation step, n' the number of electrons involved in the over-all electrode reaction, $k_{b,h}{}^{\circ}$ the heterogeneous rate constant for the re-oxidation, $(1-\alpha')$ the transfer coefficient for the re-oxidation process, and n_a' the number of electrons involved in the re-oxidation rate-determining step.

Substituting eqn. (1) for $C_R(O,t')$ gives:

$$\frac{i_o'}{n'F} = k_{b,h}{}^{\circ}\left\{2\theta\left[\frac{D_R(\tau+t')}{\pi}\right]^{1/2} - 2\left[\theta+\lambda'\right]\left[\frac{D_R t'}{\pi}\right]^{1/2}\right\} \exp\left[\frac{(1-\alpha')n_a' FE}{RT}\right] \tag{8}$$

Again assuming that D_R and D_O are equal results in the following equation for the variation of potential of the re-oxidation step with time at unequal current densities:

$$E = \frac{RT}{(1-\alpha')n_a'F}\ln\frac{i_o{}^{\circ}}{n'FC^{\circ}k_{b,h}{}^{\circ}} + \frac{RT}{(1-\alpha')n_a'F}\ln\left[\frac{\tau^{1/2}}{(\tau+t')^{1/2}-(1+a)(t')^{1/2}}\right] \tag{9}$$

When $a = 1$ then

$$E = \frac{RT}{(1-\alpha')n_a'F}\ln\frac{i_o'}{n'FC^{\circ}k_{b,h}{}^{\circ}} + \frac{RT}{(1-\alpha')n_a'F}\ln\left[\frac{\tau^{1/2}}{(\tau+t')^{1/2}-2(t')^{1/2}}\right] \tag{10}$$

which on substitution of the Sand relation for τ reduces to DELAHAY's equation (8–37)[2].

From eqn. (9) it is predicted that a plot of $\ln[\tau^{1/2}/(\tau+t')^{1/2}-(1+a)(t')^{1/2}]$ *vs.* potential should yield a straight line whose reciprocal slope equals $RT/(1-\alpha')n_a'F$. From this and the potential at time $t' = 0$, the value of the heterogeneous rate constant, $k_{b,h}{}^{\circ}$, can be evaluated.

Equation (9) was verified experimentally for the case of the irreversible re-oxidation of nickel in 1 M sodium perchlorate solution. Linear log $[f(t)]$ *vs.* potential plots at different current density ratios, were obtained in all cases. These are shown in Fig. 2. As can be seen from the graph, the linearity of each plot improves as the current density ratio decreases. This is a result of the increased precision in picking off points from the expanded potential–time curve. The fact that the slopes remain essentially constant for each curve indicates that there is little change in the rate-determining step over a ten-fold change in the current density ratio.

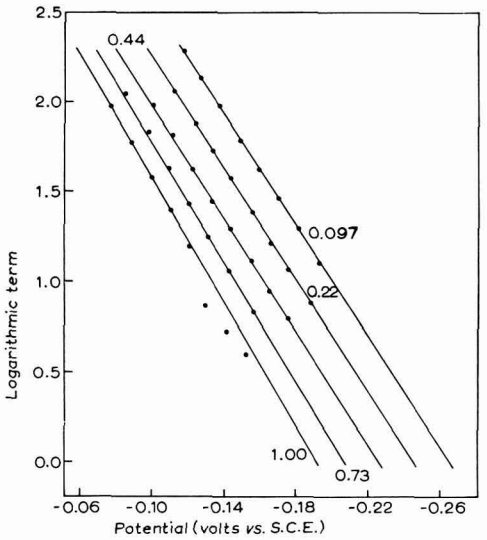

Fig. 2. Log plot for the irreversible process 1 mM Ni^{2+} in 1 M $NaClO_4$. The numbers on each curve correspond to the current density ratio used.

Values for $(1 - \alpha')n_{a'}$ and $k_{b,h}^{\circ}$ were calculated from the slopes and intercepts, respectively, for each curve and these are presented in Table 2 below.

TABLE 2

VALUES OF $(1 - \alpha')n_{a'}$ AND $k_{b,h}^{\circ}$ FOR THE RE-OXIDATION OF NICKEL ION AT DIFFERENT CURRENT DENSITY RATIOS

a	$(1 - \alpha')n_{a'}$	$k_{b,h}^{\circ} 10^4$ (cm sec^{-1})
1.000	0.462	3.15
0.729	0.423	2.47
0.435	0.396	3.40
0.217	0.390	2.20
0.097	0.395	2.47
	0.413 ± 0.026	2.74 ± 0.46

The constancy of the heterogeneous rate constant, $k_{b,h}^{\circ}$, also indicates that the nature of the rate-determining step is the same in all cases. Since the nickel system in perchlorate medium is extremely irreversible (overvoltage approximately 0.4 V) this behavior is not unusual.

DELAHAY AND MATTAX[4] report a value of $2.95 \cdot 10^{-13}$ cm sec^{-1} for the heterogeneous formal rate constant for the reduction of Ni^{2+} in 1 *M* KCl. Using this and our average value for the oxidation of nickel in 1 *M* perchlorate medium, the formal standard reduction potential of the nickelous–nickel system was calculated by means of the relationship

$$E_f^{\circ} = \frac{RT}{nF} \ln \frac{k_{f,h}^{\circ}}{k_{b,h}^{\circ}}$$

The value of -0.246 V *vs.* N.H.E. was obtained. This is in good agreement with the value of -0.250 V estimated by LATIMER[5] for this system.

The value of the forward current density for all the nickel runs was kept constant at 63.5 μA. per cm^2. At this current density the τ'/τ ratio was found to follow equation (6). The effect of increasing the Ni^{2+} concentration and the forward current density is being studied.

ACKNOWLEDGEMENT

The authors are grateful to the Syracuse University Computing Center for sponsoring time on the I.B.M. 650 Computer.

SUMMARY

The theory of current reversal chronopotentiometry has been extended to take into account unequal forward and reverse current densities. Equations have been derived for the potential–time dependence on the current density ratio for reversible and irreversible re-oxidations. The dependence of the ratio of the reverse to forward transition time on the current density ratio was established. The time at which the potential is equal to the half-wave potential for the re-oxidation step was shown to depend on the current density ratio and verified experimentally.

A study was made of the irreversible nickel–nickelous system in 1 *M* sodium perchlorate using the equations derived. A value of $k_{b,h}^{\circ}$ equal to $2.74 \cdot 10^{-4}$ cm sec^{-1} at 25°. was calculated for the re-oxidation step and the value of -0.246 V *vs.* N.H.E. established as the formal reduction potential of the Ni^{2+}–Ni system.

REFERENCES

1 T. BERZINS AND P. DELAHAY, *J. Am. Chem. Soc.*, 75 (1953) 4205.
2 P. DELAHAY, *New Instrumental Methods in Electrochemistry*, Interscience Publishers Inc., New York, 1954, Chapter 8.
3 P. DELAHAY AND G. MAMANTOV, *Anal. Chem.*, 27 (1955) 478.
4 P. DELAHAY AND C. C. MATTAX, *J. Am. Chem. Soc.*, 76 (1954) 874.
5 W. M. LATIMER, *Oxidation Potentials*, 2 nd Edn., Prentice-Hall, New York, 1952, p. 200.
6 W. F. PALKE, C. D. RUSSELL AND F. C. ANSON, *Anal. Chem.*, 34 (1962) 1171.
7 A. C. TESTA AND W. H. REINMUTH, *ibid.*, 32 (1960) 1512.

VOLTAMMETRY OF IRON IN MOLTEN LITHIUM FLUORIDE–POTASSIUM FLUORIDE–SODIUM FLUORIDE

D. L. MANNING

Analytical Chemistry Division, Oak Ridge National Laboratory, Oak Ridge, Tennessee (U.S.A.)*

(Received May 21st, 1963)

Extensive investigations have been reported on the voltammetry of electro-active species in molten salt systems[1–5]. From such work, valuable insight has been gained into the behavior of electro-active constituents in molten chloride and molten nitrate systems and to a lesser degree, sulfate and phosphate melts. Probably molten fluoride salt systems have been least investigated of all. Interest in molten fluorides has, however, increased immensely in recent years due to their potential use as constituents of reactor fuels.

In this report the voltammetry of iron(II) in molten LiF–NaF–KF (46.5–11.5–42 mole %) is described. Iron is of interest because it is a corrosion product associated with reactor fuels of the molten salt type. In addition to offering a potential means of analysis, voltammetry should also provide valuable information regarding the oxidation state of the electro-active constituent in the melt.

A controlled-potential polarograph[6] coupled with a platinum quasi-reference electrode[7,8] was used to record the current–voltage curves. The advantage of the controlled-potential polarograph, especially in fused salt voltammetry, is that an inert substance can be used as a quasi-reference electrode. The cell current does not flow through the reference electrode, therefore it remains unpolarized and at essentially constant potential, as the current–voltage curve is recorded. Half-wave potentials relative to the quasi-reference electrode are arbitrary; nevertheless, they are reproducible as long as the same electrode combination is used. This becomes especially useful when working with highly corrosive melts.

EXPERIMENTAL

The eutectic LiF–NaF–KF (46.5–11.5–42 mole %) was used as the solvent electrolyte. The salt was first purified in a platinum container enclosed in a nickel apparatus. Purification consisted of purging the molten salt with helium, followed by several hydrogen fluoride and hydrogen gas treatments, with a final treatment with helium[9].

The ORNL Model Q-1988 controlled-potential polarograph[6] was used to record the current–voltage curves.

The melt was contained in a graphite cell approximately 2 in. in diam. and $4\frac{1}{2}$ in. long. The cell was fitted with a porous graphite thimble-type inner compartment which accommodated the isolated counter electrode.

To maintain a vacuum or controlled atmosphere, the cell was enclosed in a quartz

* Operated by Union Carbide Corporation for the U.S. Atomic Energy Commission.

jacket approximately $2\frac{1}{2}$ in. in diam. and 10 in. long. The top of the quartz jacket was fitted with a 102/75 ball and socket joint, the socket portion of which served as a removable cap for the enclosure. On the cap were located five $^3/_{16}$ in. Swagelok compression-type fittings which provided access to the melt for the various electrodes, thermocouple and helium bubbling tube. Vacuum and inert atmosphere connections were provided for by means of a three-way vacuum stopcock also located on the cap. For heating, the cell assembly was placed in a 3-in. ID resistance furnace. The temperature of the furnace was controlled to about $\pm$ 2° by means of a Wheelco Model 407 temperature controller. The temperature of the melt was monitored with a platinum–platinum/rhodium (10%), thermocouple; its output was measured with a Leeds and Northrup precision temperature potentiometer connected through an ice bath to the thermocouple.

The electrodes consisted of 2 in. lengths of 0.5 and 1.0 mm diam. platinum wires which were gold-soldered on to the ends of $^1/_8 \times 12$ in. nickel rods. The tops of the nickel rods were fitted with $^3/_{16}$ in. Teflon sleeves to provide a tight connection when the electrodes were inserted through the $^3/_{16}$ in. fittings. The area of the electrode exposed to the melt was controlled by the depth at which it was immersed. The indicator electrode (0.5 mm diam.) was immersed to a depth of 7 mm. The platinum quasi-reference electrode (1 mm diam.) and the counter electrode were adjusted to about 2 cm depth; this, however, is not critical. The counter electrode dipped into the melt contained in the porous graphite thimble-type inner compartment.

To prevent moisture contamination of the salt, the cell and enclosure, with the $^3/_{16}$ in. fittings stoppered with short glass rods, were out-gassed at 600° and $< 5\ \mu$ pressure for 24 h. After cooling, the assembly was filled with dry helium (liquid nitrogen trapped) and then placed in a dry box. Approximately 100 g of the purified salt, weighted to the nearest 0.1 g was then placed in the cell. Additional salt was added to the inner compartment so that the depths of the melts in the counter electrode compartment and in the cell were kept the same. The assembly was placed in the furnace and evacuated and flushed with helium several times. With an over-pressure of helium in the system, the salt was melted. The electrodes, helium bubbling tube and thermocouple were next inserted into the cell enclosure while helium was allowed to flow rapidly through the system. The sweep continued for several minutes and then the helium was adjusted to a pressure of about 2 lbs/in.^{2}. Current–voltage curves were recorded after the desired temperature and thermal equilibrium were attained. The concentration of iron(II) in the melt was varied by electrolytic oxidation of a pure iron anode. The concentration of iron was calculated from Faraday's law, the weight of the melt and its density, 2.0 g/cm^3.

Considerable difficulty was encountered in maintaining a reproducible surface on the micro-electrode. After a few experiments, it became necessary to remove the electrode from the cell and polish it with fine-grade emery paper. After each experiment, however, the iron was removed anodically from the electrode at a potential of 0.0 V *vs.* the platinum quasi-reference electrode. When not in use, the electrodes were raised out of the melt. At no time was the melt or the salt opened to the atmosphere. All additions to the salt, transfers, etc. were carried out within a dry box.

RESULTS AND DISCUSSION

A typical current–voltage curve of iron(II) in the molten LiF–NaF–KF eutectic at

495° is shown in Fig. 1. Two waves are noted, an anodic wave which is believed to correspond to the oxidation of $Fe^{2+} \rightarrow Fe^{3+}$ with a half-wave potential of approximately + 0.1 V and a cathodic wave which exhibits a half-wave potential of about − 0.5 V *vs.* the platinum quasi-reference electrode. The latter wave represents the

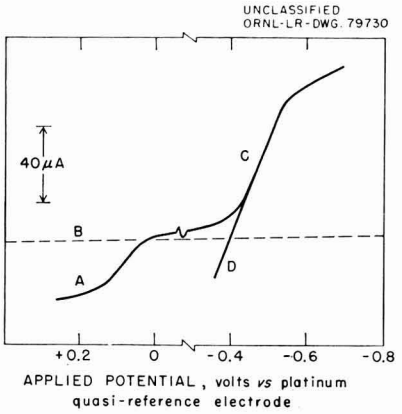

Fig. 1. Automatically recorded current–voltage curves for iron(II): Curve A, anodic; Curve B, zero current line; Curve C, reduction Fe^{2+} to metal; Curve D, reverse scan. Concn. of Fe^{2+}, 8.4 m*M*. Temp., 495°.

reduction of iron(II) to the metal. The current on the limiting current plateau usually exhibited small fluctuations which appeared to be random about an average value and also the current tended to increase somewhat. These effects are probably due to uneven growths of dendritic deposits of iron and to thermal effects that cause convective motion of the molten electrolyte in the vicinity of the indicator electrode.

The potential limits of the melt observed at the platinum micro-electrodes are the reduction of alkali (probably lithium) at about − 2.0 V and the anodic dissolution of platinum at approximately + 1.5 V *vs.* the platinum quasi-reference electrode. Prior to the anodic dissolution of the platinum micro-electrode, a reasonably well-defined anodic wave was also observed which exhibited a half-wave potential of approximately + 1.0 V. This wave was not identified. The purity of the melt from spectroscopic analyses was such as to preclude any extraneous metallic impurities. Possibilities, however, do include the oxidation of traces of oxide impurity ($O^{2-} \rightarrow {}^1/_2\, O_2$) or possible oxide ion de-polarization effects on the platinum electrode. Further investigations are contemplated to elucidate the nature of this wave.

The relationship between the limiting current, i_l, and concentration, C, of electroactive species at a solid micro-electrode is expressed by the equation[10]

$$i_l = \frac{nFADC}{l} = kAC \qquad (1)$$

where k is the area independent limiting-current constant, D is the diffusion coefficient, and l is the effective thickness of the diffusion layer. The remaining terms are n, the electron change; A, the area of the electrode; and F, the Faraday.

The concept of the diffusion layer becomes important when considering stirred

solutions or in the case of high temperature melts, where mass transport by convective means is pronounced. The reacting species is brought to this layer by stirring or convective transport and transfer through the layer occurs under the influence of diffusion. A calculation of l, the thickness of the diffusion layer, using eqn. (1) and based on an assumed value for D of 10^{-5} cm^2/sec, gives a value of about 0.3 mm, which appears to be of the right order of magnitude[8,11,12]. As a first approximation, therefore, it appears that the concept of the diffusion layer expressed in eqn. (1) is a useful approach to the study of electrode processes under these conditions. It is applicable regardless of the geometry of the cell; however, as pointed out by DELAHAY[13] the results derived using this concept should be considered only in a qualitative sense.

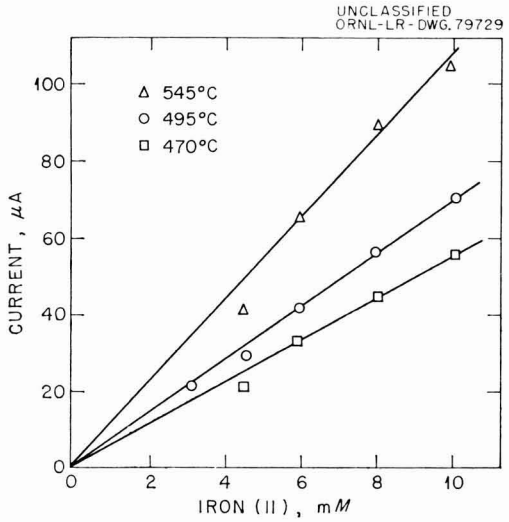

Fig. 2. Limiting current *vs.* concn. of iron. Electrode area, 9.4 mm^2.

To estimate the activation energy of the current limiting process, a plot of log D (or log k, since only D is temperature dependent) *vs.* $1/T$ was constructed as previously discussed[8]. Such a plot is shown in Fig. 3. From the slope of the line and the relationship

$$\log_{10} D = \frac{-E}{2.3\,RT} + \log_{10} A \qquad (2)$$

an E value of approximately 12 kcal is obtained. This compares favorably with other activation energies of limiting current processes in fused salts[2].

Values of k for the reduction of iron at 470, 495 and 545° are given in Table 1. The over-all coefficient of variation of these data is about 13%. A plot of the limiting current *vs.* the concentration of iron is shown in Fig. 2. These results show the limiting current is proportional to the concentration of iron and that the cathodic current–voltage curves appear to be analytically useful.

TABLE 1

EFFECT OF TEMPERATURE ON THE LIMITING CURRENT CONSTANT (k)

Temperature (°C)	*k (average)*	*Coefficient of variation (%)*
470	0.543	15
495	0.735	10
545	1.13	15

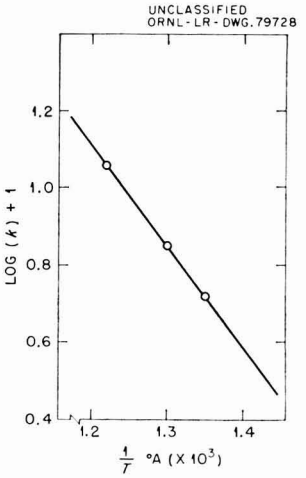

Fig. 3. Plot of log k *vs.* $1/T$. Slope of line, — 2600.

The eqns. generally utilized for reversibility tests, and which describe current–voltage curves obtained at solid micro-electrodes are

$$E = E^{\circ}_{m} - \frac{2.303\,RT}{nF}\log_{10}\frac{k_s}{f_s} + \frac{2.303\,RT}{nF}\log_{10}(i_l - i) \qquad (3)$$

and

$$E = E_{1/2} + \frac{2.303\,RT}{nF}\log_{10}\left(\frac{i_l - i}{i}\right) \qquad (4)$$

where E = applied potential
i_l = limiting current
i = current at any applied potential (E)
and the remaining symbols have their usual thermodynamic significance.

For the application of eqn. (3) which was proposed by KOLTHOFF AND LINGANE[14] it is assumed that the electrode is subject only to concentration polarization, that the metal is deposited on the electrode without alloy formation and that the reaction proceeds reversibly.

The failure of eqn. (3) to be generally applicable was pointed out by DELIMARSKII[2] following which DELIMARSKII AND GORODISKII[15] proposed eqn. (4) derived from the theory of absolute reaction rates. This eqn. is essentially identical with the eqn. proposed by HEYROVSKY and ILKOVIC[16] for the dropping mercury electrode.

Both eqns. were applied to the analyses of the cathodic iron wave and eqn. (4) was utilized to describe the anodic wave. In Fig. 4 are shown plots of $\log_{10}(i_l - i)$ *vs.* E and

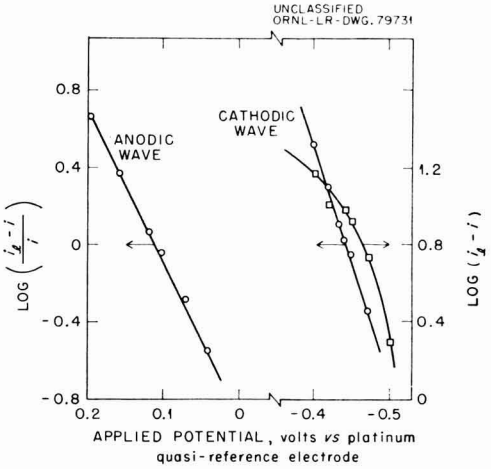

Fig. 4. Log plots for the electrode processes: anodic wave, slope 0.134 (theo. 0.156); cathodic, wave slope 0.072 (theo. 0.078).

$\log_{10}\left(\frac{i_l - i}{i}\right)$ *vs.* E which should result in a straight line with a slope of $2.303\,RT/nF$. As noted from Fig. 4, the HEYROVSKY–ILKOVIC type eqn. appears to describe the anodic wave and furthermore, seems to best describe the cathodic wave. The experimental slopes are in good agreement with theory for reversible electrode reactions. Further evidence for the applicability of this expression is that the anodic and cathodic half-wave potentials did not vary appreciably as the concentration of iron was varied. For the cathodic wave of iron, the hypothesis of DELIMARSKII[2] appears to be generally supported which suggests the formation of surface alloys on a solid electrode or a change in the surface concentration as a result of de-polarization phenomena.

Reversibility is further substantiated by the fact that the stripping curve (curve D, Fig. 1) does not hesitate as it passes through the zero-current axis. In all the reverse-scan tests, the deposited iron stripped off rapidly, which indicates that in the event of any surface alloy formation, the iron nevertheless seems to approach essentially unit activity when the electrode is covered with at least a mono-layer of deposit.

The effect of scan-rate, from 25–150 mV/min, on the general shape of the current–voltage curves was not critical. The limiting current of the iron, within the precision of the measurements, was essentially independent of the scan-rates tested. Apparently, steady-state conditions are achieved very rapidly in the melt. The majority of the curves were recorded at a scan-rate of 100 mV/min.

SUMMARY

The voltammetry of iron(II) in molten LiF–NaF–KF was investigated over the temperature range 470–545°. The current–voltage curves were recorded using a controlled-potential polarograph and a stationary platinum micro-electrode coupled with a platinum quasi-reference electrode. A third platinum electrode, which was isolated,

served as the counter electrode. The reduction of iron(II) to the metal and the oxidation of iron(II) to iron(III) appeared to proceed reversibly under the existing experimental conditions. The limiting current (wave height) of the cathodic wave was proportional to the concentration of iron in the melt. An activation energy of about 12 kcal/mole was calculated for the current limiting process which corresponded to the reduction of iron(II) to the metal.

REFERENCES

1 GEORGE J. JANZ, *Bibliography of Molten Salts*, 2nd edn., Rensselaer Polytechnic Institute, Troy, New York, 1961.
2 YU. K. DELIMARSKII AND B. F. MARKOV, *Electrochemistry of Fused Salts*, The Sigma Press, Publishers, N.W., Washington 7, D.C. 1961, pp. 297–329.
3 D. L. MARICLE AND D. N. HUME, *Anal. Chem.*, 33 (1961) 1188.
4 H. C. GAUER AND W. K. BEHL, *J. Electroanal. Chem.*, 5 (1963) 261–269.
5 H. KIDO, O. MATSUMOTO AND Y. HAYAKAWA, *J. Electrochem. Soc., Japan*, 26 (1958) E-96.
6 M. T. KELLEY, H. C. JONES AND D. J. FISHER, *Anal. Chem.*, 31 (1959) 1475.
7 M. T. KELLEY, *Controlled Potential and Derivative Polarography*, in *Advances in Polarography*, Vol. 1 (edited by I. S. LONGMUIR, Pergamon Press, New York, 1960, pp. 158-82.
8 D. L. MANNING, *Talanta*, 10 (1963) 255.
9 W. R. GRIMES, D. R. CUNEO, F. F. BLANKENSHIP, G. W. KEILHOLTZ, H. F. POPPENDICK AND M. T. ROBINSON, *Chemical Aspects of Molten-Fluoride–Salt Reactor Fuels*, in *Fluid Fuel Reactors*, edited by J. A. LANE, H. G. MACPHERSON AND FRANK MOSLAN, Addison-Wesley, Reading, Mass., 1958, p. 584.
10 I. M. KOLTHOFF AND J. J. LINGANE, *Polarography*, Interscience Publishers, Inc., New York, 1952, Vol. 1, p. 410.
11 L. E. TOPOL AND R. A. OSTERYOUNG, *J. Electrochem. Soc.*, 108 (1961) 573.
12 T. PAVLOPOULOS AND J. STRICKLAND, *ibid.*, 104 (1957) 116.
13 PAUL DELAHAY, *New Instrumental Methods in Electrochemistry*, Interscience Publishers, Inc., New York, pp. 217–227.
14 I. M. KOLTHOFF AND J. J. LINGANE, *Polarography*, Vol. 1, 2nd edn., Interscience Publishers, Inc., New York, 1952, p. 203.
15 YU. K. DELIMARSKII AND O. V. GORODISKII, *Dopovid. Akad Nauk. Ukr. RSR*, (1955), p. 540.
16 J. HEYROVSKY AND D. ILKOVIC, *Collection Czech. Chem. Commun.*, 7 (1955) 198.

THE POLAROGRAPHIC BEHAVIOR OF NICKEL(II) IN ACETONITRILE IN THE PRESENCE OF CHLORIDE ION

IVORY V. NELSON AND REYNOLD T. IWAMOTO

Department of Chemistry, University of Kansas, Lawrence, Kansas (U.S.A.)

(Received June 10th, 1963)

In the presence of high concentrations of chloride, the reduction of nickel(II) in water takes place with greater reversibility and at potentials more positive than that for the hydrated nickel ion[1-5]. This behavior has been attributed to the formation and reduction of chloride complexes of nickel(II). To explain the single continuous composite anodic-cathodic wave obtained by the method of KALOUSEK[6] for nickel(II) ion in aqueous 6 *M* calcium chloride solution, VLCEK[4] has suggested that the tetra-chloronickel(II) ion is reduced at the dropping mercury electrode to the zero-valent nickel complex $NiCl_4^{4-}$. More recently, however, TANAKA, TAMAMUSHI AND KODAMA[5] concluded from their study of the reduction of nickel(II) at the dropping mercury electrode in concentrated calcium chloride solution, that the electrode reaction must be

$$NiCl_4^{2-} + 2\,e + Hg \rightleftharpoons Ni(Hg) + 4\,Cl^-$$

They obtained no direct evidence, however, that $NiCl_4^{2-}$ is the electro-active species. Indeed, because the concentration of chloride required to bring about this phenomenon is near the solubility limit of the most soluble chloride electrolytes, no study involving variation of chloride ion concentration (which could reveal the identity of the electro-active nickel species) is possible in water.

The polarographic behavior of nickel(II) ion in nitrile solvents has been examined by several investigators[7-9]. KOLTHOFF AND COETZEE[7] observed a single reversible wave with a half-wave potential of −0.33 V *vs.* S.C.E. for the reduction of nickel(II) ion in acetonitrile 0.1 *M* in sodium perchlorate. POPOV AND GESKE[8], on the other hand, obtained a two-step wave for the reduction of nickel(II) perchlorate in the same solvent 0.1 *M* in tetra-*n*-butylammonium perchlorate. The half-wave potential of the first step was −0.69 V *vs.* the Ag–$AgNO_3$ (0.01 *M*) electrode in acetonitrile and that of the second was −1.22 V. The total diffusion current was proportional to the concentration of nickel ion; the height of the individual steps, however, was not reproducible. Two-step reduction waves for nickel ion have also been observed in benzonitrile 0.1 *M* in tetra-ethylammonium perchlorate[9]. The investigators attribute the two steps to the reduction of two nickel species. There appears to be little doubt that the second step is due to the reduction of hydrated nickel ion. The nature of the more easily reduced nickel(II) species in benzonitrile solutions 0.1 *M* in tetra-ethylammonium perchlorate, however, was not understood, except when a 0.005% concentration of methyl red was used instead of the usual 0.001%. In benzonitrile solutions 0.005%

in methyl red, only one wave corresponding to the first step of the above solutions, is obtained for the reduction of nickel ion; the second wave is not present. It has been suggested that methyl red interacts with the hydrated nickel ion to produce a nickel species more readily reduced than the hydrated ion. Moreover, since the methyl red concentration is much lower than that of nickel(II) ion, it appears that the methyl red liberated upon reduction of the more easily reduced nickel species containing methyl red, reacts rapidly with hydrated nickel ion to form more of the same nickel(II) species. Because of certain basic similarities in the behavior of nickel(II) ion at the dropping mercury electrode in (i) aqueous concentrated chloride medium and in (ii) benzonitrile containing methyl red, and because chloride complexes in many cases are formed more readily in acetonitrile than in water, *e.g.*, the zinc(II)–chloride system[7], an attempt was made to determine the nature of the more easily reduced nickel species in aqueous concentrated chloride medium by a study of the effect of chloride on the polarographic behavior of nickel(II) ion in acetonitrile. The results of this study are presented here. While this study was in progress, a communication by MARK AND REILLEY on the polarographic behavior of nickel(II) in aqueous solutions containing small amounts of pyridine appeared in the literature[10]. The behavior observed by these investigators for nickel(II) in this medium is similar to that for nickel(II) in benzonitrile in the presence of small amounts of methyl red. A complete account of their study has appeared recently[11].

EXPERIMENTAL

Reagents

Matheson, Coleman and Bell practical grade acetonitrile was refluxed and distilled twice from phosphorus pentoxide in an all-glass apparatus. Only the center portion, b.p. 82 ± 0.5°, was collected.

Tetra-ethylammonium perchlorate (Et_4NClO_4) was prepared by neutralizing a 10% tetra-ethylammonium hydroxide solution (Eastman) to pH 7 with dilute perchloric acid, evaporating almost to dryness on a hot plate, recrystallizing eleven times from water, and drying in a vacuum oven at 70° for 48 h. Hexa-aquo-nickel(II) perchlorate (G. F. Smith Chemical Co.) was dried in a vacuum oven at 60–70° for 72 h. The dried nickel salt was greenish yellow, in contrast to the deep green of the hexahydrate. From the analysis of the water content of the *dried* nickel(II) perchlorate, the formula $Ni(ClO_4)_2$, $2^1/_4$ H_2O was obtained for the dried salt. A 0.10 *M* aqueous solution of the perchlorate showed only a very faint turbidity when made 0.014 *M* in silver nitrate. Cetyl-dimethylbenzylammonium chloride (CDMBCl) was used without further treatment (K and K laboratories). Analysis of the salt showed that it contained 9.08% Cl^-. The theoretical value is 8.95%.

The water content of all the acetonitrile solutions, each containing Et_4NClO_4, nickel perchlorate and cetyl-dimethylbenzylammonium chloride, was found by the Karl Fischer technique to be *ca.* 0.02 *M*.

Procedure

Current–voltage curves were obtained with a KELLEY, JONES, Fisher[12] controlled-potential polarograph. All solutions were examined at 25°. An H-type cell, with the two compartments separated by a sintered glass disc, was used. The dropping mercury electrode was placed in one side arm, and a saturated calomel electrode together

with a platinum foil electrode to function as the auxiliary electrode in a three-electrode system, was placed in the other. The m and t values (open circuit) of the dropping mercury electrode in a 0.1 M solution of Et_4NClO_4 in acetonitrile for $h_{(uncorrected)}$ of 30 cm, were 2.18 mg/sec and 3.69 sec, respectively.

The solutions used in the polarographic study were 1.62×10^{-4} M and 2.04×10^{-4} M in nickel(II) perchlorate, 0.1 M in Et_4NClO_4, and contained varying amounts of CDMBCl. They were de-oxygenated with purified nitrogen and protected from atmospheric oxygen during the course of measurement by passing nitrogen over the surface.

The ultra-violet and visible spectral data were obtained with a Cary Model 14 recording spectrophotometer using matched 1-cm silica cells. Solutions for these measurements were 2.0×10^{-3} M and 1.0×10^{-2} M in nickel(II) perchlorate.

RESULTS

Electrochemical

Two types of polarograms were observed for the reduction of *ca.* 0.16 mM nickel(II) perchlorate in acetonitrile solutions 0.1 M in Et_4NClO_4 and containing varying amounts of CDMBCl. These are shown in Fig. 1. The type of polarogram obtained for a particu-

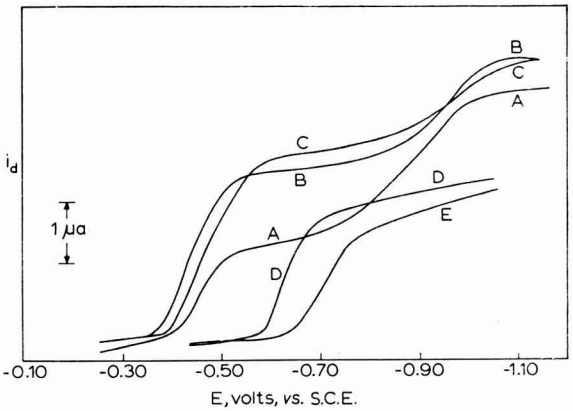

Fig. 1. Effect of varying chloride ion concn. on the polarographic wave for the reduction of nickel(II) ion in acetonitrile. Concn. of nickel(II) perchlorate, $1.62 \cdot 10^{-4}$ M; concn. of Et_4NClO_4, 0.10 M. Concn. of CDMBCl: no *added* chloride (curve A); $1.63 \cdot 10^{-4}$ M (curve B); $4.08 \cdot 10^{-4}$ M (curve C); $4.64 \cdot 10^{-3}$ M (curve D); $1.77 \cdot 10^{-2}$ M (curve E).

lar acetonitrile solution containing the above concentrations of nickel perchlorate and Et_4NClO_4 depends upon the chloride concentration and the drop time of the D.M.E. In solutions containing less than 10^{-3} M concentration of CDMBCl, and over the drop-time range of 1.5–5 sec, nickel(II) was reduced in two steps. As the concentration of added chloride was increased to 10^{-3} M, the height of the first step increased at the expense of the second. The total diffusion current changed only slightly over this chloride concentration range. However, over a range of added chloride concentration of 10^{-4} M–10^{-2} M, there was an appreciable change in the total diffusion current because of increase in viscosity. A similar change in the distribution of the total diffusion current between the first and second steps was observed, together with a decrease in

the total diffusion current, as the drop time was increased (the height of the mercury column was decreased) from 1.5–5 sec. The half-wave potential of the first step shifted with the concentration of CDMBCl from −0.43 V *vs.* S.C.E. for a $8 \cdot 10^{-5}$ *M* solution to −0.55 V *vs.* S.C.E. for a $1 \cdot 10^{-3}$ *M* solution. The nature of this dependency of the half-wave potential of the first step, on the concentration of CDMBCl (at low concentration) can be seen in the section in Fig. 2 where −log [CDMBCl] lies between 3.0 and 4.0. The plots of $-\log (i_d - i)/i$ *vs.* $E_{d.e.}$ for the first step were drawn over in the section corresponding to the top of the wave. The average value of the slopes of the plots corresponding to the foot of the wave, however, was − 1/0.034. The half-wave potentials used in Fig. 2 were obtained by extrapolating this initial section of the plots to the $-\log (i_d - i)/i = 0$ line. The second step in this type of polarogram was always drawn out with $0.059/n$ values of *ca.* 0.12. The half-wave potentials of this step were *ca.* 0.9 V *vs.* S.C.E. and essentially independent of chloride concentration.

In solutions containing between 10^{-3} to 10^{-2} *M* concentration of CDMBCl, either one- or two-step waves were obtained, depending on the drop time. At low drop times, *ca.* 2 sec, two-step waves were observed. As the drop time was increased, by lowering the height of the mercury column, the height of the first step increased at the expense of the second until a single wave corresponding to the first step was obtained. The $-n/0.059$ values, the slopes of the $-\log (i_d - i)/i$ *vs.* $E_{d.e.}$ plots, and the chloride dependency of the half-wave potential of this single wave were identical with those of the first step in the two-step polarograms. The dependency of the half-wave potential of the first step in the two-step polarograms and of the single wave, on the concentration of CDMBCl in this region of chloride concentration, is presented in Fig. 2.

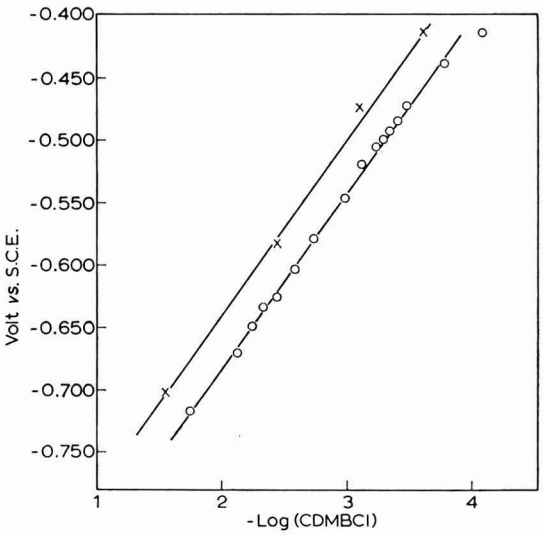

Fig. 2. Half-wave potential for the first step in the two-step waves and for the single waves for the reduction of nickel(II) in acetonitrile, as a function of the logarithm of cetyl-dimethylbenzylammonium chloride concn. Concn. of nickel(II) perchlorate, $1.62 \cdot 10^{-4}$ *M*; concn. of Et_4NClO_4, 0.10 *M*. Experimental curve, o. Theoretical curve (displaced by 0.28 of a −log [CDMBCl] unit), ×.

The non-stoichiometric relationship between i_{d_1} and i_{d_2} with respect to total nickel(II) and total chloride concentrations in solutions of low-chloride, *ca.* 10^{-5} *M*

is another interesting characteristic of the nickel(II)–chloride polarograms. For example, for a solution $2.1 \times 10^{-4} M$ in nickel(II) and $5 \times 10^{-5} M$ in chloride ($3.7 \times 10^{-5} M$ in added chloride and *ca.* $1.5 \times 10^{-5} M$ in chloride from other electrolytes added to the solution), $i_{d_1}/(i_{d_1} + i_{d_2})$ was observed to be 0.74, a value three times larger than the expected value of 0.24 assuming that all the chloride were bound to nickel(II) in a 1 : 1 complex.

The effect of drop time (height of the mercury column) and of temperature on the limiting current of the first wave are shown in Figs. 3 and 4, respectively.

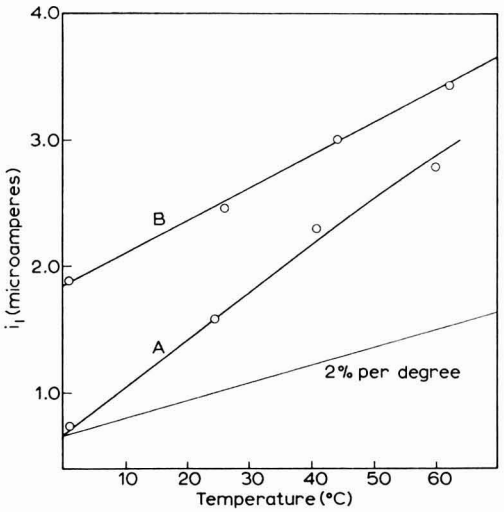

Fig. 3. Effect of temperature on the limiting current of the first step for the reduction of nickel(II) in acetonitrile in the presence of chloride at the D.M.E. Concn. of nickel(II) perchlorate, $1.62 \cdot 10^{-4} M$; concn. of Et_4NClO_4, 0.10 M; concn. of CDMBCl; *ca.* $1 \cdot 10^{-4}$ M (curve A); $9 \cdot 10^{-4}$ M (curve B).

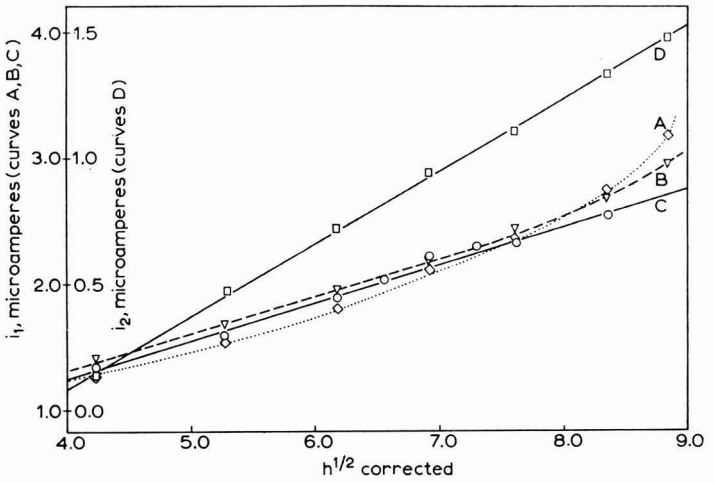

Fig. 4. Effect of drop time (height of the mercury column) on the heights of the first and second steps in the polarograms for the reduction of nickel(II) in acetonitrile in the presence of chloride. Concn. of nickel(II) perchlorate, $2.04 \cdot 10^{-4} M$; concn. of Et_4NClO_4, 0.10 M; concn. of CDMBCl; $1.86 \cdot 10^{-4} M$ (curves A and D); $8.47 \cdot 10^{-4} M$ (curve B); $1.29 \cdot 10^{-2} M$ (curve C).

Spectral

The effect of added chloride on the ultra-violet and visible spectra of nickel(II) perchlorate in acetonitrile is shown in Fig. 5. There are two points worthy of special

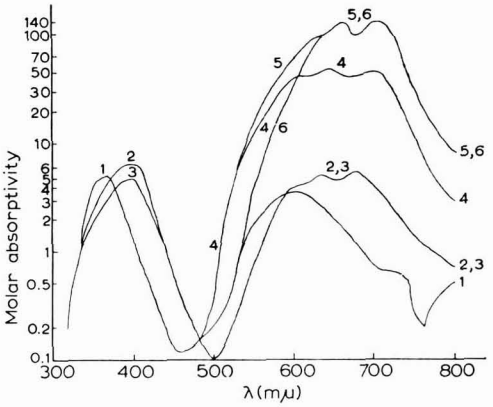

Fig. 5. Ultra-violet and visible absorption spectra of nickel perchlorate in acetonitrile in the presence of chloride ion. Concn. of $Ni(ClO_4)_2$; $1 \cdot 10^{-2}$ *M* for curves (1), (2) and (3); $2 \cdot 10^{-3}$ *M* for curves (4), (5) and (6). $[Cl^-]/[Ni(II)]$: (1), 0.0; (2), 0.5; (3), 1; (4), 2; (5), 3; (6), 5. All solutions are 0.10 *M* in Et_4NClO_4.

mention. The first is the effect of added chloride on the sharp band which is obtained at 380 mμ for nickel(II) perchlorate solutions alone. At chloride to nickel ratios of 0.5 and 1, this band appears at 400 mμ and upon further addition of chloride disappears completely. The second interesting feature is the development of the spectrum in the 500–750 mμ region.

DISCUSSION

The linear dependency of (i) the half-wave potential of the first step in the two-step polarograms for the reduction of Ni(II) in solutions of low chloride concentration and (ii) the half-wave potential of the single wave obtained for solutions of high chloride concentration, on the negative logarithm of the CDMBCl concentration is indeed surprising. Because $E^{\circ\prime}_{Ni(II),\ Ni(Hg)}$ is not known and as information with regard to it and to the approximate values of the constants for the formation reactions of the nickel–chloride complexes involving hydrated nickel(II) species and chloride, cannot be derived from the data in Fig. 2, no direct, accurate evaluation of the individual formation constants of the nickel–chloride complexes is possible. However, by assuming −0.400 V for $E^{\circ\prime}_{Ni(II),\ Ni(Hg)}$ and 10^{+5}, 10^{+5}, 10^{+4}, and 10^{+4} for the individual formation constants of $NiCl^+$, $NiCl_2$, $NiCl_3^-$, and $NiCl_4^{2-}$, and using literature values of $9 \cdot 10^{-2}$ and $3 \cdot 10^{-2}$ for the dissociation constants of the ion-pairs Et_4NClO_4 and Et_4NCl[13], we were able to calculate a theoretical curve (shown in Fig. 2) which is identical with the experimental curve except that it is displaced by + 0.28 unit on the −log [CDMBCl] axis. If values of $10^{+5.28}$, $10^{+5.28}$, $10^{+4.28}$ and $10^{+4.28}$ had been taken for the individual formation constants of the nickel–chloride complexes, the theoretical curve would have fallen exactly on the experimental curve. The agreement between the theoretical and experimental curves indicates that the first step in the two-step

polarograms, and the single polarographic wave, involve the reversible reduction of all four nickel–chloride complexes and that the individual formation constants of these complexes are very close together. Because $E^{\circ\prime}_{Ni(II),\ Ni(Hg)}$ was assumed, the k values are not the actual values. The real k values, however, are in the ratio 10^{+5}: 10^{+5}: 10^{+4}: 10^{4+} for $k_1 : k_2 : k_3 : k_4$.

The nearly similar k values are certainly in line with the spectrophotometric results. In addition to indicating the presence of $NiCl_4^{2-}$ in acetonitrile solutions containing nickel perchlorate and chloride ion our spectral study produced similar absorption spectra in the 500–750 mμ region, to those reported by GILL AND NYHOLM[14] and JØRGENSEN[15] (presented in Table 1), which shows that appreciable amounts of $NiCl_4^{2-}$

TABLE 1

Medium	*Max. (mμ)*	*Reference*
Nitromethane	610(sh)	14
(0.005 *M* $NiCl_4^{2-}$)	660(167)[a]	
	700(167)[a]	
Solid reflectance	570(sh)	15
	625(max.)	
	695(narrow band)	

[a] Molar absorptivity.

are present even in solutions in which the $[Cl^-]/[Ni(II)]$ ratio is less than 1, as can be seen in Fig. 5. The disappearance of the 380–400 mμ band (which has been attributed to hydrated nickel ion) at high chloride concentration, is in accord with the change of the nickel(II) reduction step from a two-step process to a one-step process under the same conditions.

The results of this study in acetonitrile *ca.* 0.02 *M* in H_2O suggest strongly that $NiCl_4^{2-}$, *if* present, is not the only electro-active nickel(II) species in concentrated aqueous chloride medium; all four nickel–cloride complexes are reduced reversibly. The presence of $NiCl_4^{2-}$ ion in concentrated aqueous chloride solution has been suggested by some investigators, but has not been proved definitely. In addition, this non-aqueous study suggests that the individual formation constants of the four nickel–chloride complexes in water are relatively close together, making it possible for as many as three or even all four complexes to be present simultaneously. When one considers the observation of CONNICK[16] and TAUBE[17] that — the introduction of a foreign ligand in the primary solvation sphere of certain metal ions changes drastically the lability of the remaining water molecules in the primary solvation sphere of the metal ions, resulting in greater ease of displacement of the remaining water molecules in the co-ordination sphere than in the completely hydrated ion — such a situation with regard to the individual formation constants of the nickel–chloride complexes in water is not unreasonable.

The catalytic nature of the reduction step of the nickel–chloride complexes is another interesting feature of the polarography of nickel(II) perchlorate in acetonitrile in the presence of chloride. The greater than 2% per degree effect of temperature on the height of the first wave[18], and the effect of drop time and of the concentration of chloride (particularly when the chloride concentration is less than the concentration of nickel(II)) on the distribution of the total diffusion current between the first and

second steps, all point to the reduction step involving the nickel–chloride complexes being a catalytic process. A similar phenomenon has been observed for the reduction of nickel(II) in the presence of pyridine and other amines, in aqueous medium at the D.M.E.[10,11].

ACKNOWLEDGEMENT

We wish to acknowledge the generous support of the Directorate of Chemical Sciences, Air Force Office of Scientific Research (AFOSR Grant 61-8 and 220-63) and the Dupont Chemical Company (fellowship for Ivory V. Nelson).

SUMMARY

In the presence of small amounts of chloride ion, nickel(II) undergoes a two-step reduction in acetonitrile. Analysis of the dependency of the half-wave potential of the first step on the logarithm of the CDMBCl concentration, indicates that this polarographic step involves the reversible reduction of the four nickel–chloride complexes, $NiCl_4^{2-}$, $NiCl_3^-$, $NiCl_2$ and $NiCl^+$, and that these complexes have nearly identical formation constants in acetonitrile *ca.* 0.02 *M* in H_2O. The potential and characteristic of the second step suggest that it involves the reduction of hydrated nickel II) ion. With high concentrations of choride ion, only one step, corresponding to the first step in the two-step polarograms obtained at low concentrations of chloride, is obtained. The chemistry of the nickel–chloride system in water is undoubtedly governed by a similar equilibrium situation to that in acetonitrile.

In addition, the catalytic nature of the first step has been established.

REFERENCES

1 M. PAVLICK, *Collection Czech. Chem. Commun.*, 3 (1931) 223.
2 N. YA KHLOPIN, *Zh. Anal. Chem.*, 2 (1947) 55; *C.A.*, 43 : 5327a.
3 G. F. REYNOLDS, H. I. SHALGOSKY AND T. J. WEBER, *Anal. Chim. Acta*, 8 (1953) 567.
4 A. A. VLCEK, *Z. Elektrochem.*, 61 (1957) 1014.
5 N. TANAKA, R. TAMAMUSHI AND M. KODAMA, *Bull. Chem. Soc., Japan*, 33 (1960) 14.
6 M. KALOUSEK, *Collection Czech. Chem. Commun.*, 13 (1948) 105.
7 I. M. KOLTHOFF AND J. F. COETZEE, *J. Am. Chem. Soc.*, 79 (1957) 1852.
8 A. I. POPOV AND D. H. GESKE, *ibid.*, 79 (1957) 2074.
9 R. C. LARSON AND R. T. IWAMOTO, *ibid.*, 82 (1960) 3239.
10 H. B. MARK, JR. AND C. N. REILLEY, *J. Electroanal. Chem.*, 4 (1962) 189.
11 H. B. MARK, JR. AND C. N. REILLEY, *Anal. Chem.*, 35 (1963) 195.
12 M. T. KELLEY, H. C. JONES AND H. C. FISHER, *ibid.*, 31 (1959) 1475.
13 C. W. DAVIES, *Ion Association*, Butterworths, Washington, 1962, p. 96.
14 N. S. GILL AND R. S. NYHOLM, *J. Chem. Soc.*, (1959) 3997.
15 C. K. JØRGENSEN, *Mol. Phys.*, 1 (1958) 410.
16 R. E. CONNICK, Paper presented at the 142nd National Meeting of the American Chemical Society, September, 1962, Atlantic City, N.J.
17 H. TAUBE, Franklin Lecture, University of Kansas, 1962.
18 L. MEITES, *Polarographic Techniques*, Interscience Publishers, Inc., New York, 1955, p. 56

VERIFICATION OF THE COULOMETRIC METHOD FOR THE ANALYSIS OF ABSORBED HYDROGEN

THOMAS C. FRANKLIN AND NELLIE F. FRANKLIN

Chemistry Department, Baylor University, Waco, Texas (U.S.A.)

(Received May 28th, 1963)

The coulometric method used by a number of workers[1-5] to study surface processes involving hydrogen has also been applied to the study of absorbed hydrogen[6]. It is difficult to check the results obtained by this method with those given by the normal analytical methods for hydrogen in metals since (i) the amount of hydrogen absorbed in the micro-electrodes is small and (ii) techniques such as vacuum fusion analyze for both free and combined hydrogen. The electrochemical method of analysis of absorbed hydrogen was checked against a method using a gas flow system based on the use of a rising temperature of the furnace used for heating the metal sample in an argon stream. The amount of hydrogen baked out of the metal was analyzed by the thermal conductivity method. This is a combination of the principles and apparatus used by GARN AND KESSLER[7], COE AND JENKINS[8] and MOON AND LEVY[9].

EXPERIMENTAL

Figure 1 is a block diagram of the apparatus used for the thermal conductivity method. A stream of argon was passed over the metal sample in the furnace. The furnace, originally at room temperature, was heated by a fixed voltage as applied by a variable transformer. In the region in which the hydrogen was being driven out, the temperature

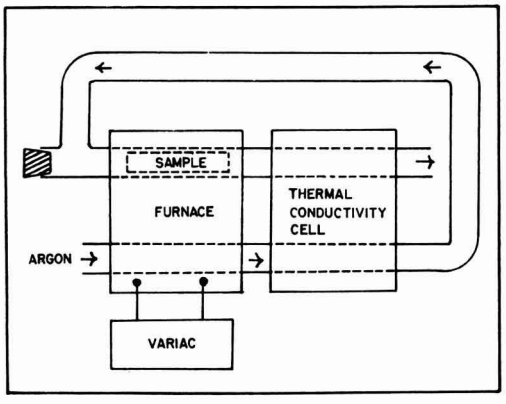

Fig. 1. Block diagram of flow system for analysis of hydrogen.

of the furnace rose almost linearly. The rate of rise of temperature was dependent on the voltage applied to the furnace.

The gas, after passing through the furnace was passed through a Gow-Mac thermal conductivity cell. The response of the thermal conductivity bridge was recorded on a Sargent SR recorder and integrated with a Disc integrator.

The metal investigated was an approximately 18-gauge palladium wire. The amount of hydrogen in the metal was varied by cathodically charging the metal in 2 *N* sulfuric acid solution for different lengths of time.

The results were checked against results obtained by a coulometric procedure previously described[1,5,6].

RESULTS

If the response of the thermal conductivity bridge during a run, was plotted against time, a maximum occurred at approximately 200°. The area under the maximum could be reproduced within 2.5%. Figure 2 is a typical plot of the area under the maximum as a function of the amount of hydrogen absorbed by the palladium measured by the coulometric procedure. It can be seen that the area under the peak is linearly proportional to the amount of hydrogen absorbed in the metal.

From this study it is seen that the area under the coulometric curves is proportional to the amount of hydrogen baked out of the palladium at low temperatures measured by the thermal conductivity method.

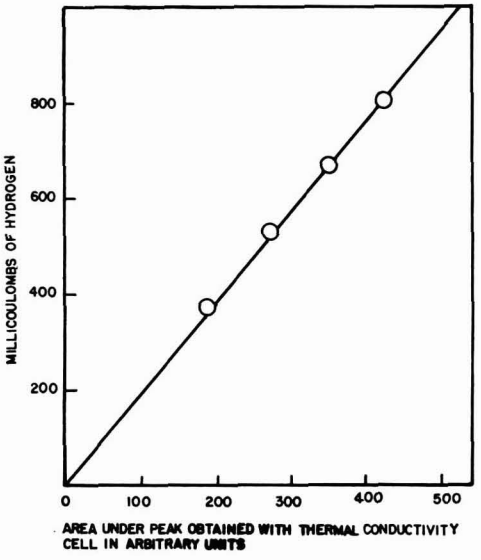

Fig. 2. A comparison of the area under the coulometric curves with the area under the thermal conductivity curves.

ACKNOWLEDGEMENT

The research reported in this paper has been sponsored by the Geophysics Research Directorate of the Air Force Cambridge Research Laboratories, Office of Aerospace Research, under contract AF 19(604)-8414.

SUMMARY

A coulometric method of analysis for hydrogen absorbed in palladium was checked against a gas flow method which used a programmed temperature rise for the sample and a thermal conductivity detector. It was found that the amount of hydrogen determined coulometrically was linearly proportional to the amount of hydrogen driven out of the metal thermally.

REFERENCES

1 T. C. FRANKLIN AND R. D. SOTHERN, *J. Phys. Chem.*, 58 (1954) 951.
2 M. OIKAWA AND T. MUKAIBO, *J. Electrochem. Soc., Japan*, 20 (1952) 568.
3 M. W. BREITER, C. A. KNORR AND V. VOLKL, *Z. Elektrochem.*, 59 (1955) 681.
4 M. W. BREITER AND S. G. IMAN, *J. Electrochem. Soc.*, 109 (1962) 622.
5 T. C. FRANKLIN AND S. L. COOKE, Jr., *ibid.*, 107 (1960) 555.
6 T. C. FRANKLIN AND J. R. GOODWYN, *ibid.*, 109 (1962) 288–292.
7 P. C. GARN AND J. E. KESSLER, *Anal. Chem.*, 33 (1961) 952.
8 F. R. COE AND N. JENKINS, *Iron Steel Inst., Spec. Rep., London*, 68 (1960) 229.
9 K. A. MOON AND C. LEVY, *J. Electrochem Soc.*, 109 (1962) 301.

THE CATALYTIC REDUCTION OF NITRITE IONS DURING POLAROGRAPHIC REDUCTION OF VANADIUM(V)

FREDERICK BAUMANN

California Research Corporation, Richmond, California (U.S.A.)

(Received May 28th, 1963)

INTRODUCTION

During the determination of vanadium using the polarographic method, enhanced limiting currents were observed with solutions which had a history of nitric acid pretreatment. Subsequent investigations established that the enhanced limiting current is caused mainly by nitrite ion. The uranyl[1]- and molybdate[2]-catalyzed reduction of nitrate and/or nitrite ions has been extensively studied by the polarographic method, but vanadium(V) catalysis has been only briefly noted[3]. This work describes the observed effect in greater detail and shows that it is consistent with the catalytic reduction of nitrite.

EXPERIMENTAL

A Leeds and Northrup Electro-Chemograph Type E was used. Extreme damping was avoided. A saturated calomel H-cell of conventional design was used. One molar ammonia (Baker and Adamson)–one molar ammonium chloride (Baker's Analyzed Reagent) electrolyte-buffer containing one-half drop Triton X-100 per liter as maximum suppressor was used. Maxima were not entirely eliminated.

Standard vanadium solutions were prepared from Baker's Analyzed Reagent ammonium vanadate. After the addition of ammonium vanadate solution to the buffer-electrolyte, the solution was warmed for 20 min to ensure conversion of vanadium to the alkaline species. This step is essential if vanadate has been previously treated in acid solution. After cooling, standard potassium nitrite solution (prepared from Baker's Analyzed Reagent) was added, the solution was diluted to volume, and a polarogram obtained immediately after de-aeration with nitrogen.

The total limiting current was measured between -1.4 and -1.6 V *vs.* the saturated calomel electrode (S.C.E.). This is on the limiting current plateau between the maximum and the reduction of the electrolyte and/or direct reduction of nitrite ions. The limiting currents were not measured at identical voltages because of shifts in the wave with change in concentration. The value 1.78 $mg^{2/3}\ sec^{-1/2}$ for $m^{2/3}t^{1/6}$ was measured for this capillary at -1.55 V *vs.* S.C.E. in 1 *M* NH_3–1 *M* NH_4Cl electrolyte.

POLAROGRAPHIC BEHAVIOUR OF VANADATE

A double wave is obtained for the reduction of vanadium(V) in the 1 *M* NH_3–1 *M* NH_4Cl electrolyte. Data for these waves are summarized in Table 1. The half-wave

TABLE 1

SUMMARY OF HALF-WAVE POTENTIAL AND LIMITING CURRENT DATA FOR THE POLAROGRAPHIC REDUCTION OF VANADIUM(V) IN THE PRESENCE OF NITRITE IONS IN 1 *M* NH_3–1 *M* NH_4Cl ELECTROLYTE AT 25°

Vanadium(V) concn. (moles/l·10⁻³)	*Nitrite concn. (moles/l·10⁻³)*	*Half-wave potential*		*Average Limiting current*	
		First wave (V vs. S.C.E.)	*Second wave (V vs. S.C.E.)*	*First wave (μA)*	*Second wave (μA)*
0.0857	0	−1.10		0.79	
—	1	−1.12		0.82	
—	5	−1.14		0.96	
—	10	−1.15		1.12	
—	15	−1.15		1.24	
0.857	0	−1.03	−1.25	3.80	2.88
—	2	−1.03	−1.26	3.94	5.28
—	5	−1.02	−1.27	3.96	8.20
—	10	−1.02	−1.27	4.02	12.2
—	15	−1.03	−1.28	4.16	14.9
4.28	0	−0.86	−1.31	5.0	17.9
—	2	−0.86	−1.35	4.9	28.4
—	4	−0.88	−1.36	5.0	40.8

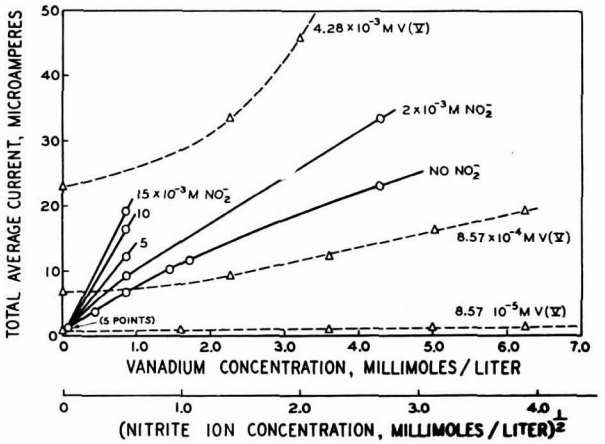

Fig. 1. Limiting currents obtained for the reduction of vanadium(V) in the presence of nitrite ions.

potential of the first wave becomes more negative with decreasing vanadium concentration. At vanadium(V) concentrations below 0.0857 m mole/l only one wave is seen. The half-wave potentials in Table 1 agree well with the data of LINGANE, who obtained −0.97 V *vs.* S.C.E. for the first wave and −1.26 V *vs.* S.C.E. for the second wave at a vanadium(V) concentration of 1.59 m*M* in 1 *M* NH_3–1 *M* NH_4Cl electrolyte containing 0.005% gelatin[4]. Within the limits of measurement all the half-wave potentials are independent of nitrite ion concentration.

The limiting current behavior is illustrated in Fig. 1. The solid curves are at constant nitrite concentration, while the broken curves represent the same data replotted at constant vanadium(V) concentration *vs.* the square root of the nitrite ion concentration. In the absence of nitrite ions, non-linear dependence of the total vanadium(V) limiting current (wave 1 + wave 2) on concentration is obtained. The non-linear dependence of the limiting current on the vanadium concentration has not been reported. The behavior is reproducible for this polarographic method has been used many years for the determination of vanadium.

The limiting current of the first wave in the absence of nitrite ions is not one-third of the total limiting current as has been reported[4], but is nearly independent of vanadium(V) concentration above $5 \cdot 10^{-4}$ *M*. SCHMID AND REILLEY attribute the first wave to an inhibited electrode reaction caused by the deposition of an insoluble vanadium species on the electrode surface[5]. The data in Table 1 and Fig. 1 agree with this adsorption wave interpretation. The shift of the half-wave potential of the first wave to more positive potentials is indicative of absorption waves where the reduced species is adsorbed on the electrode. Furthermore, observation of the limiting current of the first wave during the growth of a single drop of mercury shows a rise and then a decrease in the current before the drop falls. This is also indicative of an adsorption wave.

The limiting current of the second wave alone becomes proportional to the vanadium(V) concentration at high, vanadium(V) concentrations. The total limiting current (wave 1 + wave 2) apparently represents the reduction process of each wave operating independently rather than the direct reduction of all vanadium(V) to vanadium(II). Otherwise, the total limiting current would be expected to be proportional to vanadium(V) concentration. Only the second wave is observed in the polarographic reduction of vanadium(IV). The second wave must then involve the reduction of both vanadium(IV) and (V) species to vanadium(II). This behavior was also observed by FILIPOVIC *et al.* in phosphate buffer[3].

Enhanced current

The enhanced limiting current in the presence of nitrite ions is due entirely to an increase in the limiting current of the second wave. The dependence of the average limiting current on the square root of the nitrite ion concentration is characteristic of pseudo-first-order polarographic catalytic processes. The deviation at low concentrations reflects the fact that the nitrite concentrations were too low to maintain pseudo-first-order kinetics[6,7].

Vanadium(IV) shows an enhanced limiting current in the presence of nitrite ions and a limiting current plateau identical with the second wave of vanadium(V). The instability of vanadium(IV) species in the electrolyte, prohibited quantitative study.

The diffusion current constant $i_D/\mathrm{cm}^{2/3}t^{1/6}$ for the catalytic reduction of nitrite is $3.1\,\mu\mathrm{A\,l\,mmole^{-1}\,mg^{-2/3}\,sec^{1/2}}$ at 25° at a vanadium(V) concentration of $4.28 \cdot 10^{-3}$ *M*. This is typical of the usual polarographic sensitivity and may be useful for the determination of nitrite ions.

Vanadium(V) can be determined with greater sensitivity in a nitrite medium. The limiting current is increased approximately three-fold in a $15 \cdot 10^{-3}$ *M* nitrite medium. A higher nitrite ion concentration would result in an even greater sensitivity, but the nitrite concentration is limited by the large nitrite reduction wave which interferes with the vanadium(V) wave.

Dependence on mercury head

The average limiting current for the reduction of vanadate in the presence of nitrite ions is nearly independent of the head of mercury at $5 \cdot 10^{-3}$ moles/l nitrite and seemingly independent at $25 \cdot 10^{-3}$ moles/l nitrite. This is illustrated in Table 2. This behavior is indicative of a kinetic process.

TABLE 2

DEPENDENCE OF THE TOTAL AVERAGE LIMITING CURRENT ON THE HEAD OF MERCURY (h)

$h^{1/2}$ [a] ($cm^{1/2}$)	*Average limiting current*[b]		
	No Nitrite (μA)	$5 \cdot 10^{-3}$ *M Nitrite* (μA)	$25 \cdot 10^{-3}$ *M Nitrite* (μA)
5.22	5.2	11.1	23.3
5.76	6.1	11.2	23.0
6.90	6.8	11.3	23.4
7.70	8.7	12.2	22.4

[a] Corrected for back-pressure.
[b] $8.57 \cdot 10^{-4}$ *M* vanadium.

Effect of other ions

Nitrate, chlorate and perchlorate ions showed no effect at concentrations of 10^{-2} moles/l. Bromate, iodate and periodate gave waves which preceded or coincided with the vanadium(V) wave and were not studied further. Catalytic reduction of nitrite was observed in the same electrolyte which was also 1 *M* in ethylenediamine tetraacetate.

MECHANISM

The following sequence of reactions is proposed as contributing to the observed catalytic effect:

$$V(V) + 3\,e \rightarrow V(II) \tag{1}$$

$$V(II) + NO_2^- \xrightarrow{k} V(IV) + \text{Reduction products of } NO_2^- \tag{2}$$

$$V(IV) + 2\,e \rightarrow V(II) \tag{3}$$

The reaction

$$V(IV) + V(II) \rightarrow V(III) \tag{4}$$

seems to be unimportant since V(IV) concentration is low. The formation of a reducible complex between vanadium(II) and nitrite ion cannot be discounted, but no evidence exists for such a species. The reduction products of nitrite are complex but need not be considered here. The evidence for vanadium(IV) as the regenerated electro-reducible species is based on the fact that vanadium(IV) species also show the catalytic effect. The reduction of vanadium(III) is not observed under these conditions[4]. Furthermore, in homogneous systems the formation of vanadium(IV) with perchlorate, iodate and ferric ions is observed when excess vanadium(II) is avoided[8,9]. The reaction between V(II) and V(IV) is rapid in acidic media[8].

ACKNOWLEDGEMENT

The author is indebted to Mr. P. D. E. NELSON for experimental assistance.

SUMMARY

Enhanced limiting currents for the polarographic reduction of vanadium(V) in NH_3–NH_4Cl electrolyte are observed in the presence of nitrite ions. The limiting current is independent of the head of mercury and is proportional to the square root of the nitrite ion concentration. The enhanced current is attributed to the catalytic reduction of nitrite ion, involving the following reactions:

$$V(V) + 3\,e \rightarrow V(II)$$

$$V(II) + NO_2^- \xrightarrow{k} V(IV) + \text{reduction of products of } NO_2^-$$

$$V(IV) + 2\,e \rightarrow V(II)$$

REFERENCES

1 J. KORYTA, *Collection Czech. Chem. Commun.*, 20 (1955) 667.
2 G. P. HAIGHT, JR., *Acta Chem. Scand.*, 15 No. 10 (1961) 2012–2020.
3 I. FILIPOVIC, Z. HAHL, Z. GASPARAC AND V. KLEMENCIC, *J. Am. Chem. Soc.*, 76 (1954) 2074.
4 J. J. LINGANE, *ibid.*, 67 (1945) 182.
5 R. W. SCHMID AND C. N. REILLEY, *ibid.*, 80 (1958) 2087.
6 J. KOUTECKY, *Collection Czech. Chem. Commun.*, 18 (1953) 311.
7 P. DELAHAY AND G. L. STIEHL, *J. Am. Chem. Soc.*, 74 (1952) 3500.
8 W. R. KING, JR. AND C. S. GARNER, *J. Phys. Chem.*, 58 (1954) 29–33.
9 C. M. ELLIS AND A. I. VOGEL, *Analyst*, 81 (1956) 693.

Book Review

Representation des équilibres de solubilités et utilisation des diagrammes by ROBERT BERTHON, Gauthier-Villars, Paris, 1962, 269 pages, Fr 38.—, £ 3 15 s.

Many of us will recall being puzzled and amused by our inability to decide which way up a cube drawn on paper ought to be. The confusion originates from the compression of three dimensions into two, and in the scientific world this difficulty hits among others crystallographers, organic chemists, and users of the phase diagram. Members of the last class are particularly unfortunate because even three dimensions are not enough for a full display of properties in many polyphase systems, and various devices have to be used to depict the phase relationships. This book helps those who wish to understand and apply the geometrical intricacies of such phase diagrams. It can also be a diverting mental exercise for chemists undeterred by unfamiliar vectorial notation and straightforward French. The author's approach is through general principles and his recourse to actual systems is comparatively minor, being confined to examples drawn from aqueous inorganic systems at ordinary temperatures and constant pressure. Naturally, copious use is made of generalized diagrams, some of forbidding perspective complexity, but the text conveys their meaning with commendable verbal restraint. With so much close argument and geometrical symbolism the book can hardly be readable, but because of this it merited printing on paper of adequate weight and opacity. As it is, complex diagrams show through on each other, and the folded diagram is too fragile to consult heedlessly. Little of the subject matter has been drawn from work published after 1950, but this is not surprising in a general book on the subject. There is a table of contents at the back, and this makes the omission of a proper index just permissible. However, the specialist physical chemist can enjoy getting to grips with the complications of double satls and hydrates, particularly in the isothermal evaporation of the aqueous quinary system containing sodium, potassium, magnesium, chloride, and sulphate. The similarity between this system and sea water should be obvious, and useful discussion of practical interest is given to this and related systems. Undoubtedly, the enthusiasm of the author for his task will be shared by his serious readers.

E. C. POTTER

CONTENTS

ELSEVIER PUBLISHING COMPANY, AMSTERDAM

Printed in The Netherlands by

NEDERLANDSE BOEKDRUK INRICHTING N.V., 'S-HERTOGENBOSCH